Synthesis and Applications of Fluoroalkyl End-Capped Oligomer Gels

Doctoral Course
Graduate School of Science and Technology
Hirosaki University

Doctoral Thesis

March 2020

Shinsuke Katayama

Contents

General Introduction

1. Polymer gel

Polymer gel in general consists of three-dimensional networks, of whose structures are constructed from chemical cross-linking [Fig. 1-**(a)**] and physical interaction [Fig. 1-**(b)**], surrounded by a large number of solvent molecules.[1)] Such three-dimensional polymer gel structures are formed not only through the covalently cross-linking but also through the non-covalent bonding interactions with hydrogen bonding, ionic interactions and hydrophobic associates. [1)] Such polymer gels can be also classified according to their structures into two types: one is thermally irreversible (chemical) gels and the other is thermoreversible (physical) gels.[2, 3)]

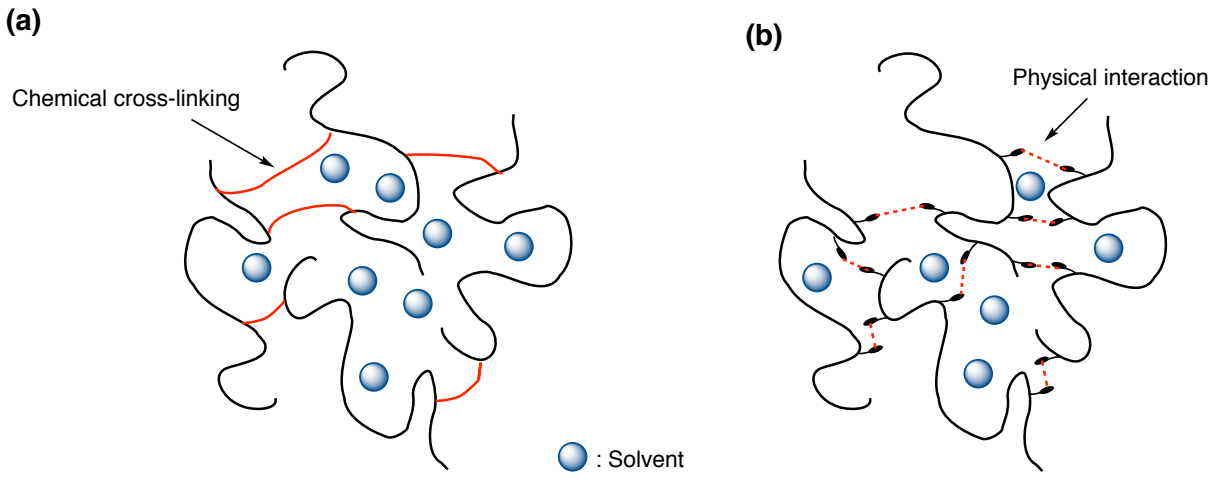

Fig. 1 Schematic illustration for the structures of chemical **(a)** and physical **(b)** polymer gels[2, 3)]

Low molecular weight compounds such as 12-hydroxystearic acid

[$CH_3(CH_2)_5CH(OH)$-$(CH_2)_{10}$-C(=O)OH] can also cause gelation through the hydrophobic association with hydrogen bonding interaction as shown in Fig. 2.[4] Especially, molecular aggregates of low molecular weight compound (gelator) can be formed through the hydrophobic association of longer alkyl units to create the fibrous state, affording the physical gel by the entanglement of the supramolecular nanofiber.[4 ~ 8]

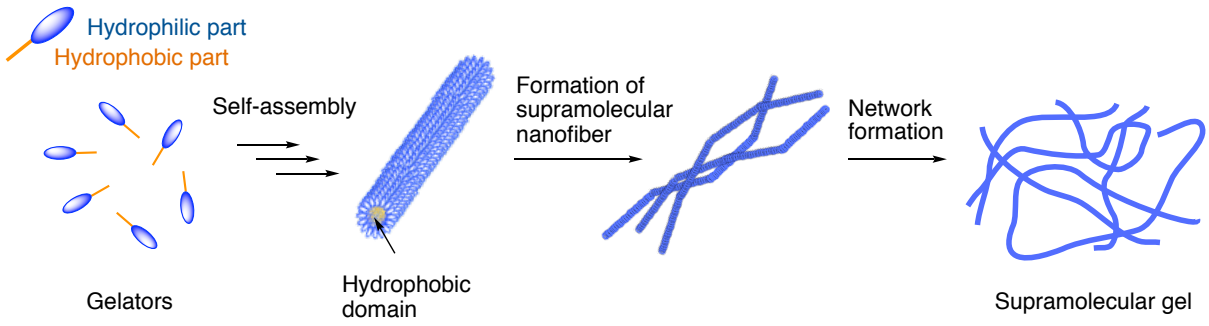

Fig. 2 Schematic illustration for the formation of supramolecular physical gel[4]

In a wide variety of polymer gels, Gong *et al.* have already developed the double-network polymer gel as shown in Fig. 3.[9 ~ 12]

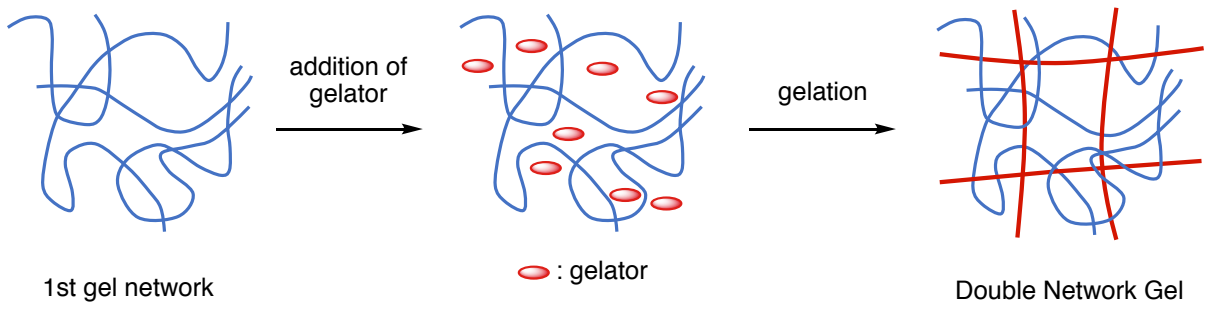

Fig. 3 Schematic illustration for the formation of double-network polymer gel

Such double-network polymer gels are effective for providing an excellent strength and rigidity that set them apart from the traditional polymer gels.[9 ~ 12)]

2. Perfluoroalkyl unit-containing organogels

There has been great interest in organofluorine compounds, due to their exhibiting a variety of unique properties such as high solubility, surface active characteristic and biological activity, which cannot be achieved by the corresponding non-fluorinated ones.[13 ~ 15)] Therefore, it is of particular interest to develop the novel organofluorine compounds possessing a gelling characteristic. In fact, there have been hitherto some reports on the development of longer perfluoroalkyl groups-containing organogelators as depicted in Scheme 1.[16 ~ 19)]

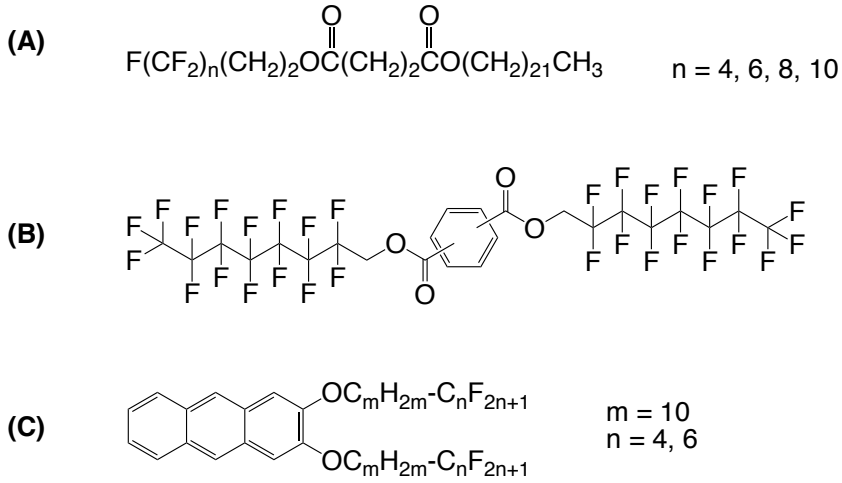

Scheme 1 Longer perfluoroalkyl groups-containing organogelators

For example, Hanabusa and Nakano *et al.* reported that perfluoroalkyl chain-containing succinic diesters can form gels by heating them in appropriate organic solvents, and the surface roughness formed by the fibrous aggregates of these organogelators enables these succinic

diesters to create the superhydrophobic surfaces (water contact angles greater than 150 degrees) [see Scheme 1-**(A)**].[16] However, we have some difficulties to keep such unique gelling characteristics for a long time; because these gelators consist of the low molecular weight organic compounds.[6]

On the other hand, studies on the fluorinated polymer gels have been very limited so far, although fluorinated polymers can exhibit unique and remarkable properties, such as thermal stability, chemical inertness, low refractive indices, and surface active characteristic that set them apart from the corresponding non-fluorinated polymers.[20 ~ 22] Therefore, from the developmental viewpoint of fluorinated polymeric functional materials, studies on the fluorinated polymer gels are of particular importance. In fact, there have been hitherto some reports on the fluorinated polymer gels, such as formation of thermally reversible poly(vinylidene fluoride) [PVDF] gels in a specific solvent[23] and the fluorinated microgel-core star polymers bearing poly(methyl methacrylate) as the corona units (see Scheme 2).[24]

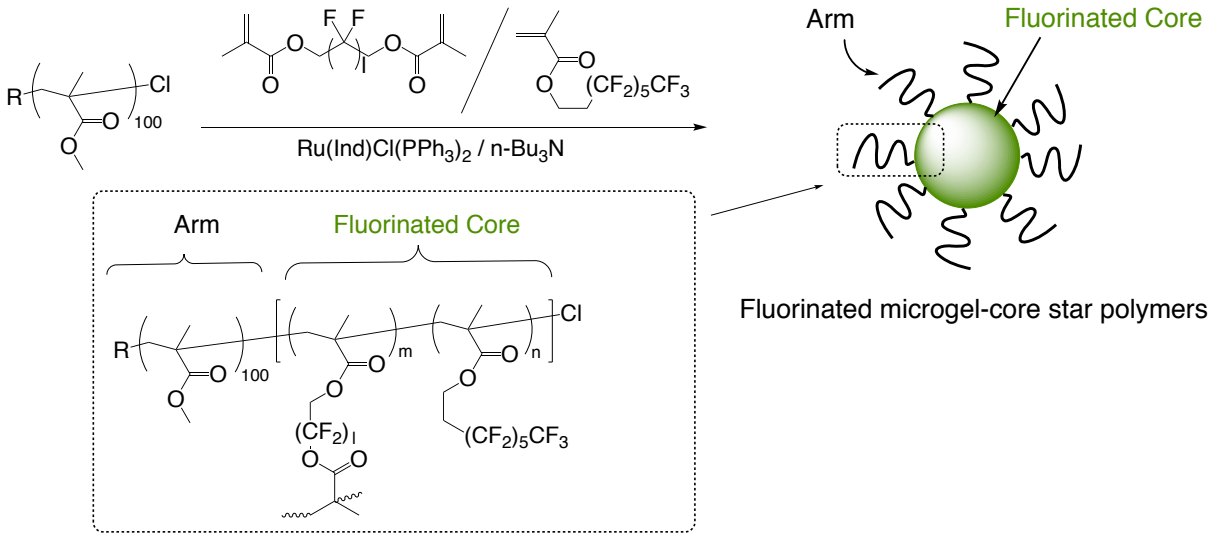

Scheme 2 Synthesis of fluorinated microgel-core star polymers bearing poly(methyl methacrylate) as the corona units[24]

3. Fluoropolymers

As indicated above, fluorinated polymers such as poly(tetrafluoroethylene) [PTFE] and tetrafluoroethylene - perfluorovinylether copolymer [PFA] (see Scheme 3) exhibit a wide variety of unique properties, such as high heat resistance, oxidation resistance, low dielectric constant, chemical inertness to acids, bases and organic solvents, and surface active properties that set them apart from the corresponding non-fluorinated polymers. [25 ~ 27)]

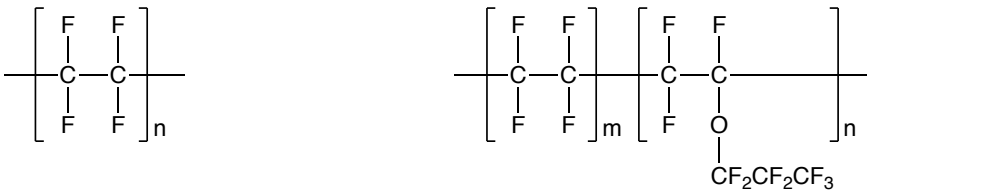

Poly(tetrafluoroethylene) [PTFE]

Poly[tetrafluoroethylene-co-perfluoro(propylvinyl ether)] [PFA]

Scheme 3 Some of typical fluoropolymers

However, these fluorinated polymers exhibit extremely low solubility in organic solvents.[28 ~ 30)] In contrast, partially protonated ring-containing fluoropolymers have a solubility in polar aprotic solvents such as acetone, acetonitrile, and tetrahydrofuran.[29, 30)] The introduction of hydrocarbon units into fluorinated polymers is an effective tool, from the developmental viewpoint of novel fluorinated polymers possessing a good solubility toward a variety of solvents. In fact, as shown in Scheme 4, an ABA triblock-type fluoroalkyl end-capped oligomeric surfactant [R_F-$(M)_n$-R_F: R_F = fluoroalkyl group; M = radical polymerizable monomers such as acrylic acid] has been already synthesized by reaction of fluoroalkanoyl peroxide with the radical polymerizable monomer.[31)] This ABA triblock-type fluoroalkyl

end-capped oligomer can be obtained through the primary radical termination of R_F· radical or radical chain transfer of the peroxide to the propagation radical as shown in Scheme 3.[31, 32)]

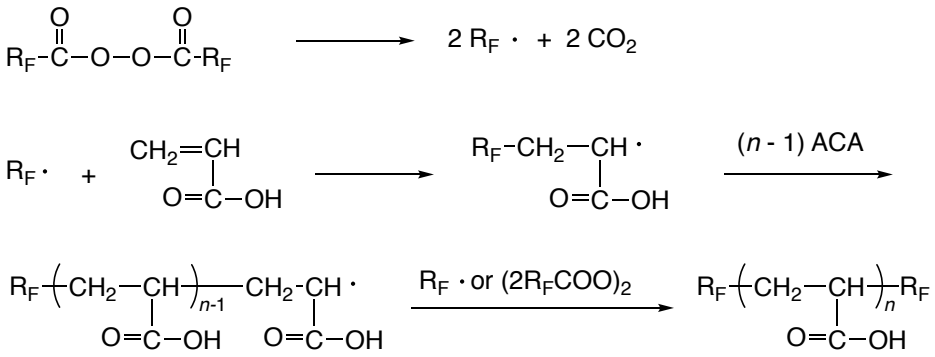

R_F = perfluoroalkyl, perfluoro-oxa-alkyl group

Scheme 4 Synthesis of two fluoroalkyl end-capped acrylic acid oligomer

These fluoroalkyl end-capped oligomers such as fluoroalkyl end-capped acrylic acid oligomer can exhibit an excellent solubility not only in traditional polar organic solvents but also in water.[31)]

Similarly, two fluoroalkyl end-capped acrylic acid - trimethylvinylsilane cooligomers [R_F-($CH_2CHCOOH)_x$-($CH_2CHSiMe_3)_y$-R_F] have been synthesized by the cooligomerization of fluoroalkanoyl peroxide with the corresponding monomers.[33, 34)] These fluoroalkyl end-capped cooligomers can form the nanometer size-controlled self-assembled molecular aggregates with aggregation of terminal fluoroalkyl segments in aqueous and organic media as shown in Fig. 4.[35, 36)]

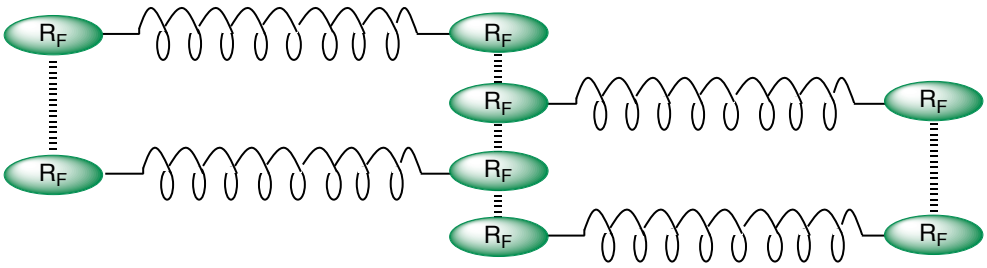

Fig. 4 Schematic model of micelles formed with fluoroalkyl end-capped acrylic acid trimethylvinylsilane cooligomers

On the other hand, the corresponding non-fluorinated cooligomers cannot form such molecular aggregates, and these cooligomers have an entanglement interaction in aqueous and organic media.[35, 36)]

In this way, fluoroalkyl end-capped oligomers can form the self-assembled molecular aggregates as shown in Fig. 4. Thus, the exploration of two fluoroalkyl end-capped oligomers possessing additional functional units, which can provide a van der Waals interaction, is of particular interest from the developmental viewpoint of novel fluorinated oligomer gels.

4. Thesis outline

In this study, preparation and properties of novel fluoroalkyl end-capped oligomer gels will be described.

Chapter 1 shows that fluoroalkylated end-capped 2-acrylamido-2-methylpropanesulfonic acid oligomers form gels not only in water but also in organic polar solvents under non-crosslinked conditions (see Fig. 5). These fluorinated gelling oligomers thus obtained have a strong metal ion binding power. In addition, it is demonstrated that these fluorinated gelling

oligomers are potent and selective inhibitors of HIV-1 replication in cell culture. It is also demonstrated that these fluorinated gelling oligomers possess antibacterial activity against *Staphylococcus aureus*.

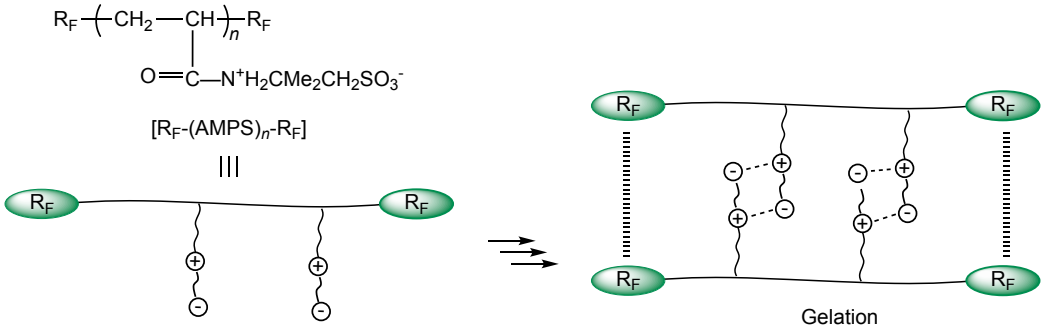

Fig. 5 Schematic illustration for the gel formation of R_F-(AMPS)$_n$-R_F oligomers

In chapter 2, the synthesis and properties of fluoroalkylated end-capped *N*-tris(hydroxymethyl)methylacrylamide oligomers by reaction of fluoroalkanoyl peroxide with the corresponding monomer are described (see Fig. 6).

These fluoroalkylated oligomers are demonstrated to cause a gelation, where the aggregations of fluoroalkyl segments and the hydrogen-bonding interactions are involved in establishing a physical gel network in water or in organic media.

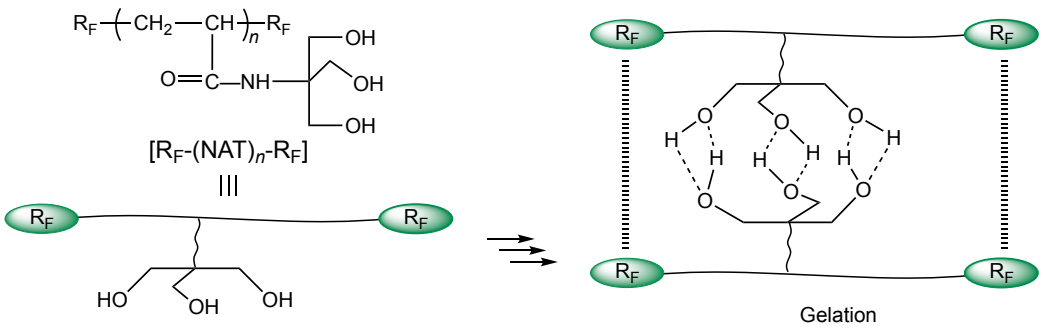

Fig. 6 Schematic illustration for the gel formation of R_F-(NAT)$_n$-R_F oligomers

In chapter 3, synthesis and properties of fluoroalkylated end-capped oligomers containing hydroxy segments, such as 2-hydroxypropyltrimethylammonium segments and carboxy-hydroxymethylamido segments are described (see Fig. 7).

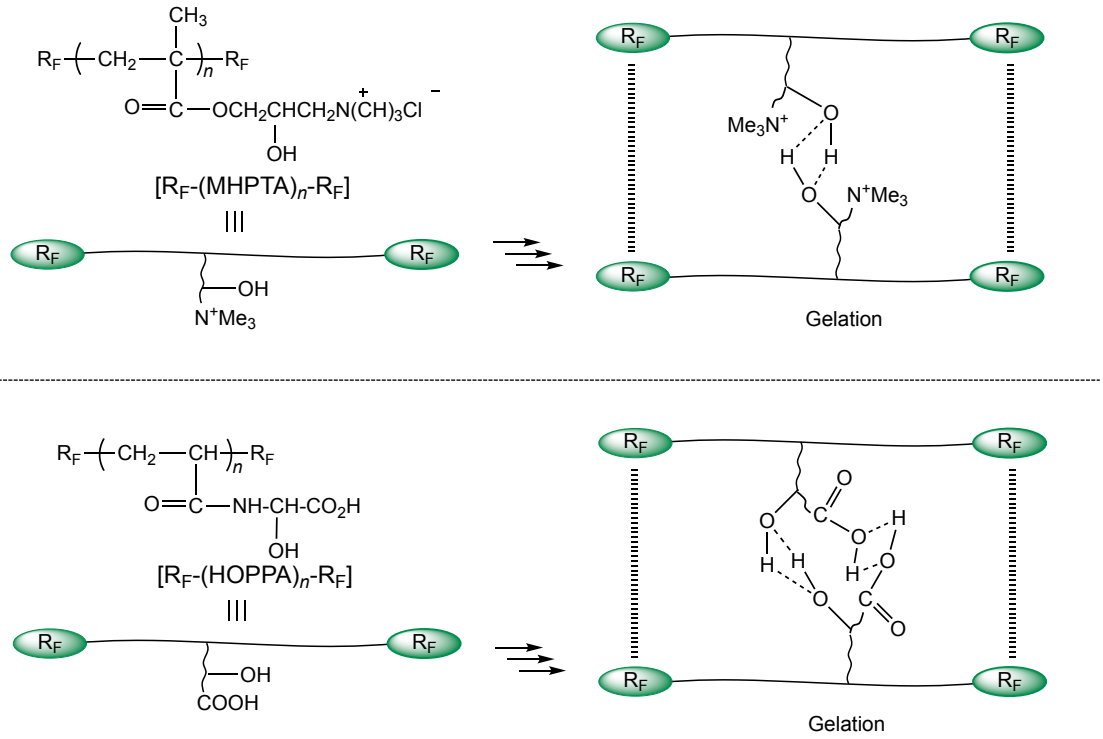

Fig. 7 Schematic illustration for the gel formation of R_F-(MHPTA)$_n$-R_F oligomers and R_F-(HOPPA)$_n$-R_F oligomers

It is demonstrated that these fluorinated oligomers can cause gelation in water or in polar organic solvents, whose behavior is governed by the synergistic interactions of the aggregation of fluoroalkyl segments within oligomers and intermolecular hydrogen bonding between hydroxy or carboxy segments under non-cross-linked conditions.

Chapter 4 shows that two fluoroalkyl end-capped vinyltrimethoxysilane oligomer [R_F-(CH_2–$CHSi(OMe)_3$)$_n$-R_F] can undergo the sol-gel reaction in the presence of *N*-(3-triethoxysilylpropyl)gluconamide [Glu-Si(OEt)$_3$] under alkaline conditions to afford the

corresponding fluorinated oligomeric silica nanocomposite gels containing gluconamide units [R_F-(VM-SiO_2)$_n$-R_F/Glu-SiO_2] (see Fig. 8).

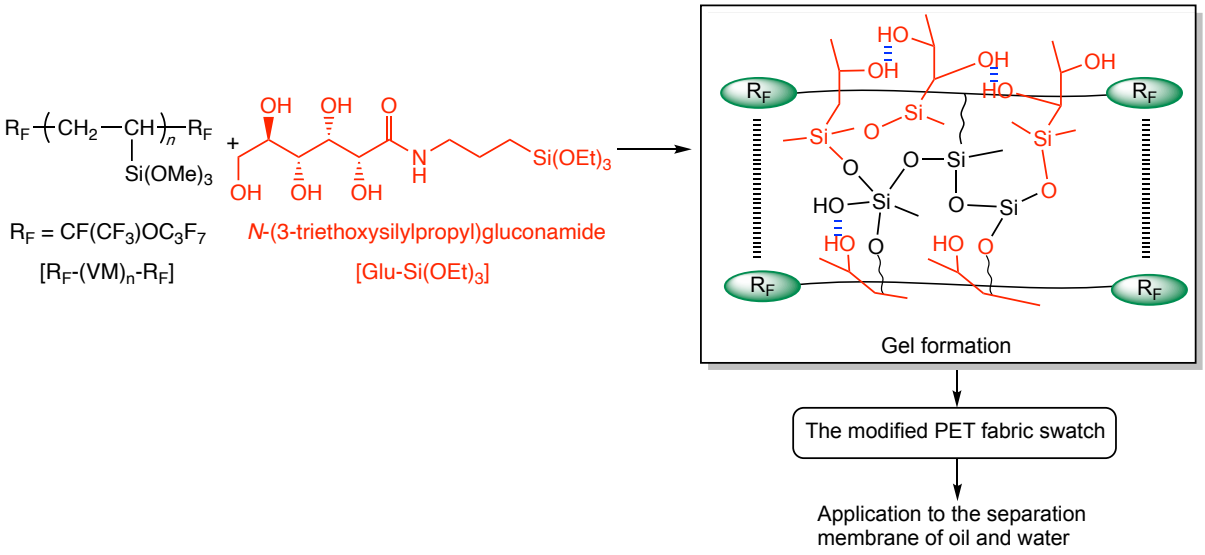

Fig. 8 Schematic illustration for the gel formation of R_F-(VM-SiO_2)$_n$-R_F/Glu-SiO_2 nanocomposites

It is also demonstrated that the modified surfaces treated with these obtained nanocomposites provide the unique wettabilities such as highly oleophobic/superhydrophobic, highly oleophobic/superhydrophilic, and superoleophilic/superhydrophobic characteristics.

Chapter 5 shows that fluoroalkyl end-capped 2-acrylamido-2-methylpropanesulfonic acid oligomer [R_F-(AMPS)$_n$-R_F] can react with poly(vinyl alcohol) [PVA] to supply the corresponding R_F-(AMPS)$_n$-R_F/PVA composite gels. In addition, it is demonstrated that the transparent colorless R_F-(AMPS)$_n$-R_F/PVA composite films are prepared by casting the homogeneous aqueous methanol sol solutions containing the corresponding fluorinated oligomeric composites (see Fig. 9). Moreover, mechanical properties and the water-adsorption ability of these films are superior to those of the original PVA film, which

was prepared under acidic conditions.

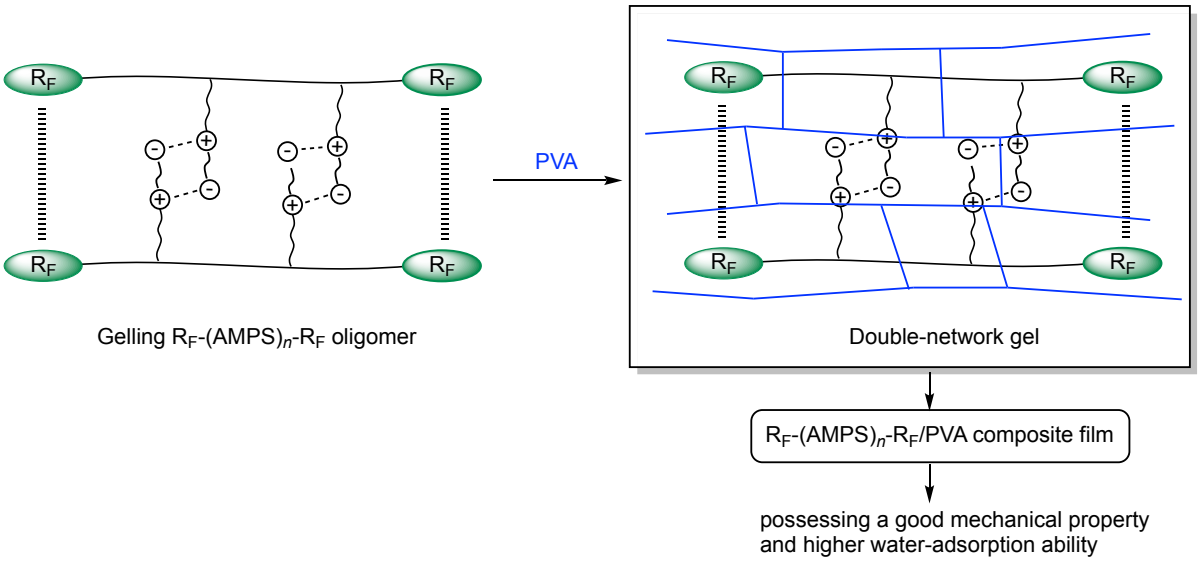

Fig. 9 Schematic illustration for the double-network gel formation of R_F-(AMPS)$_n$-R_F/PVA composites

In this way, gelling characteristic of R_F-(AMPS)$_n$-R_F oligomers (see Fig. 5) is applicable to the composite reactions with poly(vinyl alcohol), providing new R_F-(AMPS)$_n$-R_F/PVA composites possessing double-network gelling ability illustrated in Fig. 9. These findings are demonstrated in detail in Chapter 5. In addition, gelling ability of R_F-(NAT)$_n$-R_F oligomers, R_F-(MHPTS)$_n$-R_F oligomers, and R_F-(HOPPA)$_n$-R_F oligomers related to the hydroxy segments (see Figs. 6 and 7) is applicable to new gelling fluorinated nanocomposites through the sol-gel reaction of R_F-(VM)$_n$-R_F oligomer with Glu-Si(OEt)$_3$ illustrated in Fig. 8, and the evaluation of the membrane separability of hydrocarbon oil and fluorocarbon oil by using these obtained nanocomposites is detailed in Chapter 4. Their outline is also demonstrated in the following Fig. 10.

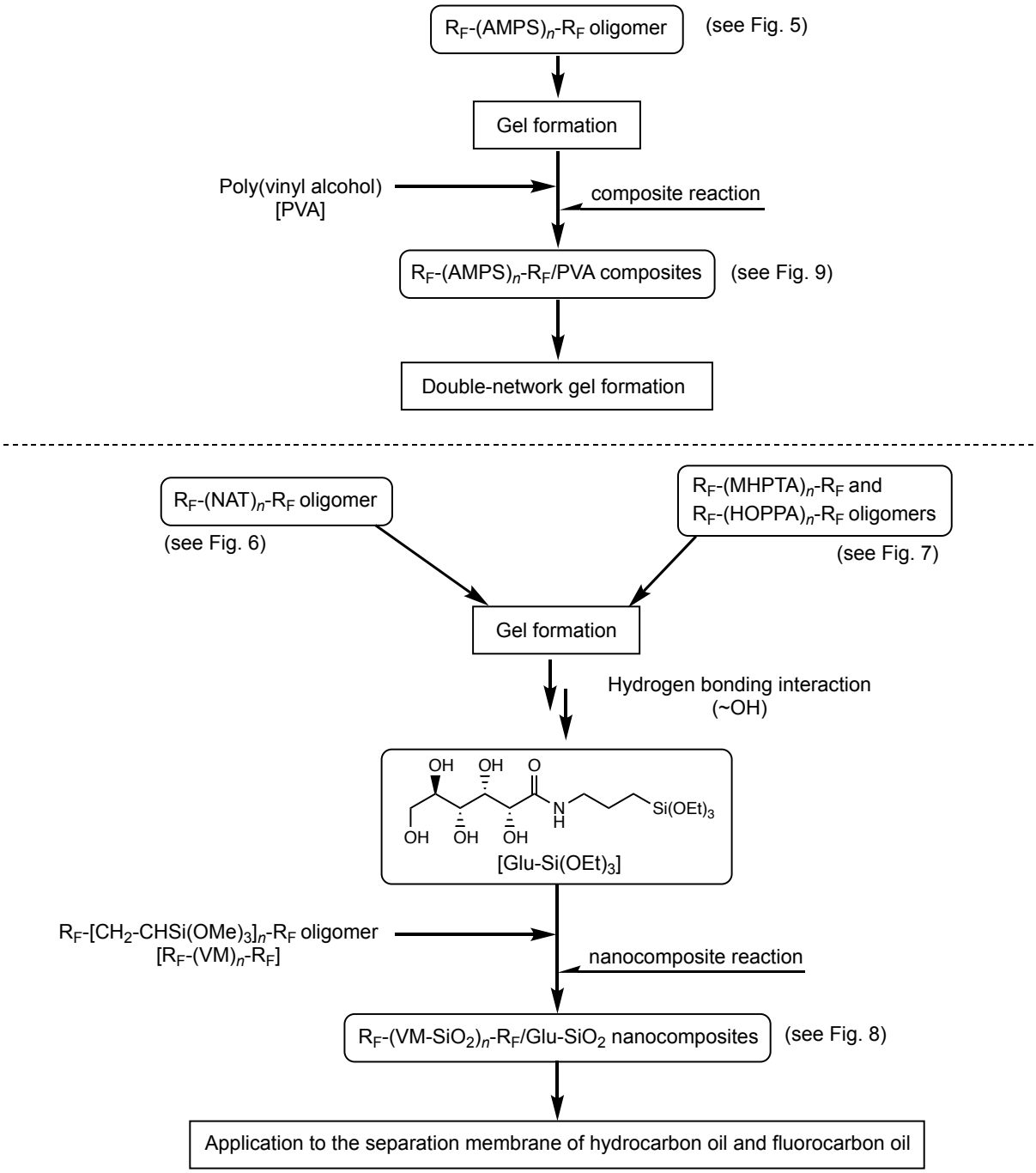

Fig. 10 Schematic outline of R_F-(AMPS)$_n$-R_F/PVA composite gels and R_F-(VM-SiO$_2$)$_n$-R_F/Glu-SiO$_2$ nanocomposite gels

References

1) Editorial Committee of Kobunshi-jiten, *Kobunshi-jiten (Dictionary of Polymer)*, ed. by the Polymer Society of Japan, Asakura, Tokyo, 1988, p. 129.

2) S. H. Gulrez, S. Al-Assaf, and G.-O. Phillips, *Hydrogels: Methods of Preparation, Characterisation and Applications*, A. Carpi (Ed.), Progress in Molecular and Environmental Bioengineering – From Analysis and Modeling to Technology Applications, 2011, IntechOpen, London, p117.

3) K. Hanabusa, *Materials Life,* **12**, 193 (2000).

4) H. Shigemitsu and I. Hamachi, *Acc. Chem. Res.,* **50**, 740 (2017).

5) A. Noro, M. Hayashi, and Y. Matsushita, *Soft Mater.*, **8**, 6416 (2012).

6) K. Hanabusa and M. Suzuki, *Polym. J.*, **46**, 776 (2014).

7) E. A. Appel, J. del Barrio, X.J. Loh, and O.A. Scherman, *Chem. Soc. Rev.*, **41**, 6195 (2012).

8) M. J. Webber, E.A. Appel, E.W. Meijer, and R. Langer, *Nat. Mater.*, **15**, 13 (2016).

9) K. Yasuda, J.-P. Gong, Y. Katsuyama, A. Nakayama, Y. Tanabe, E. Kondo, M. Ueno, and Y. Osada, *Biomaterials*, **26**, 4468 (2005).

10) K. Yasuda, N. Kitamura, J.-P. Gong, K. Arakaki, H. J. Kwon, S. Onodera, Y. M. Chen, T. Kurokawa, F. Kanaya, Y. Ohmiya, and Y. Osada, *Macromol Biosci.*, **9**, 307 (2009).

11) H. Yin, T. Akasaki, T.-L. Sun, T. Nakajima, T. Kurokawa, T. Nonoyama, T. Taira, Y. Saruwatari, and J.-P. Gong, *J. Mater. Chem. B*, **1**, 3685 (2013).

12) T.-L. Sun, T. Kurokawa, S. Kuroda, A.B. Ihsan, T. Akasaki, K. Sato, M.A. Haque, T. Nakajima, and J.-P. Gong, *Nat. Mater.*, **12**, 932 (2013).

13) H. C. Fielding, Organofluorine Chemicals and Their Industrial Applications", ed. by R. E. Banks, Ellis Horwood Ltd., London (1979) p. 214.

14) N. Ishikawa, *Yukagaku,* **26,** 613 (1977).

15) M. Inoue, *Farumashia,* **50**, 14 (2014).

16) M. Yamanaka, K. Sada, M. Miyata, K. Hanabusa, and K. Nakano, *Chem. Commun.,* 2248 (2006).

17) T. Yoshida, T. Hirakawa, T. Nakamura, Y. Yamada, H. Tatsuno, M. Hirai, Y. Morita, and H. Okamoto, *Bull. Chem. Soc. Jpn*., **88**, 1447 (2015).

18) T. Shimasaki, Y. Ohno, M. Tanaka, M. Amano, Y. Sasaki, H. Shibata, M. Watanabe, N. Teramoto, and M. Shibata, *Bull. Chem. Soc. Jpn*., **92**, 97 (2019).

19) H. Miyajima, M. C. Z. Kasuya, and K. Hatanaka, *J. Fluorine Chem.,* **222-223**, 24 (2019).

20) K. Johns and G. Stead, *J. Fluorine Chem.*, **104**, 5 (2000).

21) G. W. Tyndall and P. B. Leezenberg, *Tribol. Lett.*, **4**, 103 (1998).

22) H. I. Rowan, *Engineered Materials Handbook*, **2**, 115 (1988).

23) J. W. Cho, H. Y. Song, and S. Y. Kim, *Polymer,* **34**, 1024 (1993).

24) Y. Koda, T. Terashima, A. Nomura, M. Ouchi, and M. Sawamoto, *Macromolecules*, **44**, 4574 (2011).

25) G. G. Hougham, P. E. Cassidy, K. Johns, and T. Davidson, Ed., "*Fluoropolymers 2: Properties*", Kluwer Academic/ Plenum Publishers, New York (1999).

26) K. M. Choi and J. W. Stansbury, *Chem. Mater.*, **8**, 2704 (1996).

27) E. T. Kang and Y. Zhang, *Adv. Mater.*, **12**, 1481 (2000).

28) P. Smith and K. H. Gardner, *Macromolecules*, **18**, 1222 (1985).

29) Z.-Y. Yang, A. E. Feiring, and B. E. Smart, *J. Am.Chem. Soc.,* **116**, 4135 (1994).

30) H. Miyake and T. Takakura, *Fluororesin. In Development of Fluoro Functional Materials*, M. Yamada and M. Matsuo (Eds), CMC, Tokyo, 1997, p. 46.

31) H. Sawada; Y.-F. Gong, Y. Minoshima, T. Matsumoto, M. Nakayama, M. Kosugi, and T. Migita, *J. Chem. Soc., Chem. Commun*., 537, (1992).

32) H. Sawada, Y. Minoshima, and H. Nakajima, *J. Fluorine Chem.,* **65**, 169 (1993).

33) H. Sawada, N. Itoh, T. Kawase, M. Mitani, H. Nakajima, M. Nishida, and M. Moriya, *Langmuir,* **10**, 994 (1994).

34) H. Sawada, K. Tanba, N. Itoh, C. Hosoi, M. Oue, M. Baba, T. Kawase, M. Mitani, and H. Nakajima, *J. Fluorine Chem.*, **77**, 51 (1996).

35) J. Nakagawa, K. Kamogawa, H. Sakai, T. Kawase, H. Sawada, J. Manosroi, A. Manosroi, and M. Abe, *Langmuir,* **14**, 2055 (1998).

36) J. Nakagawa, K. Kamogawa, N. Momozawa, H. Sakai, T. Kawase, H. Sawada, Y. Sano, and M. Abe, *Langmuir,* **14**, 2061 (1998).

CHAPTER 1

Fluorinated Functional Materials Possessing Biological Activities: Gel Formation of Novel Fluoroalkylated End-Capped 2-Acrylamido-2-methylpropanesulfonic Acid Oligomers Under Non-Crosslinked Conditions

1.1 Introduction

Fluorinated polymeric materials exhibit numerous excellent properties which cannot be achieved by the corresponding non-fluorinated materials. However, in general they are very poorly soluble in various solvents.[1 ~ 4)] Therefore, it is interesting to search for highly soluble fluorinated polymeric materials with excellent properties imparted by fluorine. Recently, it has been reported that a series of fluoroalkylated end-capped silicon co-oligomers containing carboxy groups, which are prepared by using fluoroalkanoyl peroxides as key intermediates, are highly soluble in various solvents, and are effective in reducing the surface tension of these solvents.[5, 6)] These fluorosilicon co-oligomers were also found to be potent and selective inhibitors against HIV-1 (human immunodeficiency virus type 1) replication *in vitro*.[5, 6)] Furthermore, fluoroalkylated end-capped oligomers containing trimethylammonium segments[7)] or sulfo segments[8)] can be also synthesized by using fluoroalkanoyl peroxide as a key intermadiate. These fluoroalkylated oligomers containing trimethylammonium or sulfo segments exhibited not only unique properties imparted by fluorine but also biological activities, although they have only two fluoroalkylated end-caps.[7, 8)] Partially fluoroalkylated polymers were prepared by a variety of anionic polymerizations[9 ~ 12)] and a fluoroalkylated end-capped moiety was introduced through the ester bond[13 ~ 15)] to perfluoroalkyl-terminated polymers, and

the interesting properties of these polymers have been reported.

In view of the development of new fluoroalkylated end-capped polymeric materials, it is very interesting to explore the fluoroalkylated end-capped oligomers containing both cationic and anionic segments by using fluoroalkanoyl peroxides. Hitherto, the synthesis of non-fluorinated zwitterionic (betaine-type) polysoaps has been reported by Laschewsky and Zerbe;[16] however, there has been so far no report on the synthesis of fluoroalkylated end-capped betaine-type oligomers. From the developmental view point of novel fluoroalkylated betaine-type oligomers, it is of particular interest to synthesize novel fluoroalkylated end-capped 2-acrylamido-2-methylpropanesulfonic acid oligomer. This chapter shows the synthesis and gel formation of fluoroalkylated end-capped 2-acrylamido-2-methylpropanesulfonic acid oligomers, with emphasis on an application to new fluorinated gelling functional materials possessing biological activities.

1.2 Experimental

1.2.1 Measurements

NMR spectra were measured using a Varian Unity-plus 500 (500 MHz) spectrometer, while IR spectra were recorded on a HORIBA FT-300 FT-IR spectrophotometer. Molecular weights were calculated by using a JASCO-PU-980-Shodex-SE-11 gel permeation chromatography calibrated with standard poly (ethylene glycol) by using 0.5 mol dm^{-3} Na_2HPO_4 solution as the eluent. Absorption spectra were recorded on a Shimadzu UV-240 spectrophotometer. Solution viscosities were measured by using a falling-sphere Haake Viscometer D1-G.

1.2.2 Materials

A series of fluoroalkanoyl peroxides [$(R_FCOO)_2$] and a polymeric perfluoro-oxaalkane diacyl peroxide were prepared by the method described in the literature.[17 ~ 20] 2-Acrylamido-2-methylpropanesulfonic acid was purchased from Tokyo Kasei Kogyo Co., Ltd. Trimethylvinylsilane was purchased from Shin-Etsu Co., Ltd. Chromium(III) nitrate and cobalt(II) chloride were purchased from Wako Chemicals.

1.2.3 General procedure for the synthesis of fluoroalkylated end-capped AMPS oligomers

Perfluorobutyryl peroxide (3 mmol) in a 1:1 mixture (AK-225) of 1,1-dichloro-2,2,3,3,3-pentafluoropropane and 1,3-dichloro-1,2,2,3,3-pentafluoropropane (110 g) was added to an aqueous solution (50 %, w/w) of AMPS (9 mmol). The heterogeneous mixture was stirred vigorously at 40 ºC for 5 h under nitrogen. After evaporation of the solvent, the crude product obtained was reprecipitated from water-tetrahydrofuran to give an α,ω-bis(perfluoropropylated) 2-acrylamido-2-methylpropanesulfonic acid oligomer (1.13 g).

This oligomer exhibited the following spectral characteristics: IR ν (cm^{-1}) 3448 (OH, NH), 1641 [C(=O)N^+H_2-], 1310 (CF_3), 1259 (SO_3^-), 1228 (CF_2), 1101 (SO_3^-); ^{1}H NMR (D_2O) δ 1.51 ~ 2.12 (CH_2), 1.60 (CH_3), 2.29 ~ 2.71 (CH), 3.65 ~ 4.22 (CH_2); ^{19}F NMR (D_2O, ext. CF_3CO_2H) δ -3.45 (6F), -40.60 (4F), -50.20 (4F).

The other products obtained exhibited the following spectral characteristics.

R_F-(AMPS)$_n$-R_F [R_F = $CF(CF_3)OC_3F_7$]:

IR ν (cm^{-1}) 3469 (OH, NH), 1647 [C(=O)N^+H_2-], 1304 (CF_3), 1228 (CF_2); ^{1}H NMR (D_2O) δ 1.49 ~ 2.11 (CH_2), 1.60 (CH_3), 2.31 ~ 2.69 (CH), 3.61 ~ 4.15 (CH_2); ^{19}F NMR (D_2O, ext. CF_3CO_2H) δ -1.56 to -5.10 (16F), -48.00 (4F).

R_F-(AMPS)$_n$-R_F [R_F = $CF(CF_3)OCF_2CF(CF_3)OC_3F_7$]:

IR ν (cm^{-1}) 3370 (OH, NH), 1647 [$C(=O)N^+H_2$-], 1303 (CF_3), 1255 (SO_3^-), 1226 (CF_2), 1101 (SO_3^-); ^{1}H NMR (D_2O) δ 1.38 ~ 1.83 (CH_2), 1.53 (CH_3), 1.97 ~ 2.30 (CH), 3.19 ~ 3.57 (CH_2); ^{19}F NMR (D_2O, ext. CF_3CO_2H) δ -4.42 to -8.42 (26F), -54.0 to -56.26 (6F); -66.78 (2F).

R_F-(AMPS)$_n$-R_F [R_F = $CF(CF_3)OCF_2CF(CF_3)OCF_2CF(CF_3)OC_3F_7$]:

IR ν (cm^{-1}) 3465 (OH, NH), 1641 [$C(=O)N^+H_2$-], 1238 (CF_2); ^{1}H NMR (D_2O) δ 1.51 ~ 2.12 (CH_2), 1.54 (CH_3), 2.35 ~ 2.71(CH), 3.65 ~ 4.17 (CH_2); ^{19}F NMR (D_2O, ext. CF_3CO_2H) δ -0.98 to -5.50 (36F), -49.10 (6F), -69.10 (4F).

Similarly, a series of fluoroalkylated end-capped AMPS co-oligomers were prepared by co-oligomerizations with fluoroalkanoyl peroxides. These exhibited the following spectral characteristics.

R_F-(AMPS)$_x$-($CH_2CHSiMe_3$)$_y$-R_F [R_F = C_3F_7]:

IR ν (cm^{-1}) 3409 (OH, NH), 1649 [$C(=O)N^+H_2$-], 1304 (CF_3), 1227 (CF_2); ^{1}H NMR (D_2O) δ -0.20 ~ 0.46 (CH_3), 1.51 ~ 2.12 (CH_2), 1.54 (CH_3), 2.29 ~ 2.71(CH), 3.65 ~ 4.22 (CH_2); ^{19}F NMR (D_2O, ext. CF_3CO_2H) δ -3.50 (6F), -40.60 (4F), -50.20 (4F).

R_F-(AMPS)$_x$-($CH_2CHSiMe_3$)$_y$-R_F [R_F = $CF(CF_3)OC_3F_7$]:

IR ν (cm^{-1}) 3453 (OH, NH), 1645 [$C(=O)N^+H_2$-], 1304 (CF_3), 1232 (CF_2); ^{1}H NMR (D_2O) δ -0.23 ~ 0.36 (CH_3), 1.49 ~ 2.11 (CH_2), 1.54 (CH_3), 2.31 ~ 2.69 (CH), 3.61 ~ 4.15 (CH_2); ^{19}F

NMR (D_2O, ext. CF_3CO_2H) δ -1.58 to -5.12 (16F), -48.00 (4F).

R_F-(AMPS)$_x$-($CH_2CHSiMe_3$)$_y$-R_F [R_F = $CF(CF_3)OCF_2CF(CF_3)OC_3F_7$]:

IR ν (cm^{-1}) 1647 [C(=O)N^+H_2-], 1227 (CF_2); ^{1}H NMR (D_2O) δ -0.18 ~ 0.33 (CH_3), 1.61 ~ 2.31 (CH_2), 1.44 (CH_3); 2.33 ~ 2.72 (CH), 3.59 ~ 4.08 (CH_2); ^{19}F NMR (D_2O, ext. CF_3CO_2H) δ -3.64 to -7.10 (26F), -48.91 (6F), -67.48 (2F).

R_F-(AMPS)$_x$-(CH_2CMeCO_2Me)$_y$-R_F [R_F = C_3F_7]:

IR ν (cm^{-1}) 3452 (OH, NH), 1641 [C(=O)N^+H_2-], 1228 (CF_2); ^{1}H NMR (D_2O) δ 1.51 ~ 2.13 (CH_2, CH_3), 2.29 ~ 2.58(CH), 3.65 ~ 4.20 (CH_2, CH_3); ^{19}F NMR (D_2O, ext. CF_3CO_2H) δ -3.50 (6F), -40.65 (4F), -50.20 (4F).

R_F-(AMPS)$_x$-(CH_2CMeCO_2Me)$_y$-R_F [R_F = $CF(CF_3)OC_3F_7$]:

IR ν (cm^{-1}) 1645 [C(=O)N^+H_2-], 1315 (CF_3), 1238 (CF_2); ^{1}H NMR (D_2O) δ 1.49 ~ 2.11 (CH_2, CH_3), 2.33 ~ 2.70 (CH), 3.60 ~ 4.15 (CH_2, CH_3); ^{19}F NMR (D_2O, ext. CF_3CO_2H) δ -1.62 to -5.00 (16F), -48.30 (4F).

R_F-(AMPS)$_x$-(CH_2CMeCO_2Me)$_y$-R_F [R_F = $CF(CF_3)OCF_2CF(CF_3)OC_3F_7$]:

IR ν (cm^{-1}) 1642 [C(=O)N^+H_2-], 1236 (CF_2); ^{1}H NMR (D_2O) δ 1.52 ~ 2.26 (CH_2, CH_3), 2.33 ~ 2.78 (CH), 3.59 ~ 4.08 (CH_2, CH_3); ^{19}F NMR (D_2O, ext. CF_3CO_2H) δ -3.60 to -7.10 (26F), -48.96 (6F), -67.48 (2F).

Similarly, fluoroalkylene unit-containing AMPS polymer {-[R_F-(AMPS)$_q$]$_p$-} was

prepared by reaction of a polymeric perfluoro-oxaalkane diacyl peroxide with AMPS. This exhibited the following spectral characteristics.

-[CF(CF$_3$)[OCF$_2$CF(CF$_3$)]$_n$O(CF$_2$)$_5$O-[CF(CF$_3$)CF$_2$O]$_m$-CF(CF$_3$)-(AMPS)$_q$]$_p$-; n + m = 3:

IR ν (cm^{-1}) 3492 (OH, NH), 1643 [C(=O)N$^+$H$_2$-], 1226 (CF$_2$); ^{1}H NMR (D$_2$O) δ 0.82 ~ 1.80 (CH$_2$), 1.35 (CH$_3$), 1.82 ~ 2.23 (CH), 2.97 ~ 3.76 (CH$_2$); ^{19}F NMR (D$_2$O, ext. CF$_3$CO$_2$H) δ -5.06 to -10.70 (21F), -48.24 (2F), -51.38 (10F), -71.11 (3F).

1.2.4 Viscosity measurements

The viscosities of aqueous solutions of fluoroalkylated AMPS oligomers were measured at 5 ~ 50 °C using a falling-sphere viscometer (Haake Viscometer D1-G).

1.2.5 A typical procedure for gelation test

A procedure for studying the gel-formation ability was based on a method reported by Hanabusa *et al.*[21, 22] Briefly, weighed fluoroalkylated end-capped AMPS oligomer was mixed with water or organic fluid in a tube. The mixture was treated under ultrasonic conditions until the solid dissolved. The resulting solution was kept at 30 °C for 1 h, and then the gelation was assessed visually. When it was formed, the gel was stable and the tube was able to be inverted without changing the shape of the gel.

1.2.6 Metal ions binding by fluorinated AMPS oligomer hydrogel

Fluoroalkylated end-capped AMPS co-oligomer hydrogels was swelled with water in a measuring flask. After the addition of the required amount of aqueous metal ion solution into the flask, the flask was allowed to stand for 1 day at 25 ℃. The metal-ion concentration of supernatant liquid after the incubation was spectrophotometrically determined..

1.2.7 Antiviral assays

Antiviral activity of the compounds against HIV-1 (HTLB−IIIb starin) replication was based on the inhibition of the virus-induced cytopathic effect in MT−4 cells as described previously.[23)]

1.2.8 Antibacterial assessment

The antibacterial activity of the oligomers was evaluated against *Staphylococcus aureus* by a viable cell counting method as described previously.[7)]

1.3 Results and discussion

The reactions of fluoroalkanoyl peroxides with 2-acrylamido-2-methylpropanesulfonic acid (AMPS) were carried out in heterogeneous solvent systems [AK-225 (mixed solvents of 1,1-dichloro-2,2,3,3,3-pentafluoropropane and 1,3-dichloro-1,2,2,3,3-pentafluoropropane) and water] by stirring vigorously at 40 ºC for 5h under nitrogen. The process is outlined in Scheme 1-1.

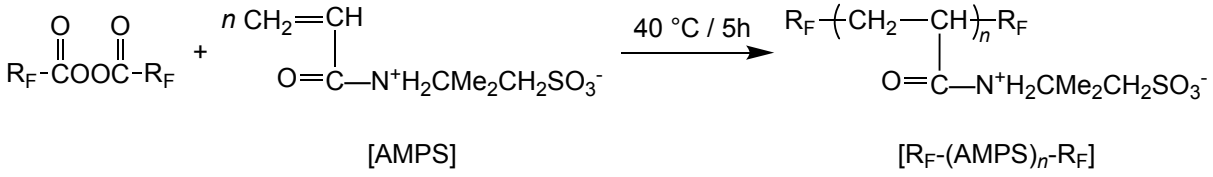

R_F = C_3F_7, $CF(CF_3)[OCF_2CF(CF_3)]_mOC_3F_7$; m = 0, 1, 2

Scheme 1-1 Synthesis of R_F-(AMPS)$_n$-R_F homo-oligomers at 40 ºC for 5 h

AMPS was found to react with fluoroalkanoyl peroxides under mild conditions to afford fluoroalkylated end-capped AMPS homo-oligomers [R_F-(AMPS)$_n$-R_F] in 35 ~ 58 % isolated yields as shown in Table 1-1.

Table 1-1 Homo- and co-oligomerizations of AMPS with fluoroalkanoyl peroxides

R_F in peroxide	AMPS	comonomer	Product		
/ mmol	/ mmol	/ mmol	Yield / %[a]	$\overline{M}$n ($\overline{M}$w/$\overline{M}$n)[b]	x : y [c]
C_3F_7			R_F-(AMPS)$_n$-R_F		
3	9	—	39	24500 (28)	—
$CF(CF_3)OC_3F_7$			R_F-(AMPS)$_n$-R_F		
3	9	—	58	20500 (131)	—
$CF(CF_3)OCF_2CF(CF_3)OC_3F_7$			R_F-(AMPS)$_n$-R_F		
3	9	—	38	12000 (282)	—
$CF(CF_3)OCF_2CF(CF_3)OCF_2CF(CF_3)OC_3F_7$			R_F-(AMPS)$_n$-R_F		
2	6	—	35	24000 (76)	—
C_3F_7		CH_2=CHSiMe$_3$	R_F-(AMPS)$_x$-($CH_2CHSiMe_3$)$_y$-R_F		
3	9	9	57	11000 (291)	90 : 10
$CF(CF_3)OC_3F_7$		CH_2=CHSiMe$_3$	R_F-(AMPS)$_x$-($CH_2CHSiMe_3$)$_y$-R_F		
3	9	9	38	10000 (400)	78 : 22
$CF(CF_3)OCF_2CF(CF_3)OC_3F_7$		CH_2=CHSiMe$_3$	R_F-(AMPS)$_x$-($CH_2CHSiMe_3$)$_y$-R_F		
3	9	9	30	17400 (166)	98 : 2
C_3F_7		CH_2=$CMeCO_2Me$	R_F-(AMPS)$_x$-(CH_2CMeCO_2Me)$_y$-R_F		
3	9	9	52	11300 (216)	93 : 7
$CF(CF_3)OC_3F_7$		CH_2=$CMeCO_2Me$	R_F-(AMPS)$_x$-(CH_2CMeCO_2Me)$_y$-R_F		
3	9	9	41	14300 (211)	94 : 6
$CF(CF_3)OCF_2CF(CF_3)OC_3F_7$		CH_2=$CMeCO_2Me$	R_F-(AMPS)$_x$-(CH_2CMeCO_2Me)$_y$-R_F		
3	9	9	41	8300 (726)	92 : 8

a) The yields are based on starting materials [AMPS, Co-monomers and the decarboxylated peroxide unit (R_F-R_F).
b) The molecular weight of each polymer was determind by GPC; however, it is suggested that the obtained values by GPC indicate the apparent molecular weights owing to the strong aggregations of fluoroalkyl segments in aqueous solutions.
c) Copolymerization ratio was determined by ^{1}H NMR analysis.

Similarly, in the co-oligomerization of AMPS with fluoroalkanoyl peroxides, a series of fluoroalkylated end-capped AMPS co-oligomers were obtained in 30 ~ 57 % isolated yields by using comonomers such as trimethylvinylsilane and methyl methacrylate as shown in the

following Scheme 1-2 and Table 1-1.

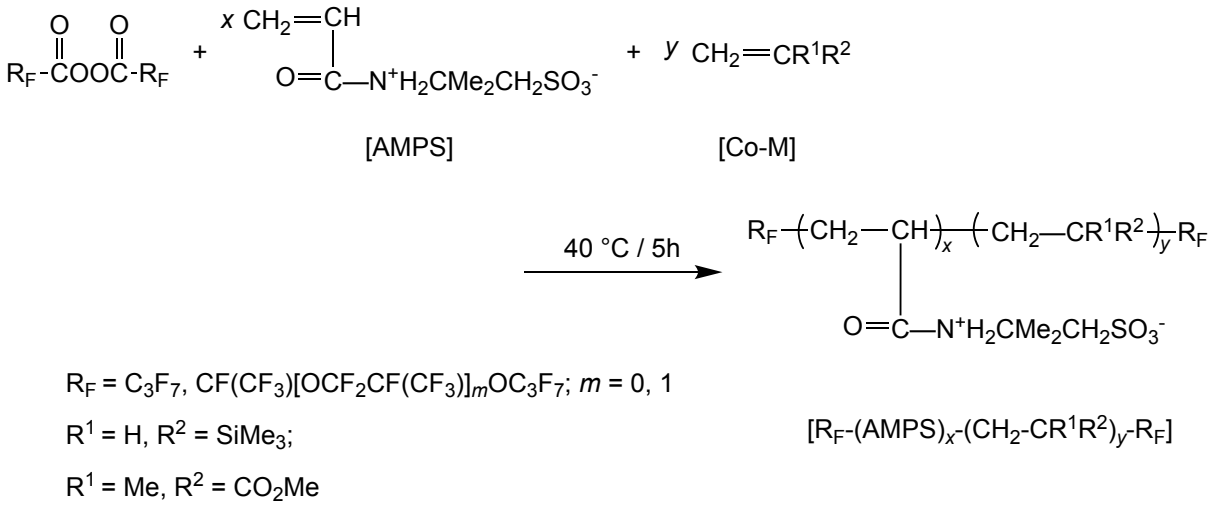

R_F = C_3F_7, $CF(CF_3)[OCF_2CF(CF_3)]_mOC_3F_7$; m = 0, 1

R^1 = H, R^2 = $SiMe_3$;

R^1 = Me, R^2 = CO_2Me

Scheme 1-2 Synthesis of R_F-$(AMPS)_x$-$(CH_2CR^1R^2)$-R_F co-oligomers

As shown in Table 1-1, not only perfluoropropylated but also a series of perfluoro-oxaalkylated end-capped homo- and co-oligomers were obtained under mild conditions, and the co-oligomerization ratios of these oligomers were determined by ^{1}H NMR analyses. Under the oligomerization conditions, in which the concentration of the peroxide was almost the same as that of AMPS (trimethylvinylsilane or methyl methacrylate) as shown in Table 1-1, mainly oligomers with two fluoroalkylated end-groups would be obtained via primary radical termination or radical chain transfer to the peroxide. In fact, two fluoroalkylated end-capped acrylic acid oligomers [R_F-$(CH_2CHCO_2H)_n$-R_F] can be obtained by the reactions of

fluoroalkanoyl peroxides with acrylic acid under similar conditions.[24, 25)]

The molecular weights ($\overline{Mn}$) of these oligomers measured by GPC [gel permeation chromatography calibrated with standard poly(ethylene glycol) by using 0.5 mol dm^{-3} Na_2HPO_4 solution as the eluent] were relatively high (8300 ~ 24500). Considering the fact that water-soluble fluoroalkylated end-capped oligomers containing trimethylammonium and sulfo segments easily form molecular aggregates in aqueous solutions,[7, 8)] this finding suggests that the GPC values indicate the apparent molecular weights. Interestingly, the $\overline{Mw}/\overline{Mn}$ values of these fluoroalkylated oligomers are extremely high (28 ~ 726) compared to that of the corresponding non-fluorinated oligomer [-$(AMPS)_n$-: $\overline{Mn}$ = 5400 ($\overline{Mw}/\overline{Mn}$ = 3.25)], which was prepared by using 2,2'-azobis (2-methylpropionamidine) dihydrochloride. This result also suggests that these fluoroalkylated AMPS oligomers form aggregates.

The fluoroalkylated AMPS oligomers were found to be easily soluble not only in water but also in polar organic solvents such as methanol, ethanol, *N,N*-dimethylformamide and dimethyl sulfoxide at under dilute conditions (below ca. 0.5 g dm^{-3}). In order to clarify the solution properties of the fluoroalkylated oligomers, the viscosity of an aqueous solution of fluoroalkylated AMPS oligomer [C_3F_7- $(AMPS)_n$-C_3F_7] was measured under dilute conditions (0.1 g dm^{-3}), and the viscosities of aqueous solutions of perfluoropropylated oligomers containing trimethylammonium segments [C_3F_7-$(AETM)_n$-C_3F_7] and non-fluorinated AMPS

oligomer [-(AMPS)$_n$-] were also measured under similar conditions for comparison. These results are shown in Fig. 1-1.

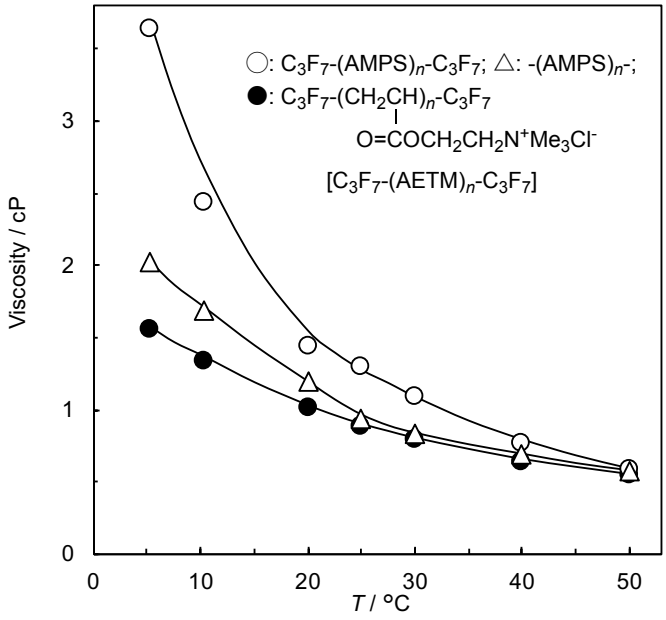

Fig. 1-1 Effect of temperature on viscosity of aqueous oligomer solutions

As shown in Fig. 1-1, the viscosity of an aqueous solution of C_3F_7-(AMPS)$_n$-C_3F_7 at 5 ºC was higher than that of C_3F_7-(AETM)$_n$-C_3F_7 and -(AMPS)$_n$- under dilute conditions (0.1 g dm^{-3}). On the other hand, the viscosities of C_3F_7-(AMPS)$_n$-C_3F_7 including both C_3F_7-(AETM)$_n$-C_3F_7 and -(AMPS)$_n$- were also found to decrease on heating the solutions from 5 ~ 50 ºC.

However, surprisingly, at concentrations above 1.0 g dm^{-3} all fluoroalkylated end-capped AMPS oligomer-solvent systems formed gels. To study this unique gelation, the viscosity of

aqueous solutions of these fluoroalkylated end-capped oligomers was measured at 30 ºC. The results are shown in Fig. 1-2.

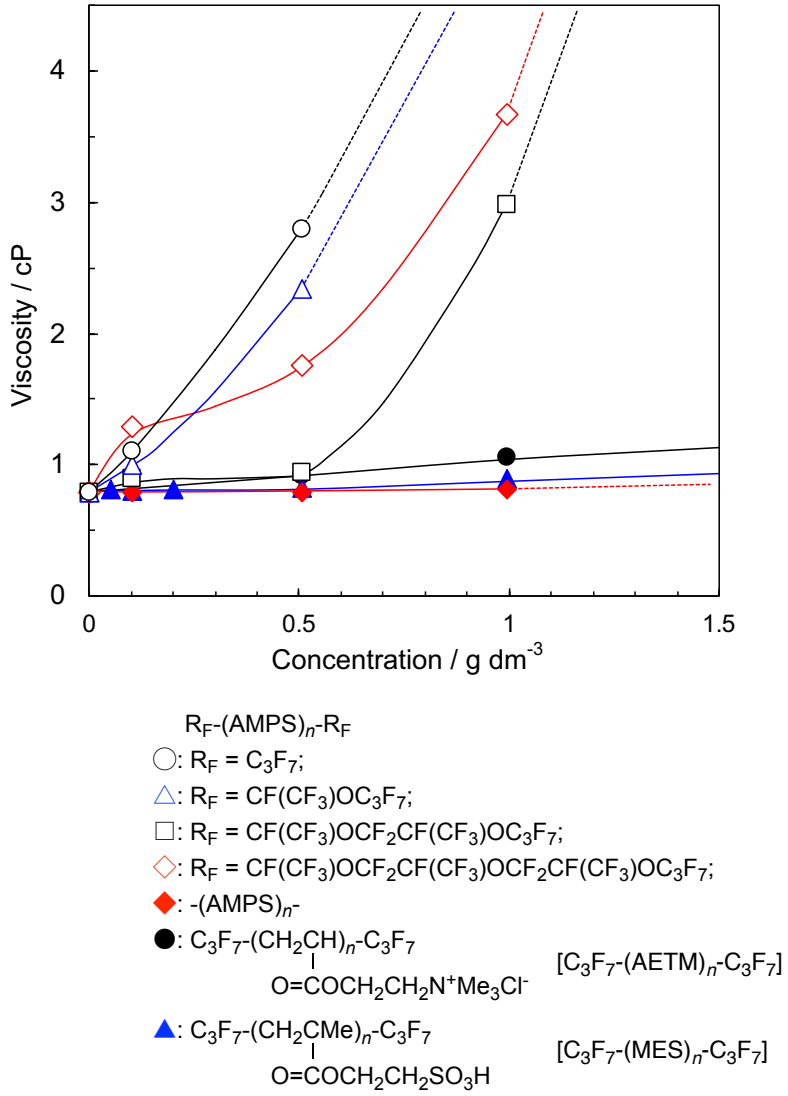

Fig. 1-2 Effect of concentration on viscosity of fluoroalkylated end-capped oligomer measured at 30 ºC by using a falling-sphere viscometer

As shown in Fig. 1-2, the viscosities of -(AMPS)$_n$-, C_3F_7-(AETM)$_n$-C_3F_7 and perfluoropropylated oligomer containing sulfo segments [C_3F_7-(MES)$_n$-C_3F_7] increased little with increasing concentrations, and the gel did not form, although these fluoroalkylated oligomers were shown to form molecular aggregates like micelles in aqueous solutions.[3,4] On the other hand, the viscosity of the fluoroalkylated end-capped AMPS oligomers increased greatly with increasing concentration, and it became impossible to measure their viscosity owing to the gelation at concentrations above 0.5 or 1.0 g dm^{-3}. The measurement of the melting temperature of the gel was tried; however, the gel did not melt either in water or in organic solvents even when it was heated to around 95 ºC. It is suggested that the fluoroalkylated end-capped AMPS oligomers could cause a gelation involving a strong aggregation of fluoroalkyl segments to a physical gel network in water, methanol, ethanol, *N,N*-dimethylformamide and dimethyl sulfoxide at higher concentrations. By contrast, non-fluorinated AMPS oligomer was completely soluble in these media, and no gel formed.

The gelation abilities of some fluoroalkylated end-capped AMPS oligomers were also studied by measuring the minimum concentrations of these oligomers necessary for gelation according to the method reported of Hanabusa *et al*.[21, 22, 26] The minimum concentrations for gelation (C_{min}) in water and dimethyl sulfoxide (DMSO) at 30 ºC are listed in Table 1-2.

Table 1-2 Minimum concentrations for gelation (C_{min}) of fluoroalkylated AMPS homo- and co-oligomers (in g dm^{-3} solvent) necessary for gelation at 30 ºC

oligomer	C_{min} / g dm^{-3} (gelator/medium)	
	water	DMSO
R_F-(AMPS)$_n$-R_F; R_F = C_3F_7	25	13
R_F-(AMPS)$_n$-R_F; R_F = $CF(CF_3)OCF_2CF(CF_3)OC_3F_7$	31	11
R_F-(AMPS)$_n$-R_F; R_F = $CF(CF_3)OCF_2CF(CF_3)OCF_2CF(CF_3)OC_3F_7$	33	21
R_F-(AMPS)$_x$-($CH_2CHSiMe_3$)$_y$-R_F; R_F = C_3F_7	6	6
R_F-(AMPS)$_x$-($CH_2CHSiMe_3$)$_y$-R_F; R_F = $CF(CF_3)OC_3F_7$	6	8
R_F-(AMPS)$_x$-($CH_2CHSiMe_3$)$_y$-R_F; R_F = $CF(CF_3)OCF_2CF(CF_3)OC_3F_7$	7	9
R_F-(AMPS)$_x$-(CH_2CMeCO_2Me)$_y$-R_F; R_F = C_3F_7	2	5
R_F-(AMPS)$_x$-(CH_2CMeCO_2Me)$_y$-R_F; R_F = $CF(CF_3)OC_3F_7$	5	7
R_F-(AMPS)$_x$-(CH_2CMeCO_2Me)$_y$-R_F; R_F = $CF(CF_3)OCF_2CF(CF_3)OC_3F_7$	9	5

As shown in Table 1-2, the gelling ability of fluoroalkylated end-capped co-oligomers is somewhat superior to that of the homo-oligomers, with C_{min} 2 ~ 9 g dm^{-3} for co-oligomers and 11 ~ 33 g dm^{-3} for homo-oligomers. This result is in fair agreement with the values of $\overline{Mw}/\overline{Mn}$ of oligomers in Table 1-1, and the more polydisperse oligomers exhibited the higher gelling ability. These findings would suggest that the co-oligomers are likely to promote the gelation sterically compared to the corresponding homo-oligomers.

These fluoroalkylated oligomers also exhibited a quite similar property to the common water-swollen crosslinked polymeric hydrogels. That is, these fluoroalkylated AMPS oligomers in water exhibited extremely high water adsorption, with the weight of adsorbed

water by fluoroalkylated gelling co-oligomers: C_3F_7-$(AMPS)_x$-$(CH_2CHSiMe_3)_y$-C_3F_7 and C_3F_7-$(AMPS)_x$-$(CH_2CMeCO_2Me)_y$-C_3F_7 201 and 213 times the weight of the dry gel, respectively. These values are similar to that of AMPS oligomer hydrogel prepared by radical polymerization of AMPS and *N,N'*-methylenebisacrylamide initiated by H_2O_2.[27)]

The striking characteristic of the AMPS oligomers is their gelation both in water and in organic polar solvents under non-crosslinking conditions. This is because fluoroalkyl segments are solvophobic and aggregate in aqueous and organic media. In fact, it was reported that the solvophobic fluorocarbon tails in fluorinated amphiphiles are responsible for the formation of stable bilayer membrances in water and organic solvents.[28 ~ 32)] Semifluorinated alkanes, such as $F(CF_2)_{10}(CH_2)_{12}H$, are also known to exhibit gel-like characteristics in hydrocarbon solvents [$H(CH_2)_pH$; p = 8, 10, 12, 14].[33)] Such aggregation of fluoroalkyl segments in these media should be enhanced due to the self-organization of oligomers which causes gelation in these media.

The AMPS oligomers can form gels in both water and organic media due to the synergistic interaction between the aggregations of fluoroalkyl units, and the ionic interactions of the amide cations and the sulfonate anions as shown in the following Schematic illustration.

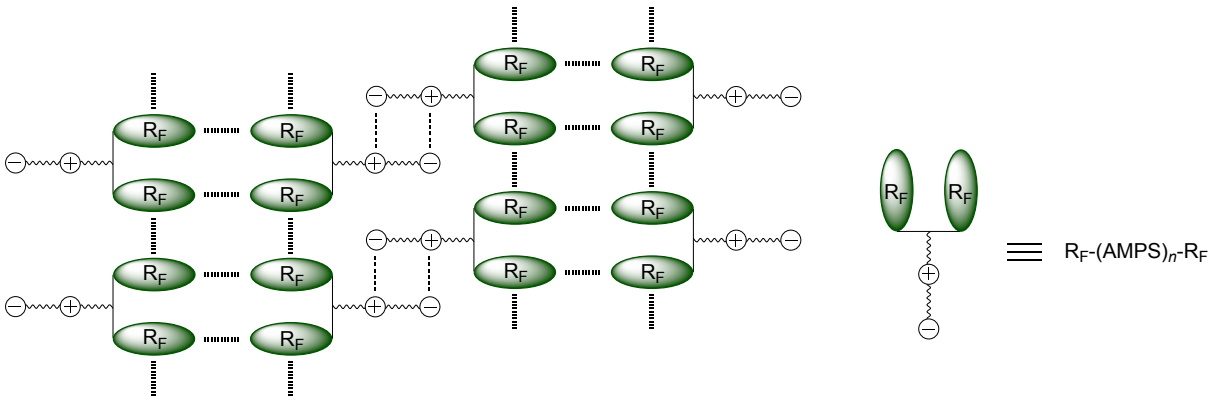

Fig. 1-3 Schematic illustration for gelation of R_F-(AMPS)$_n$-R_F

On the other hand, in the case of the corresponding non-fluorinated oligomer [-(AMPS)$_n$-], only the ionic interactions would operate and the gelation would not occur. Furthermore, in the case of C_3F_7-(AETM)$_n$-C_3F_7 or C_3F_7-(MES)$_n$-C_3F_7, only the aggregation of the end-capped fluoroalkyl segments would operate, owing to the electrostatic repulsion of cationic segments (AETM) or anionic segments (MES) between the central oligomer chains, and these oligomers could not form gels (see Fig. 1-2).

In general, it is well-known that acrylated and methacrylated polymers containing longer perfluoroalkyl groups are strongly repelled by water or hydrocarbons owing to the strong electronegativity of fluorine. In contrast, the characteristics of the present fluoroalkylated end-capped AMPS oligomers are to cause gelation under non-crosslinking conditions. This feature would be due to their unique structure (fluoroalkylated end-capped structure), and the

end-capped fluoroalkyl segments in oligomers could strongly aggregate rather than being repelled by aqueous or organic media. Therefore, it is suggested that AMPS oligomers containing fluoroalkylene units but no fluoroalkyl end-capped units, $\{[\text{-}R_F\text{-}(AMPS)_q]_p\text{-}\}$, could not gel since the interaction between the aggregation of internal fluoroalkylene units in the polymers should become weaker than that of the aggregation of end-capped fluoroalkyl units in oligomers. It was previously reported that a polymeric perfluoro-oxaalkane diacyl peroxide $\{[\text{-}(O{=}C)R_FC(=O)OO]_p\text{-}\}$ is a useful tool for the introduction of the perfluoro-oxaalkylene unit ($\text{-}R_F\text{-}$) into acrylic acid polymers.[17, 18] Thus, the synthesis of fluoroalkylene unit-containing AMPS polymers was tried by using a polymeric perfluoro-oxaalkane diacyl peroxide. The result is shown in Scheme 1-3.

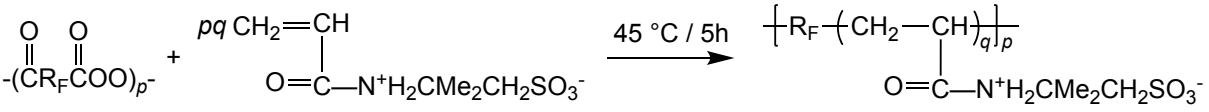

[AMPS]

2 mmol

0.2 mmol[a)]

-[R_F-(AMPS)$_q$]$_p$-

Yield: 45%[b)]

$\overline{M}$n($\overline{M}$w/$\overline{M}$n) = 120000 (1.46)

$\text{-}R_F\text{-}$ = $\text{-}CF(CF_3)[OCF_2CF(CF_3)]_nO(CF_2)_5O\text{-}[CF(CF_3)CF_2O]_mCF(CF_3)\text{-}$; $(n + m) = 3$

Scheme 1-3 Synthesis of the -[R_F-(AMPS)$_q$]$_p$-
a) Calculated on the basis of the peroxide monomer unit.
b) Yield based on AMPS and decarboxylated peroxide unit ($\text{-}R_F\text{-}$).

As shown in Scheme 1-3, the reaction of AMPS with a polymeric perfluoro-oxaalkane diacyl peroxide proceeded smoothly to give AMPS polymer containing perfluoro-oxaalkylene units {-[R_F-(AMPS)$_q$]$_p$-}. The AMPS polymer containing fluoroalkylene units thus obtained was found to be easily soluble not only in water but also in methanol, ethanol, *N*,*N*-dimethylformamide and dimethyl sulfoxide even at higher concentrations above 1.0 g dm^{-3}, and the gel could not form in any of these media. This finding suggests that the internal fluoroalkylene units in the polymer are not likely to aggregate sterically with each other compared to the end-capped fluoroalkyl units. Therefore, it is concluded that fluoroalkylated end-capped AMPS oligomers can cause gelation where strong aggregation of the end-capped fluoroalkyl segments is involved sterically in establishing the physical gel network in aqueous and organic media.

Hitherto, the synthesis of chemically-cross-linked AMPS polymer gels has been reported by Osada *et al*., and this polymer hydrogel crosslinked by *N*,*N*'-methylenebisacrylamide has a high adsorptive property towards various metal ions.[27] Therefore, it is interesting to study the adsorptive property towards metal ions on the swelling equilibrium of the fluoroalkylated end-capped AMPS oligomer hydrogel.

The swelling equilibrium of R_F-(AMPS)$_x$-(CH_2CMeCO_2Me)$_y$-R_F [R_F = $CF(CF_3)OCF_2CF(CF_3)OC_3F_7$] hydrogel was studied in aqueous solutions of metal ions (Cr^{3+}

and Co^{2+}). The metal-ion concentrations of the supernatant liquid after incubation (at 25 °C for 24 h) was spectrophotometrically determined from absorbance at 580 nm (Cr^{3+}) or 510 nm (Co^{2+}). The binding of the metal ions by this fluorinated gel was studied for a wide range of metal-ion concentrations, and the results are shown in Fig. 1-4.

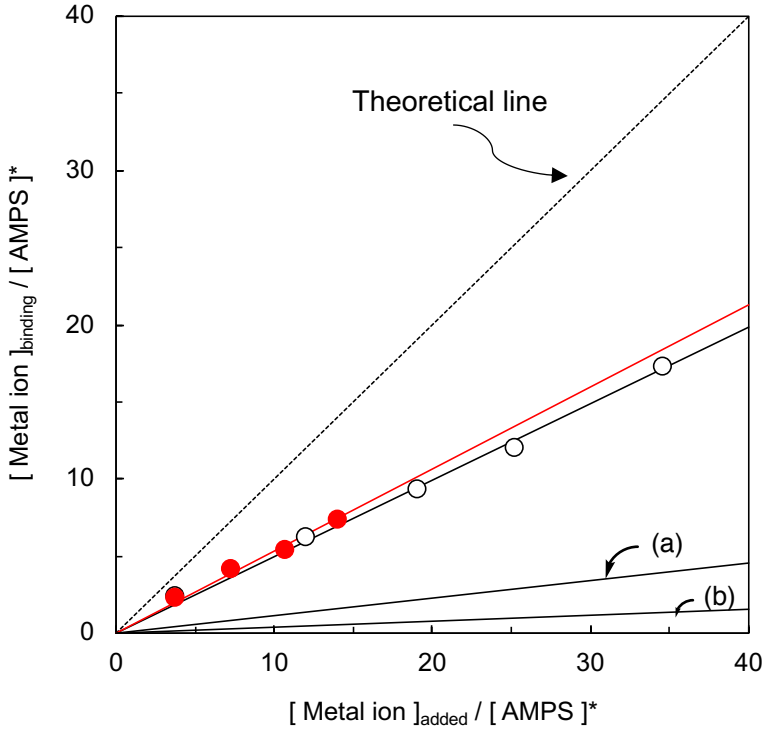

Fig. 1-4 Relationship between relative amounts of Metal ions binding to $[R_F\text{-}(AMPS)_x\text{-}(CH_2CMeCO_2Me)_y\text{-}R_F$; $R_F = CF(CF_3)OCF_2CF(CF_3)OC_3F_7]$ and relative amount of initial metal ions: (◯) Co^{2+}; (●) Cr^{3+}; (----) theoretical line (corresponds to a 100% binding ratio; (a) Cr^{3+} ion (AMPS polymer curved by *N,N'*-methylenebisacrylamide-H_2O_2 system) (see ref. 27); (b) Co^{2+} ion (AMPS polymer curved by *N,N'*-methylenebisacrylamide-AIBN system) (see ref. 27). †[AMPS] indicates calculated concentration (mol dm^{-3}) based on polymer monomer unit.

A remarkable decrease in the absorbance of Cr^{3+} or Co^{2+} was observed after the addition of the fluoroalkylated hydrogel to each metal ion solution. As shown in Fig. 1-4, the Cr^{3+} and

Co^{2+} ion bindings increased linearly with an increase in the initial concentration of Cr^{3+} or Co^{2+} with ca. 60% binding ratio {based on the relative amount of Cr^{3+} (or Co^{2+}) binding to gel ($[Metal\ ion]_{binding}/[AMPS]$) and relative amount of initial metal ion ($[Metal\ ion]_{add}/[AMPS]$)}. Furthermore, this fluoroalkylated hydrogel was found to have a similar adsorptive property towards Co^{2+} and Cr^{3+} ions. This finding would mean that these metal ions bind ionically to the anionic parts of the oligomer networks in the fluorinated gel, and this ionic interaction is not affected by the gel structure. On the other hand, bound Co^{2+} or Cr^{3+} ion was not released from the fluoroalkylated gel into water. This result also suggests that the interaction for the binding of the metal ions to the hydrogel is not coordination but ionic.

Interestingly, the fluoroalkylated end-capped AMPS oligomer hydrogel was shown to have a higher metal ion binding power than the corresponding AMPS polymer hydrogels crosslinked by *N*,*N*'-methylenebisacrylamide–H_2O_2 or AIBN (azobisisobutyronitrile) system[27] as in Fig. 1-4. As a result, it can be said that the metal ions should interact in part with not only the anionic parts of the fluorinated hydrogel but also the fluoroalkyl segments in the fluorinated AMPS hydrogel possessing strong electron-withdrawing properties.

In this way, it was verified that the aggregation of fluoroalkyl segments in water and in organic media becomes a new driving factor for gelation as well as the well-known interactions such as hydrogen bonding and ionic interaction. Furthermore, it was clarified that the hydrogels

which are built up through the aggregation of the fluoroalkyl segments have similar metal ion adsorptive properties to the well-known chemically crosslinked polymer hydrogels.

Because the fluoroalkylated AMPS oligomers are gelling, it is of particular interest to investigate their potential as biologically active materials. Thus, a series of fluoroalkylated end-capped AMPS oligomers have been evaluated for activity against HIV-1 replication in MT-4 cells (see Table 1-3).

Table 1-3 Inhibitory effect of fluoroalkylated 2-acrylamido-2-methylpropanesulfonic oligomers on the replication of HIV-1 in MT-4 cells

oligomer	$\overline{Mn}$	EC_{50}[a] / μg ml^{-1}	CC_{50}[b] / μg ml^{-1}
R_F-(AMPS)$_n$-R_F; R_F = C_3F_7	24500	1.6	>100
R_F-(AMPS)$_n$-R_F; R_F = $CF(CF_3)OCF_2CF(CF_3)OC_3F_7$	12000	1.6	>100
R_F-(AMPS)$_n$-R_F; R_F = $CF(CF_3)OCF_2CF(CF_3)OCF_2CF(CF_3)OC_3F_7$	24000	1.7	>100
R_F-(AMPS)$_x$-($CH_2CHSiMe_3$)$_y$-R_F; R_F = C_3F_7	11000	0.6	>100
R_F-(AMPS)$_x$-($CH_2CHSiMe_3$)$_y$-R_F; R_F = $CF(CF_3)OC_3F_7$	10000	2.3	>100
R_F-(AMPS)$_x$-($CH_2CHSiMe_3$)$_y$-R_F; R_F = $CF(CF_3)OCF_2CF(CF_3)OC_3F_7$	17400	1.7	>100
R_F-(AMPS)$_x$-(CH_2CMeCO_2Me)$_y$-R_F; R_F = C_3F_7	11300	1.9	>100
R_F-(AMPS)$_x$-(CH_2CMeCO_2Me)$_y$-R_F; R_F = $CF(CF_3)OC_3F_7$	14300	0.23	>100
-(AMPS)$_n$-	5400	1.6	36
dextran sulfate (MW = 5000)		3.5	>100

a) Fifty percent effective concentration, based on the inhibition of HIV-1 induced cytopathic effects in MT-4 cell.
b) Fifty percent cytotoxic concentration, based on the impairment of viability of mock-infected MT-4 cells.

As shown in Table 1-3, the 50% effective concentrations of the oligomers were 0.23 ~

2.3 μg ml^{-1} in MT-4 cells, whereas they were not toxic at concentrations up to 100 μg ml^{-1}. These values are superior to those of dextran sulfate, which has been considered to be a potent and selective polymeric inhibitor of HIV-1 replication in cell culture to date.[34] On the other hand, non-fluorinated oligomers were toxic to the host cells. The mechanism of action of the gelling oligomers may also explain the inhibition of virus adsorption, as previously demonstrated for fluoroalkylated acrylic acid oligomers.[23, 35, 36] Interestingly, there is some correlation between the activity against HIV-1 and the C_{min} values (medium: water). As the activity against HIV-1 shown in Table 1-3 becomes higher, the C_{min} values (see Table 1-2) become in general smaller. Thus, fluoroalkylated end-capped AMPS co-oligomers such as C_3F_7-(AMPS)$_x$-($CH_2CHSiMe_3$)$_y$-C_3F_7, $C_3F_7OCF(CF_3)$-(AMPS)$_x$-(CH_2CMeCO_2Me)$_y$-$CF(CF_3)OC_3F_7$ exhibit a higher anti-HIV-1 activity than the corresponding homo-oligomers, and these co-oligomers possess in general a higher gelling ability. Therefore, it is suggested that the oligomers possessing a higher gelling ability (that is, the oligomers which are more adsorbable) would interact strongly with the virus leading to more potent inhibitory effects against HIV-1 replication.

It has already reported that fluoroalkylated end-capped oligomers containing trimethylammonium segments possess antibacterial activity against *Staphylococcus aureus*.[7] Hence, the present fluoroalkylated end-capped AMPS oligomers are also expected to show

antibacterial activity since these oligomers contain the amide segments. These AMPS oligomers have been evaluated for their antibacterial activity against *S. aureus* by viable cell counting method as already reported.[7] About 10^8 cells per ml of *S. aureus* were exposed to 1 mg ml^{-1} of the oligomers in saline.

Fluoroalkylated end-capped AMPS homo- and co-oligomers were in general inactive. However, of these AMPS oligomers, perfluoropropylated AMPS–trimethylvinylsilane co-oligomer [C_3F_7-$(AMPS)_x$-$(CH_2CHSiMe_3)_y$-C_3F_7] was found to show anti-bacterial activity (from 2.2×10^8 to 2×10^2 colony forming units levels). In addition, this co-oligomer was shown to possess a higher anti-HIV-1 activity (see Table 1-3).

Hitherto, the development of antibacterial cationic materials possessing fluoroalkyl segments has been limited.[37, 38] However, C_3F_7-$(AMPS)_x$-$(CH_2CHSiMe_3)_y$-C_3F_7 was able to exhibit effectively not only anti-HIV-1 activity but also antibacterial activity.

In this way, it was demonstrated that the fluorinated AMPS oligomers have not only a gelling ability but also anti-HIV-1 activity or antibacterial activity, although these compounds are high molecular mass materials containing only fluoroalkylated end-groups in one oligomeric molecule. Hence, these new fluorinated compounds are expected to be widely applicable in various fields as new attractive fluorinated gelling functional materials possessing biological activities.

3.4 Conclusions

New fluoroalkylated end-capped 2-acrylamido-2-methylpropanesulfonic acid homo-oligomers were prepared by reaction of fluoroalkanoyl peroxides with 2-acrylamido-2-methylpropanesulfonic acid (AMPS). Similarly, fluoroalkylated end-capped co-oligomers were prepared by reaction of fluoroalkanoyl peroxides with AMPS and the co-monomers such as trimethylvinylsilane and methyl methacrylate. These thus-obtained fluoroalkylated end-capped AMPS oligomers were found to form gels not only in water but also in organic polar solvents such as methanol, ethanol, *N,N*-dimethylformamide and dimethyl sulfoxide under non-crosslinked conditions. On the other hand, AMPS polymer containing fluoroalkylene units $\{[-R_F-(AMPS)_q]_p-\}$ could cause no gelation under similar conditions. This suggests that fluoroalkylated end-capped AMPS oligomers can cause gelation where strong aggregation of the end-capped fluoroalkyl segments is involved sterically in establishing the physical gel network in these media. Interestingly, these fluoroalkylated end-capped AMPS oligomer hydrogels had a strong metal ion binding power. Moreover, it was demonstrated that these fluoroalkylated gelling oligomers are potent and selective inhibitors of HIV-1 replication in cell culture. In addition, one of these gelling oligomers was found to possess antibacterial activity against *Staphylococcus aureus*. Therefore, these fluorinated gelling oligomers are suggested to have high potential for new functional materials through their gelling ability and

biological activity.

References

1) L. A. Wall, *Fluoropolymer*, Wiley, New York, 1972, Vol. XXV.

2) P. R. Resnick, *Polym. Prepr. (Am. Chem. Soc. Div. Polym. Chem.)*, **31**, 312 (1990).

3) N. Nakamura, T. Kawasaki, M. Unoki, K. Oharu, N. Sugiyama, I. Kaneko, and G. Kojima, *Preprints of the First Pacific Polymer Conference*, Am. Chem. Soc. Div. Polym. Chem., Maui, HI, Dec. 1989 ; American Chemical Society, Washington, DC, 1989, p. 369.

4) Z.-Y. Yang, A. E. Feiring and B. E. Smart, *J. Am. Chem. Soc.*, **116**, 4135 (1994).

5) H. Sawada, N. Itoh, T. Kawase, M. Mitani, H. Nakajima, M. Nishida, and Y. Moriya, *Langmuir*, **10**, 994 (1994).

6) H. Sawada, K. Tanba, N. Itoh, C. Hosoi, M. Oue, M. Baba, T. Kawase, M. Mitani, and H. Nakajima, *J. Fluorine Chem.*, **77**, 51 (1996).

7) H. Sawada, S. Katayama, M. Oue, T. Kawase, Y. Hayakawa, M. Baba, T. Tomita, and M. Mitani, *J. Jpn. Oil Chem. Soc.*, **45**, 161 (1996).

8) H. Sawada, H. A. Ohashi, A. M. Baba, T. Kawase, and Y. Hayakawa, *J. Fluorine Chem.*, **79**, 149 (1996).

9) J. F. Elman, B. D. Johs, T. E. Long, and J. T. Koberstein, *Macromolecules*, **27**, 5341 (1994).

10) S. Affrossman, M. Hartshorne, T. Kiff, R. A. Pethrick, and R. W. Richards, *Macromolecules*, **27**, 1588 (1994).

11) M. O. Hunt, Jr., A. M. Belu, R. W. Linton, and J. M. DeSimone, *Macromolecules*, **26**, 4854 (1993).

12) S. Affrossman, P. Bertrand, M. Hartshorne, T. Kiff, D. Leonard, R. A. Pethrick, and R. W. Richards, *Macromolecules*, **29**, 5432 (1996).

13) B. Xu, L. Li, A. Yekta, Z. Masoumi, S. Kanagalingam, M. A. Winnik, K. Zhang, P. M. Macdonald, and S. Menchen, *Langmuir*, **13**, 2447 (1997).

14) J. Wang, G. Mao, C. K. Ober, and E. J. Kramer, *Polym. Prepr. (Am. Chem. Soc., Div. Polym. Chem.)*, **38**, 953 (1997).

15) Z. Su, D. Wu, S. L. Hsu, and T. J. McCarthy, *Polym. Prepr. (Am. Chem. Soc., Div. Polym. Chem.)*, **38**, 951 (1997).

16) A. Laschewsky and I. Zerbe, *Polymer*, **32**, 2070 (1991).

17) H. Sawada, E. Sumino, M. Oue, M. Mitani, H. Nakajima, M. Nishida, and Y. Moriya, *J. Chem. Soc., Chem. Commun.*, 143 (1994).

18) H. Sawada, E. Sumino, M. Oue, M. Baba, T. Kira, S. Shigeta, M. Mitani, H. Nakajima, M. Nishida, and Y. Moriya, *J. Fluorine Chem.*, **74**, 21 (1995).

19) H. Sawada and M. Nakayama, *J. Fluorine Chem.*, **51**, 117 (1990).

20) H. Sawada, M. Yoshida, H. Hagii, K. Aoshima and M. Kobayashi, *Bull. Chem. Soc. Jpn.*, **59**, 215 (1986).

21) K. Hanabusa, R. Tanaka, M. Suzuki, M. Kimura, and H. Shirai, *Adv. Mater.*, **9**, 1095 (1997)

22) K. Hanabusa, K. Okui, K. Karaki, M. Kimura, and H. Shirai, *J. Colloid Interface Sci.*, **195**, 86 (1997).

23) M. Baba, T. Kira, S. Shigeta, T. Matsumoto, and H. Sawada, *J. Acquir. Immun. Defic. Syndr.*, **7**, 24 (1994).

24) H. Sawada, Y.-F. Gong, Y. Minoshima, T. Matsumoto, M. Nakayama, M. Kosugi, and T. Migita, *J. Chem. Soc., Chem. Commun.*, 537 (1992).

25) H. Sawada, Y. Minoshima, and Y. Nakajima, *J. Fluorine Chem.*, **65**, 169 (1992).

26) K. Hanabusa, Y. Naka, T. Koyama and H. Shirai, *J. Chem. Soc., Chem. Commun.*, 2683 (1994).

27) Y. Osada and M. Takase, *Nippon Kagaku Kaishi*, 439 (1983).

28) T. Kunitake, Y. Okahata and S. Yasunami, *J. Am. Chem. Soc.*, **104**, 5547 (1987).

29) T. Kunitake and N. Higashi, *J. Am. Chem. Soc.*, **107**, 692 (1985).

30) T. Kunitake and N. Higashi, *Macromol. Chem. Phys. Suppl.*, **14**, 81 (1985).

31) Y. Ishikawa, K. Kuwahara, and T. Kunitake, *Chem. Lett.*, 1737 (1989).

32) Y. Ishikawa, H. Kuwahara, and T. Kunitake, *J. Am. Chem. Soc.*, **111**, 8530 (1989).

33) R. J. Twieg, T. P. Russell, R. Siemens and J. F. Rabolt, *Macromolecules*, **18**, 1361 (1985).

34) M. Baba, R. Pauwels, J. Balzarini, J. Arnout, J. Desmyter, and E. De Clercq, *Proc. Natl. Acad. Sci. USA*, **85**, 6132 (1988).

35) H. Sawada, A. Ohashi, M. Oue, M. Baba, M. Abe, M. Mitani, and H. Nakajima, *J. Fluorine Chem.*, **75**, 121 (1995).

36) H. Sawada, K. Yamamoto, M. Oue, T. Kawase, Y. Hayakawa, M. Baba, and M. Mitani, *J. Jpn. Oil Chem. Soc.*, **45**, 37 (1996).

37) H. Sawada, A. Wake, T. Maekawa, T. Kawase, Y. Hayakawa, T. Tomita, and M. Baba, *J. Fluorine Chem.*, **83**, 125 (1997).

38) H. Sawada, K. Tanba, T. Tomita, T. Kawase, M. Baba, and T. Ide, *J. Fluorine Chem.*, **84**, 141 (1997).

CHAPTER 2

Gelation of Fluoroalkylated End-Capped Oligomers Containing Triol Segments under Non-Crosslinked Conditions, and Binding or Releasing of Metal Ions by These Oligomers

2.1 Introduction

Polyacrylamide gels, such as poly[*N*-tris(hydroxymethyl)methylacrylamide] gels crosslinked by *N*,*N*′-methylene-bisacrylamide, have been widely used as anticonvective media for the electrophoretic separation of biomolecules,[1)] and their derivatives have also been applied to a drug-delivery system.[2, 3)] Hitherto, there has been attractive interest in organofluorine compounds owing to possessing various unique properties which cannot be achieved by the corresponding non-fluorinated ones.[4)] Therefore, it is of particular interest to explore fluorinated polyacrylamide gels; however, although the preparation and application of these compounds have been limited, these compounds have been the subject of considerable research of both fundamental and applied nature. Recently, it has been discovered that fluoroalkylated end-capped betaine-type oligomers, $\{R_F\text{-}[CH_2\text{-}CHC(=O)N^+H_2C(CH_3)_2CH_2SO_3^-]_n\text{-}R_F\}$, can cause gelation derived from the synergistical interaction of the aggregations of fluoroalkyl segments and the ionic interactions of the betaine segments in water or organic media.[5)] Therefore, the hydrogen-bonding interaction can be strongly expected to participate in the gelator which is constructed by the fluoroalkyl units.

From such points of view, it is of particular important to synthesis new fluoroalkylated end-capped acrylamide oligomers which can cause physical gelation, the driving factors of which are intermolecular hydrogen bonding and the aggregations of fluoroalkyl segments. This

Chapter shows that the synthesis and properties of fluoroalkylated end-capped *N*-tris(hydroxymethyl)methylacrylamide oligomers by the reactions of fluoroalkanoyl peroxides with the corresponding monomers.

2.2 Experimental

2.2.1 Measurements

NMR spectra were measured using a Varian Unity-plus 500 (500 MHz) spectrometer, while IR spectra were recorded on a Horiba FT-300 FT-IR spectrophotometer. Absorption spectra were recorded on a Shimadzu UV-240 spectrophotometer. Solution viscosities were measured by using a falling-sphere Haake Viscometer D1-G.

2.2.2 Materials

A series of fluoroalkanoyl peroxides [$(R_FCOO)_2$] were prepared by the reactions of the corresponding acyl halides and hydrogen peroxide in the presence of aqueous sodium hydroxide according to the previously reported method.[6, 7)]

N-Tris(hydroxymethyl)methylacrylamide was purchased from Acros Organics Inc.. Trimethylvinylsilane and dimethyl-1,4,7-trioxanonylvinylsilane were purchased from

Shin-Etsu Co., Ltd.. Chromium(III) nitrate and cobalt(II) chloride were purchased from Wako Chemicals.

2.2.3 General procedure for the synthesis of fluoroalkylated NAT oligomers

Perfluor-2-methyl-3-oxahexanoyl peroxide (4 mmol) in 1 : 1 mixed solvents (AK-225) of 1,1-dichloro-2,2,3,3,3-pentafluoropropane and 1,3-dichloro-1,2,2,3,3-pentafluoropropane (50 g) was added to an aqueous solution (50%, w/w) of NAT (20 mmol). The heterogeneous solution was stirred vigorously at 45 °C for 5 h under nitrogen. The crude product obtained was washed with methanol well to remove the unreacted NAT monomer, and dried over in vacuo to give a bis(perfluoro-1-methyl-2-oxapentylated)-*N*-tris(hydroxymethyl)methylacrylamide (3.45 g). This oligomer exhibited the following spectra characteristics: IR ν (cm^{-1}) 3355 (OH, NH), 1652 (C=O), 1394 (CF_3), 1270 (CF_2); ^{1}H NMR (D_2O) δ 1.10 ~ 2.22 (CH_2, CH), 3.28 ~ 4.19 (CH_2); ^{19}F NMR (D_2O, ext. CF_3CO_2H) δ -5.82 ~ -10.82 (16F), -54.65 (6F).

The other products obtained exhibited the following spectral characteristics:

R_F-(NAT)$_x$-R_F [R_F = C_3F_7; Run 1 in Table 2-1]:

IR ν (cm^{-1}) 3361 (OH, NH), 1648 (C=O), 1386 (CF_3), 1280 (CF_2); ^{1}H NMR (D_2O) δ 1.10 ~ 2.24 (CH_2, CH), 3.28 ~ 4.15 (CH_2); ^{19}F NMR (D_2O, ext. CF_3CO_2H) δ -5.64 (6F), -43.18 (4F), -54.65 (4F).

R_F-(NAT)$_x$-R_F [R_F = C_3F_7; Run 2 in Table 2-]):

IR ν (cm^{-1}) 3424 (OH, NH), 1648 (C=O), 1388 (CF_3), 1261 (CF_2); ^{1}H NMR (D_2O) δ 1.04 ~ 2.48 (CH_2, CH), 3.33 ~ 3.98 (CH_2); ^{19}F NMR (D_2O, ext. CF_3CO_2H) δ -5.77 (6F), -43.18 (4F), -54.52 (4F).

R_F-(NAT)$_x$-R_F [R_F = $CF(CF_3)OC_3F_7$; Run 4 in Table 2-1]:

IR ν (cm^{-1}) 3378 (OH, NH), 1650 (C=O), 1392 (CF_3), 1245 (CF_2); ^{1}H NMR (D_2O) δ 1.03 ~ 2.24 (CH_2, CH), 3.03 ~ 4.28 (CH_2); ^{19}F NMR (D_2O, ext. CF_3CO_2H) δ -6.93 ~ -7.74 (16F), -54.05 (6F).

R_F-(NAT)$_x$-R_F [R_F = $CF(CF_3)OCF_2CF(CF_3)OC_3F_7$; Run 5 in Table 2-1]:

IR ν (cm^{-1}) 3386 (OH, NH), 1650 (C=O), 1390 (CF_3), 1245 (CF_2); ^{1}H NMR (D_2O) δ 1.01 ~ 2.21 (CH_2, CH), 2.78 ~ 4.18 (CH_2); ^{19}F NMR (D_2O, ext. CF_3CO_2H) δ -3.99 ~ -7.74 (26F), -54.36 (6F), -72.28 (2F).

R_F-(NAT)$_x$-R_F [R_F = $CF(CF_3)OCF_2CF(CF_3)OC_3F_7$; Run 6 in Table 2-1]:

IR ν (cm^{-1}) 3390 (OH, NH), 1648 (C=O), 1392 (CF_3), 1267 (CF_2); ^{1}H NMR (D_2O) δ 1.04 ~ 2.54 (CH_2, CH), 3.40 ~ 4.12 (CH_2); ^{19}F NMR (D_2O, ext. CF_3CO_2H) δ -3.99 ~ -6.93 (26F), -54.60 (6F), -71.21 (2F).

Similarly, a series of fluoroalkylated NAT co-oligomers were prepared by co-oligomerizations with fluoroalkanoyl peroxides. These exhibited the following spectral

characteristics:

R_F-(NAT)$_x$-($CH_2CHSiMe_3$)$_y$-R_F [R_F = C_3F_7; Run 7 in Table 2-1]:

IR ν (cm^{-1}) 3337 (OH, NH), 1648 (C=O), 1390 (CF_3), 1268 (CF_2); ^{1}H NMR (D_2O) δ -0.22 ~ -0.01 (CH_3), 0.98 ~ 2.47 (CH_2, CH), 3.34 ~ 4.36 (CH_2); ^{19}F NMR (D_2O, ext. CF_3CO_2H) δ -5.71 (6F), -43.25 (4F), -52.24 (4F).

R_F-(NAT)$_x$-($CH_2CHSiMe_3$)$_y$-R_F [R_F = $CF(CF_3)OC_3F_7$;Run 8 in Table 2-1]:

IR ν (cm^{-1}) 3411 (OH, NH), 1648 (C=O), 1392 (CF_3), 1245 (CF_2); ^{1}H NMR (D_2O) δ -0.13 ~ 0.11 (CH_3), 0.74 ~ 2.65 (CH_2, CH), 3.28 ~ 4.22 (CH_2); ^{19}F NMR (D_2O, ext. CF_3CO_2H) δ -3.97 ~ -7.74 (16F), -54.68 (6F).

R_F-(NAT)$_x$-($CH_2CHSiMe_3$)$_y$-R_F [R_F = $CF(CF_3)OCF_2CF(CF_3)OC_3F_7$;Run 9 in Table 2-1]:

IR ν (cm^{-1}) 3415 (OH, NH), 1649 (C=O), 1392 (CF_3), 1245 (CF_2); ^{1}H NMR (D_2O) δ = -0.24 ~ -0.08 (CH_3), 0.82 ~ 2.22 (CH_2, CH), 2.90 ~ 4.21 (CH_2); ^{19}F NMR (D_2O, ext. CF_3CO_2H) δ -3.99 ~ -7.50 (26F), -54.70 (6F), -62.75 (2F).

R_F-(NAT)$_x$-($CH_2CHSiMe_2O(CH_2)_2O(CH_2)_2OCH_2Me$)$_y$-$R_F$

[R_F = $CF(CF_3)OCF_2CF(CF_3)OC_3F_7$;Run 10 in Table 2-1]:

IR ν (cm^{-1}) 3405 (OH, NH), 1650 (C=O), 1386 (CF_3), 1247 (CF_2); ^{1}H NMR (D_2O) δ -0.29 ~ 0.11 (CH_3), 0.52 ~ 2.44 (CH_2, CH), 3.27 ~ 4.18 (CH_2); ^{19}F NMR (D_2O, ext. CF_3CO_2H) δ -3.78 ~ -10.78 (26F), -55.82 (6F), -70.98 (2F).

R_F-(NAT)$_x$-(CH_2CMeCO_2Me)$_y$-R_F [R_F = $CF(CF_3)OC_3F_7$; Run 11 in Table 2-1]:

IR ν (cm^{-1}) 3397 (OH, NH), 1650 (C=O), 1322 (CF_3), 1241 (CF_2); ^{1}H NMR (D_2O) δ 0.62 ~ 2.52 (CH_3, CH_2, CH), 3.28 ~ 4.22 (CH_3, CH_2); ^{19}F NMR (D_2O, ext. CF_3CO_2H) δ -5.64 ~ -10.13 (16F), -54.36 (6F).

R_F-(NAT)$_x$-(CH_2CMeCO_2Me)$_y$-R_F [R_F = $CF(CF_3)OCF_2CF(CF_3)OC_3F_7$; Run 12 in Table 2-1]:

IR ν (cm^{-1}) 3423 (OH, NH), 1646 (C=O), 1394 (CF_3), 1243 (CF_2); ^{1}H NMR (D_2O) δ 0.84 ~ 2.39 (CH_3, CH_2, CH), 3.31 ~ 4.18 (CH_3, CH_2); ^{19}F NMR (D_2O, ext. CF_3CO_2H) δ -3.99 ~ -9.18 (26F), -54.57 (6F), -70.64 (2F).

2.2.4 Viscosity measurements

The viscosities of aqueous solutions of fluoroalkylated NAT homo- and co-oligomers were measured at 30 °C using a falling-sphere viscometer (Haake Viscometer D1-G).

2.2.5 A typical procedure for gelation test

A procedure for studying the gel-formation ability was based on a method reported by Hanabusa *et al*.[8] Briefly, weighted fluoroalkylated NAT oligomer was mixed with water or organic fluid in a tube. The mixture was treated under ultrasonic conditions until the solid was dissolved. The resulting solution was kept at 30 °C for 1 h, and then the gelation was checked out visually. When it was formed, the gel was stable and the tube was able to be inverted without changing the shape of the gel.

2.2.6 Metal ions binding or releasing by fluoroalkylated NAT oligomer hydrogels

Fluoroalkylated NAT oligomer hydrogels were swelled with water in a measuring flask. After the addition of the required amount of aqueous metal ion solution into the flask, the flask was allowed to stand for 1 d at 25 °C. The metal-ion concentration of supernatant liquid after the incubation was spectrophotometrically determined.

The metal ion was released from the metal binding to the hydrogel into water for 1 d at 25 °C, and then the metal ion concentration of supernatant liquid was determined spectrophotometrically.

2.3 Results and discussion

The reactions of fluoroalkanoyl peroxides with *N*-tris(hydroxymethyl)methylacrylamide [NAT] in 1 : 1 mixed solvents (AK-225) of 1,1-dichloro-2,2,3,3,3-pentafluoropropane and 1,3-dichloro-1,2,2,3,3-pentafluoropropane were carried out at 45 °C for 5h under nitrogen. The process is outlined in Scheme 2-1. NAT was found to react smoothly with the peroxides under mild conditions to give fluoroalkylated end-capped oligomers containing triol segments [R_F-(NAT)$_n$-R_F].

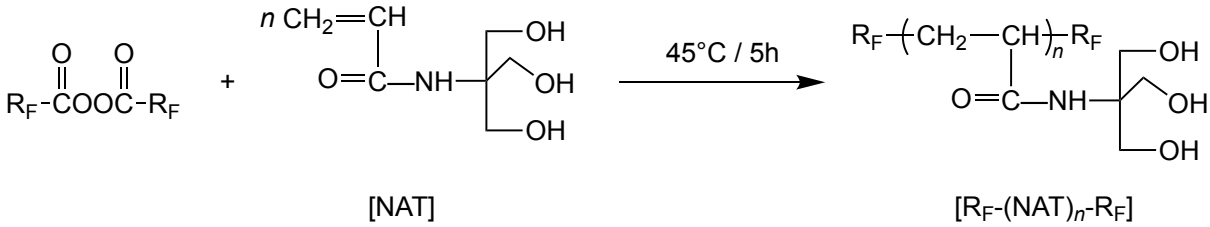

R_F = C_3F_7, $CF(CF_3)[OCF_2CF(CF_3)]_mOC_3F_7$; *m* = 0, 1

Scheme 2-1 Synthesis of R_F-(NAT)$_n$-R_F homo-oligomers at 45 ºC for 5 h

Similarly, co-oligomerization with co-monomers such as trimethylvinysilane, dimethyl-1,4,7-trioxanonylvinylsilane, and methyl methacrylate was found to proceed under mild conditions to afford the corresponding fluoroalkylated end-capped co-oligomers, as shown in the following Scheme 2-2.

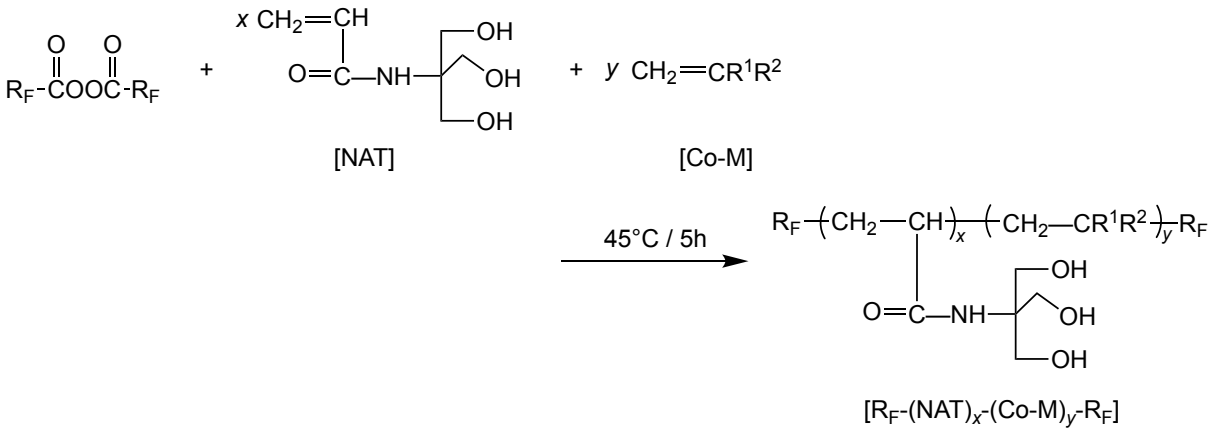

R_F = C_3F_7, $CF(CF_3)[OCF_2CF(CF_3)]_mOC_3F_7$; m = 0, 1

R^1 = H, R^2 = $SiMe_3$;

R^1 = H, R^2 = $SiMe_2$-$O(CH_2)_2O(CH_2)_2OEt$;

R^1 = Me, R^2 = CO_2Me

Scheme 2-2 Synthesis of R_F-$(NAT)_x$-$(Co\text{-}M)_y$-R_F co-oligomer at 45 ºC for 5 h

The results for these reactions are summarized in Table 2-1.

Table 2-1 Synthesis of fluoroalkylated NAT homo- and co-oligomers at 45 ºC for 5h

Run	R_F in peroxide	NAT	$CH_2=CR^1R^2$	Product	
	/ mmol	/ mmol	/ mmol	Yield / %[a]	x : y [b]
	C_3F_7			R_F-(NAT)$_n$-R_F	
1	5	21	—	55	—
2	4	9	—	45	—
	$CF(CF_3)OC_3F_7$				
3	4	20	—	43	—
4	5	5	—	29	—
	$CF(CF_3)OCF_2CF(CF_3)OC_3F_7$				
5	3	13	—	42	—
6	3	5	—	48	—
	C_3F_7		$CH_2=CHSiMe_3$	R_F-(NAT)$_x$-(CH_2-CR^1R^2)$_y$-R_F	
7	4	21	21	55	83 : 17
	$CF(CF_3)OC_3F_7$				
8	5	21	21	53	67 : 33
	$CF(CF_3)OCF_2CF(CF_3)OC_3F_7$				
9	3	13	15	50	96 : 4
	$CF(CF_3)OCF_2CF(CF_3)OC_3F_7$		$CH_2=CHSiMe_2$-O(CH_2)$_2$O(CH_2)$_2$OEt		
10	3	13	14	25	95 : 5
	$CF(CF_3)OC_3F_7$		$CH_2=CMeCO_2Me$		
11	4	21	22	52	88 : 12
	$CF(CF_3)OCF_2CF(CF_3)OC_3F_7$				
12	3	13	13	54	90 : 10

a) The yields are based on starting materials [NAT, Co-monomers and the decarboxylated peroxide unit (R_F-R_F).
b) Co-oligomerization ratio determined by ^{1}H NMR.

As shown in Table 2-1, not only perfluoropropylated, but also perfluoro-oxaalkylated NAT homo- and co-oligomers, were obtained under mild conditions, and the co-oligomerization ratios of these oligomers were determined by ^{1}H NMR analyses. The obtained co-oligomers afforded a different reactivity in the co-oligomerization ratios. This finding would depend upon that the present homo- and co-oligomerizations of NAT with fluoroalkanoyl peroxides are heterogeneous systems including water. In these fluoroalkylated NAT homo- and co-oligomers (Table 2-1), each molecular weight of the oligomers was unable to measure by GPC (gel permeation chromatography) analyses under various conditions owing to the highly viscoelastic fluids or gel formation. In contrast, it was previously reported that fluoroalkylated end-capped acrylic acid oligomers [R_F-$(CH_2CHCO_2H)_n$-R_F] can be synthesized by the reactions of fluoroalkanoyl peroxides with acrylic acid under similar conditions, and that their molecular weights ($\overline{Mn}$: 5000 ~ 13000) are easily measured by GPC analyses.[9, 10] To clarify this unique gelling behavior, the viscosity of aqueous solutions of these fluoroalkylated end-capped oligomers was measured at 30 °C. The results are shown in Fig. 2-1.

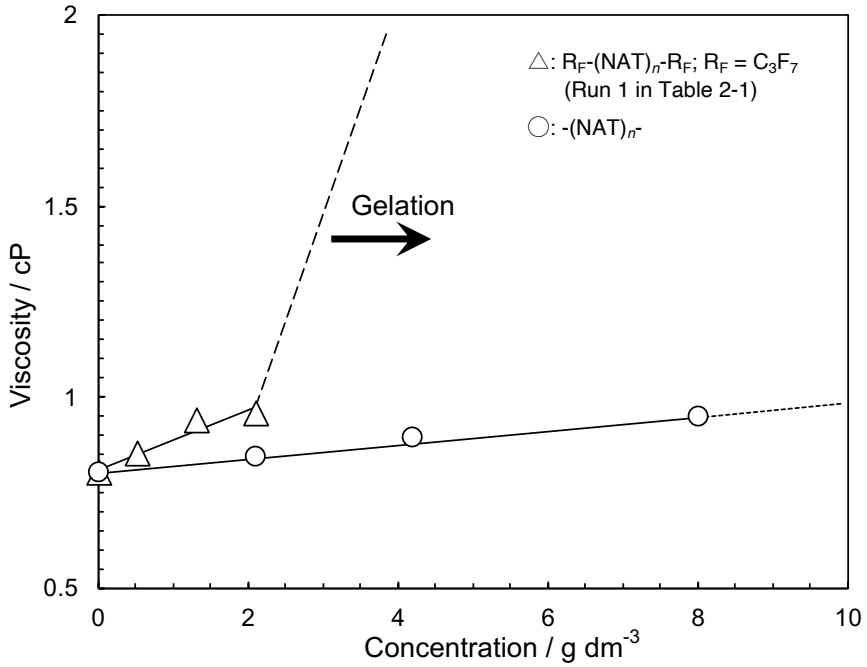

Figure 2-1 Effect of concentration on viscosity of R_F-(NAT)$_n$-R_F and -(NAT)$_n$- at 30°C

A shown in Fig. 2-1, the viscosities of non-fluorinated NAT oligomer [-(NAT)$_n$-] did not increase remarkably with increasing its concentration. On the other hand, fluoroalkylated NAT oligomer increased extremely with increasing the concentration, and it became impossible to measure its viscosity owing to causing a gelation at concentrations above 2 g dm^{-3}.

Similarly, other fluoroalkylated end-capped oligomers were found to increase extremely with increasing the concentration to cause gelation in water. The striking characteristics of the fluoroalkylated NAT oligomers as gelling agents are to harden organic solvents, such as dimethyl sulfoxide (DMSO) and *N*,*N*-dimethylformamide (DMF). In contrast, non-fluorinated NAT oligomer was completely soluble not only in water, but also in organic solvents, such as

DMSO and DMF.

The temperature where the gel melts was also tried to measure; however, the gel melted neither in water nor in DMSO, even when the gel was heated from 30 °C to around 95 °C. This suggests that the fluoroalkyl segments are strongly connected with the establishment of a gel network. For a similar gel formation of fluorinated compounds, Tweig *et al.* reported that semifluorinated alkanes, such as $F(CF_2)_{10}(CH_2)_{12}H$, exhibit gel-like characteristics in hydrocarbon solvents, [H $(CH_2)_pH$; p = 8, 10, 12, 14].[11] To study this gel-formation ability, the minimum concentrations of fluoroalkylated NAT oligomers necessary for gelation were measured according to a method reported by Hanabusa *et al*.[8] The results on the minimum concentrations for gelation (C_{min}) in water and in DMSO at 30 °C are given in Table 2-2.

There was no gel-formation ability for a non-fluorinated NAT oligomer owing to its good solubility. However, surprisingly, each fluoroalkylated oligomer in Table 2-1 can form a physical gel and harden not only water, but also organic polar solvents, such as DMSO at low concentrations, as shown in Table 2-2. In general, the gelling ability of fluoroalkylated homo-oligomers is superior to that of the co-oligomers, except for perfluoropropylated ones (Table 2-2), taking into account that C_{min}s are 18 ~ 47 g dm^{-3} for homo-oligomers and 34 ~ 82 g dm^{-3} for co-oligomers at 30 °C. This finding suggests that the fluoroalkylated homo-oligomers are likely to have stronger association through intermolecular hydrogen bondins between triol

segments to cause physical gelation compared to those of the co-oligomers.

Table 2-2 Minimum gel concentration C_{min} of fluoroalkylated NAT homo- and co-oligomers (in g per dm^3 Solvent) necessary for gelation at 30 °C

Run [a]	Oligomer	C_{min} / g dm^{-3} (gelator/midium)	
		H_2O	DMSO
	R_F-(NAT)$_n$-R_F		
1	$R_F = C_3F_7$	72	72
2	$= C_3F_7$	38	73
3	$R_F = CF(CF_3)OC_3F_7$	18	24
4	$= CF(CF_3)OC_3F_7$	39	37
5	$R_F = CF(CF_3)OCF_2CF(CF_3)OC_3F_7$	42	47
6	$= CF(CF_3)OCF_2CF(CF_3)OC_3F_7$	31	19
	R_F-(NAT)$_x$-(CH_2-CHSiMe_3)$_y$-R_F		
7	$R_F = C_3F_7$	15	47
8	$R_F = CF(CF_3)OC_3F_7$	64	66
9	$R_F = CF(CF_3)OCF_2CF(CF_3)OC_3F_7$	57	63
	R_F-(NAT)$_x$-(CH_2-CHSiMe_2-O(CH_2)$_2$O(CH_2)$_2$OEt)$_y$-R_F		
10	$R_F = CF(CF_3)OCF_2CF(CF_3)OC_3F_7$	50	34
	R_F-(NAT)$_x$-(CH_2-CMeCO_2Me)$_y$-R_F		
11	$R_F = CF(CF_3)OC_3F_7$	82	63
12	$R_F = CF(CF_3)OCF_2CF(CF_3)OC_3F_7$	54	54

a) Each different from those of Table 2-1.

The non-fluorinated NAT oligomer could not cause gelation. Therefore, the physical gelling behavior for the fluorinated NAT oligomers is not governed by only the intermolecular hydrogen bonding between triol segments, but the strong aggregations between end-capped fluoroalkyl segments in oligomers are essential for causing the gelation. Throughout these

results, it is reasonable to assume that the present fluoroalkylated NAT oligomer gel is built up through the synergistic interactions of both the aggregations of fluoroalkyl segments and the intermolecular hydrogen bondings between triol segments. This feature is attributable to the fact that fluoroalkyl segments are solvophobic in aqueous and organic media, and enhance the aggregation due to the strong interaction between fluoroalkyl segments.

Much attention has been paid to the effect of metal ions or surfactants on the swelling equilibrium of polymer gels from both fundamental and technological standpoints.[12, 13] For example, Osada *et al.* reported that poly(2-acryloylamino-2-methyl-1-propanesulfonic acid) gels crosslinked by *N*,*N*′-methylenebisacrylamide have high adsorptive properties against metal ions, such as Cr^{3+} and Co^{2+}.[14] Thus, it is very interesting to study the adsorptive properties against metal ions on the swelling equilibrium of the new fluoroalkylated NAT oligomer hydrogels. In fact, quantitative measurements of the uptake of Cr^{3+} have been tried by the use of fluoroalkylated NAT oligomers. The metal-ion concentration of supernatant liquid after incubation (at 25 °C for 24 h) was spectrophotometrically determined from a calibration curve showing the relationship between the metal-ion concentration and absorbance at 580 nm (Cr^{3+}). These results are shown in Fig. 2-2.

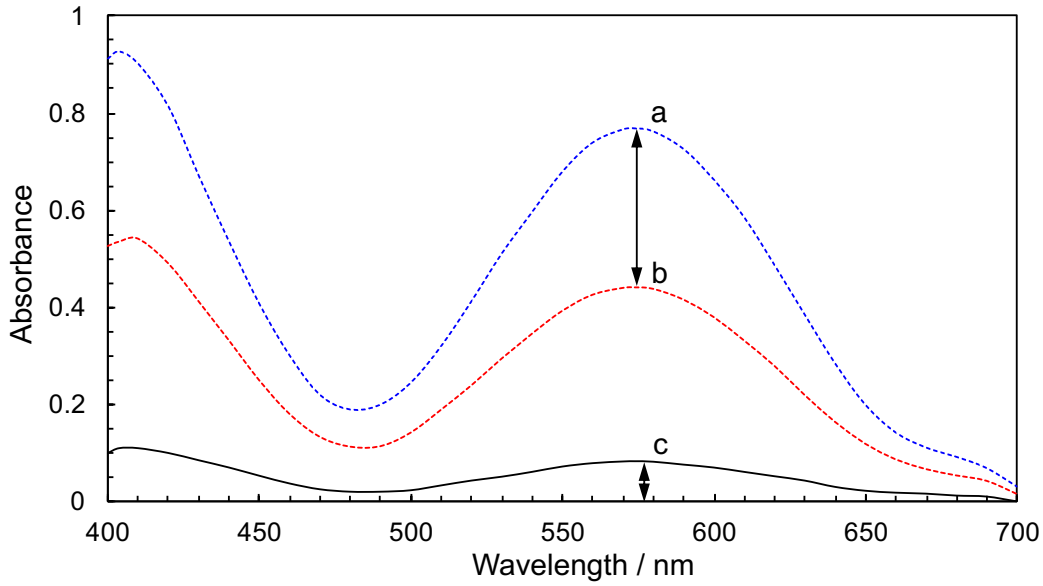

(a) $Cr(NO_3)_3$: 60 mmol dm^{-3}.
(b) Cr^{3+} binding to R_F-$(NAT)_x$-$(CH_2CHSiMe_3)_y$-R_F gel (R_F = C_3F_7; Run 7 in Table 2-1; 6.57 g dm^{-3}).
(c) Cr^{3+} released in water from Cr^{3+} binding to R_F-$(NAT)_x$-$(CH_2CHSiMe_3)_y$-R_F gel.

Figure 2-2 The UV-visible spectra of aqueous solutions of $Cr(NO_3)_3$ in the presence (b) and absence (a) of R_F-$(NAT)_x$-$(CH_2CHSiMe_3)_y$-R_F gel, and the UV-visible spectra of aqueous solutions in the presence of Cr^{3+} binding to R_F-$(NAT)_x$-$(CH_2CHSiMe_3)_y$-R_F gel (c) after the incubation at 25 ºC for 24 h

As shown in Fig. 2-2, there was a decrease (a – b) in the absorbance of Cr^{3+} at 580 nm after the addition of the fluorinated hydrogel. This indicates that the Cr^{3+} ion strongly binds to R_F-$(NAT)_x$-$(CH_2CHSiMe_3)_y$-R_F hydrogel. A similar Cr^{3+} or Co^{2+} binding tendency was observed in poly(2-acryloylamino-2-methyl-1-propanesulfonic acid) gels crosslinked by *N*,*N*′-methylenebisacrylamide.[14)]

More interestingly, as shown in Fig. 2-2, the results on the absorbance of Cr^{3+} released into water (c) and the absorbance of Cr^{3+} binding to gel (a - b) show that Cr^{3+} can be easily

released from Cr^{3+}-bound R_F-(NAT)$_x$-($CH_2CHSiMe_3$)$_y$-R_F hydrogel into water after incubation at 25 °C for 24 h.

Furthermore, the uptake and release of Cr^{3+} by various fluoroalkylated NAT oligomer hydrogels were studied for a wide range of metal-ion concentrations; these results are demonstrated in Figs. 2-3 and 2-4, respectively.

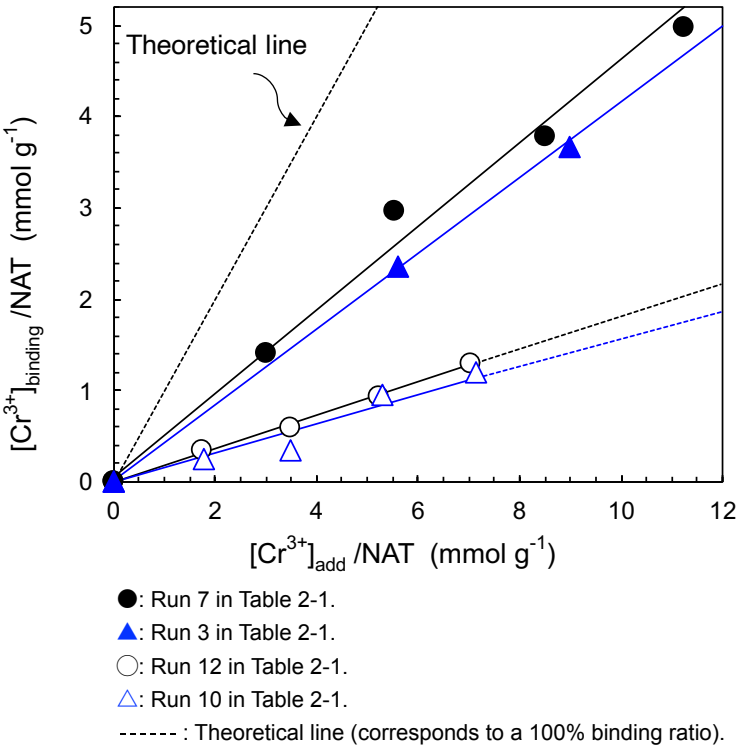

Figure 2-3 Relationship between relative amounts of Cr^{3+} binding to fluoroalkylated NAT oligomer hydrogels and relative amount of initial Cr^{3+}

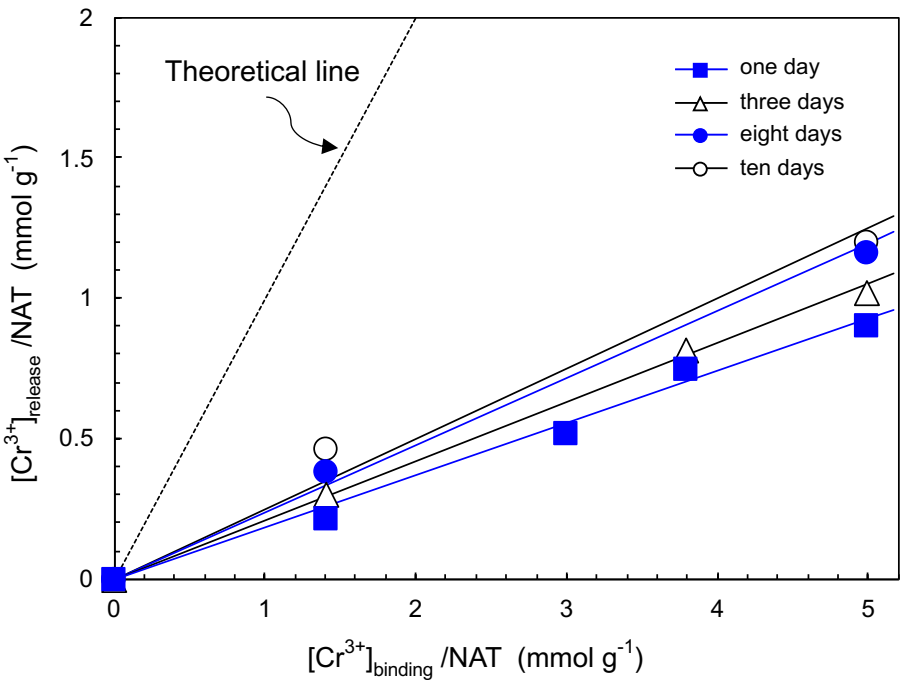

Figure 2-4 Relationship between relative amounts of released Cr^{3+} in water and relative amount of Cr^{3+} binding to Run 7 hydrogel under various incubation conditions.

As shown in Fig. 2-3, the uptake of Cr^{3+} increased linearly with an increase in the initial concentration of Cr^{3+}, and fluorinated hydrogels possessing lower C_{min} values (i.e., Run 7 in Table 2-1: C_{min} = 15 g dm^{-3}) were found to have a stronger Cr^{3+} binding power with ca. 40 % binding ratio (the ratio based on the relative amount of Cr^{3+} binding to gel and relative amount of initial Cr^{3+}).

On the other hand, as shown in Fig. 2-4, the release of Cr^{3+} increased linearly along with an increase in the initial concentration of Cr^{3+} binding to the fluoroalkylated hydrogels; it was clarified that Cr^{3+} can be released from Cr^{3+}-bound fluoroalkylated NAT oligomer hydrogels into water with ca. 18 % (Run 7) or 25 % (Run 3 in Table 2-1: C_{min} = 18 g dm^{-3}; data not shown)

releasing ratio after the incubation at 25 °C for 1 d. This releasing ratio is based on the relative amount of Cr^{3+} released into water and the relative amount of Cr^{3+} binding to gel. Thus, an oligomer hydrogel possessing a lower C_{min} value (Run 7) was clarified to have a lower metal-ion releasing power.

Furthermore, the release of Cr^{3+} from Cr^{3+}-bound fluoroalkylated NAT oligomer hydrogel (Run 7) possessing the lowest C_{min} was studied at 25 °C under various incubation conditions. The results are shown in Fig. 2-4.

As shown in Fig. 2-4, the releasing ratios were found to increase along with an increase in the incubation times from 18 % (1 d) to 24 % (10 d).

Similar results for the uptake and release of Co^{2+} ($CoCl_2$) by fluoroalkylated NAT oligomer hydrogels were obtained under the same spectrometrical conditions at 510 nm, and the uptake and release of Co^{2+} increased linearly with an increase in the initial concentration of Co^{2+} (data not shown), and an increase in the initial concentration of Co^{2+} binding to the hydrogels (data not shown) to afford ca. 50% (Run 7) and ca. 40% (Run 3) binding ratios, and ca. 18% (Run 7) and ca. 23% (Run 3) releasing ratios, respectively.

From these results, it can be said that the fluoroalkylated NAT oligomer hydrogels possessing lower C_{min} values enable the metal ions to bind more strongly to the triol segments in the oligomer networks via the coordinate interaction, since the stronger aggregation of

fluoroalkyl segments and the intermolecular hydrogen bondings are necessary for the establishment of the physical gel network to exhibit lower C_{min} values. In contrast, the metal ions are likely to release easily from metal ions-bound fluorinated hydrogels possessing higher C_{min} values into water. This finding would depend on that the binding of metal ions to oligomer hydrogels is via the coordinate interaction, and the oligomer gels possessing higher C_{min} values have a weaker interaction among the oligomer networks in the gel.

The uptake of Cr^{3+} by fluoroalkylated NAT hydrogel (Run 7) was studied at 25 °C for a wider range (ca. 44 mmol g^{-1}) of Cr^{3+} concentrations than that of Fig. 2-3 in order to determine the binding number of Cr^{3+} to the hydrogel by applying the Langmuir isotherm. The results are shown in Fig. 2-5.

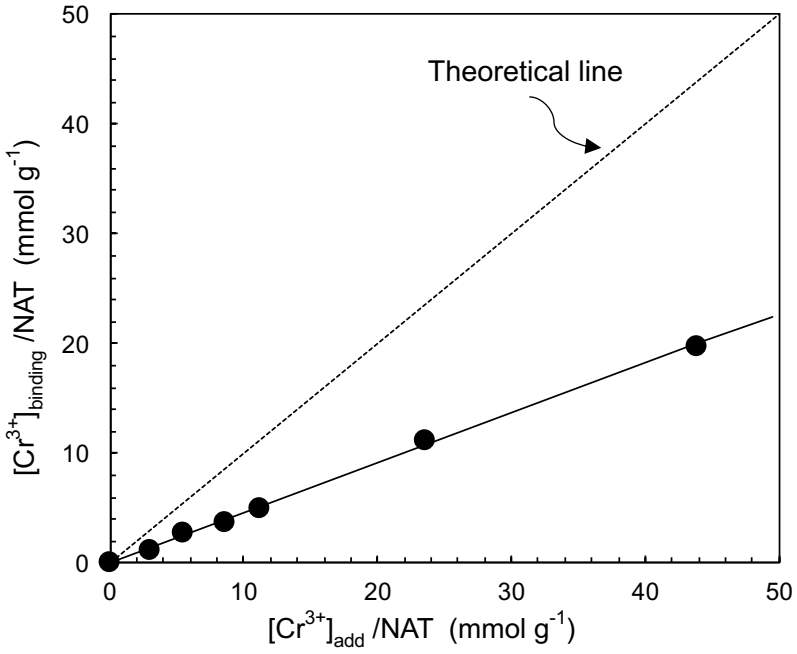

Figure 2-5 Relationship between relative amounts of Cr^{3+} binding to Run 7 hydrogel and relative amount of initial Cr^{3+}

However, as shown in Fig. 2-5, the uptake of Cr^{3+} increased linearly with an increase in the initial concentration of Cr^{3+}. Thus, the following equilibrium reaction should be applicable rather than Langmuir isotherm:

$$m\mathrm{M}^{n+} + \mathrm{R_F\text{-}Gel} \underset{K_2}{\overset{K_1}{\rightleftharpoons}} \mathrm{R_F\text{-}Gel\ (M}^{n+})_m, \qquad (1)$$

where R_F–Gel, M^{n+}, and R_F–Gel $(M^{n+})_m$ denote the fluoroalkylated NAT oligomer hydrogel, metal ion, and the fluoroalkylated NAT oligomer hydrogel with metal ions, respectively.

The equilibrium constant (K) can be then defined as

$$K = \frac{[\mathrm{R_F\text{-}Gel\ (M}^{n+})_m]}{[\mathrm{M}^{n+}]^m\,[\mathrm{R_F\text{-}Gel}]}, \qquad (2)$$

where the brackets signify the equilibrium concentration of the species. Taking into account the fact that the degree of saturation (Y) of metal ion binding is given by

$$Y = \frac{[\mathrm{R_F\text{-}Gel\ (M}^{n+})_m]}{[\mathrm{R_F\text{-}Gel\ (M}^{n+})_m] + [\mathrm{R_F\text{-}Gel}]}, \qquad (3)$$

and also that $[M^{n+}] = C$, we obtain the following relation which is useful in determining the m and K values:

$$\log\left(\frac{Y}{1-Y}\right) = m\log C + \log K\,. \qquad (4)$$

We can determine the m and K values in the Cr^{3+} uptake or release of Run 7 hydrogel

from plots of log [Y/(1–Y)] vs. log C using both Eq. 4 and the results shown in the data for Run 7 hydrogel in Fig. 2-4 (Cr^{3+} release) and Fig. 2-5 (Cr^{3+} uptake).

The m and K values were estimated by means of the slope of each straight line. The m and K_1 values for binding (incubation time: 1 d) estimated by means of the slope of the straight line were 0.9 and 12.3 $dm^3\ g^{-1}$, respectively. In contrast, the m and K_2 values for release estimated by means of the slope of each straight line were shown in Table 2-3.

Table 2-3 The m and K_2 values for release estimated by means of the slope of each straight line

Incubation time / d	m	K_2 / $dm^3\ g^{-1}$
1	1.1	9.2
3	0.9	4.5
8	0.8	4.4
10	1.1	3.0

From these results, it was clarified that one molecule of metal ion was bound to one binding site in the gel. Thus, this result suggests that the metal ions bind only to the oligomer networks lying near to the gel surface due to the presence of a strong hydrophobic fluoroalkyl segment in the oligomers. The equilibrium constants K_2 (9.2 ~ 3.0 $dm^3\ g^{-1}$) were smaller than K_1 value (12.3 $dm^3\ g^{-1}$). This finding corresponds well with the results for the binding and the release ratios of the Run 7 hydrogel in Figs. 2-4 and 2-5.

2.4 Conclusions

It was demonstrated that fluoroalkylated end-capped oligomers containing triol segments can be prepared under very mild conditions by using fluoroalkanoyl peroxides as the key intermediates. Very interestingly, these fluoroalkylated oligomers were found to cause a physical gelation not only in water, but also in organic solvents, whose behavior is governed by the synergistic interaction of strong aggregations of fluoroalkyl segments in oligomers and intermolecular hydrogen bonding between triol segments under non-crosslinked conditions. Thus, it was demonstrated that the aggregation of fluoroalkyl segments in polymeric compounds in water and/or in organic media become a new driving factor for gelation as well as the well-known interactions, such as hydrogen bond and ionic interaction. Hitherto, it is well known that longer fluoroalkylated compounds exhibit a strong repellent property against water or hydrocarbons owing to the strong electronegativity of fluorine. However, since fluoroalkyl groups are introduced into only oligomer end-sites, these fluoroalkyl segments could aggregate easily each other rather than have repellent interactions in aqueous or organic media. In fact, Kunitake *et al*. reported that the fluorocarbon tails in the fluorinated amphiphiles should provide the solovophobic property to form stable bilayer membrances in water[15 ~ 17] and in organic solvents.[18, 19] Thus, such unique aggregate in these media would be remarkably enhanced due to the stability by the self-organization of oligomers to cause gelation in these media.

Additionally, these fluoroalkylated oligomer hydrogels were demonstrated to have not only a metal ion binding, but also a metal-ion releasing power. Especially, these oligomer hydrogels possessing lower C_{min} values had a higher metal binding power, whereas, the hydrogels possessing higher C_{min} values had a higher releasing power. Therefore, these fluoroalkylated oligomers would be applicable to various fields, such as water softening, scale removal, and metal cleaning.

References

1) M. Kozulic, B. Kozulic, and K. Mosbach, *Anal. Biochem.*, **163**, 506 (1987).

2) S. Kitano, K. Kataoka, Y. Koyama, T. Okano, and Y. Sakurai, *Makromol. Chem.*, *Rapid Commun.*, **12**, 227 (1991).

3) S. Kitano, Y. Koyama, K. Kataoka, T. Okano, and Y. Sakurai, *J. Control Release*, **19**, 162 (1992).

4) H. Sawada, *Chem. Rev.*, **96**, 1779 (1996).

5) H. Sawada, S. Katayama, Y. Nakamura, T. Kawase, and Y. Hayakawa, *Polymer*, **39**, 743 (1998).

6) H. Sawada and M. Nakayama, *J. Fluorine Chem.*, **51**, 117 (1990).

7) H. Sawada, M. Yoshida, H. Hagii, K. Aoshima, and M. Kobayashi, *Bull. Chem. Soc. Jpn.*, **59**, 215 (1986).

8) K. Hanabusa, Y. Watanabe, M. Kimura, T. Koyama, and H. Shirai, *Sen'i Gakkaishi*, **52**, 129 (1996).

9) H. Sawada, Y.-F. Gong, Y. Minoshima, T. Matsumoto, M. Nakayama, M. Kosugi, and T. Migita, *J. Chem. Soc.*, *Chem. Commun.*, 537 (1992).

10) H. Sawada, Y. Minoshima, and H. Nakajima, *J. Fluorine Chem.*, **65**, 169 (1993).

11) R. J. Twieg, T. P. Russell, R. Siemens, and J. F. Rabolt, *Macromolecules*, **18**, 1361

(1985).

12) A. R. Khokhlov, E. Y. Kramarenko, E. E. Makhaeva, and S. G. Starodubtzev, *Macromolecules*, **25**, 4779 (1992).

13) H. Inomata, S. Goto, K. Otake, and S. Saito, *Langmuir*, **8**, 1030 (1992).

14) Y. Osada and M. Takase, *Nippon Kagaku Kaishi*, 439 (1983).

15) T. Kunitake, Y. Okahata, and S. Yasunami, *J. Am. Chem. Soc.*, **104**, 5547 (1987).

16) T. Kunitake and N. Higashi, *J. Am. Chem. Soc.*, **107**, 692 (1985).

17) T. Kunitake and N. Higashi, *Macromol. Chem. Phys. Suppl.*, **14**, 81 (1985).

18) Y. Ishikawa, H. Kuwahara, and T. Kunitake, *Chem. Lett.*, 1737 (1989).

19) Y. Ishikawa, H. Kuwahara, and T. Kunitake, *J. Am. Chem. Soc.*, **111**, 8530 (1989).

CHAPTER 3

Synthesis and Properties of Gelling Fluoroalkylated End-Capped Oligomers Containing Hydroxy Segments

3.1 Introduction

Fluorinated polymers are very interesting and useful class of materials due to their unique balance of properties such as low surface free energy, low coefficient of friction, and solvent and chemical resistance.[1, 2] However these fluorinated compounds in general exhibit extremely low solubility in organic solvents. Therefore, it has been deeply desirable to explore highly soluble fluorinated macromolecules possessing excellent properties imparted by fluorine that set them apart from the usual fluorinated polymers. From such points of view, the partially fluorinated polymeric compounds, especially fluoroalkylated end-capped macromolecules with carbon-carbon bond formation, prepared by using fluoroalkanoyl peroxides as key intermediates, were found to exhibit a high solubility in various solvents and an excellent surface active property imparted by fluorine and biological activities, although these polymers have only fluoroalkylated end-capped materials.[3] Partially fluoroalkylated polymers were prepared by a variety of anionic polymerizations[4 ~ 7] and a fluoroalkylated end-capped moiety was introduced through the ester bond[8 ~ 10] to perfluoroalkyl-terminated polymers, and the interesting properties have been reported. In a series of such fluoroalkylated end-capped macromolecules, it was reported that fluoroalkylated end-capped oligomers containing betaine-type segments cause a gelation derived from the synergistical interaction of the aggregations of fluoroalkyl segments and ionic interaction between the betaine-type

segments.[11] Furthermore, in the fluoroalkylated end-capped oligomers containing triol segments, it was demonstrated that the hydrogen bonding interaction between triol segments can be participated in the gelator which is constructed by the fluoroalkyl units.[12] Previously, Tweig *et al.* reported similar gel formation of low-molecular semifluorinated alkanes such as $F(CF_2)_{10}(CH_2)_{12}H$ in hydrocarbon solvents [$H(CH_2)_pH$; p = 8, 10, 12, 14].[13] However, studies on such interesting gelations of polymeric organofluorine compounds have been hitherto very limited except for the recent reports.[11, 12] Therefore, it is very interesting to explore partially fluorinated polymeric compounds which cause gelation through the aggregation of fluoroalkyl segments.

This chapter describes the synthesis and properties of fluoroalkylated end-capped oligomers containing 2-hydroxypropyltrimethylammonium or carboxy(hydroxy)methylamido segments.

3.2 Experimental

3.2.1 Measurements

NMR spectra were measured using a Varian Unity plus 500 (500 MHz) spectrometer, while IR spectra were recorded on a HORIBA FT-300 FT-IR spectrophotometer. Absorption spectra were recorded on a Shimadzu UV-240 spectrophotometer. Solution viscosity was measured by using a falling-sphere Haake Viscometer D1- G.

3.2.2 Materials

A series of fluoroalkanoyl peroxides [$(R_FCOO)_2$] was prepared by reactions of the corresponding acyl halides and hydrogen peroxide in the presence of aqueous sodium hydroxide according to the previously reported methods.[14, 15)] 3-Methacryloxy-2-hydroxypropyltrimethylammonium chloride (MHPTA) was supplied by NOF Corporation. 2-Hydroxy-2-[(1-oxoprop-2-enyl)amino]acetic acid (HOPPA) was purchased from Acros Organics Inc. Chromium(III) nitrate and cobalt(II) chloride were purchased from Wako Chemicals.

3.2.3 General procedure for the synthesis of fluoroalkylated end-capped oligomers

Perfluorobutyryl peroxide (4 mmol) in 1 : 1 mixed solvents (AK-225) of 1,1-dichloro-2,2,3,3,3-pentafluoropropane and 1,3-dichloro-1,2,2,3,3-pentafluoropropane (65 g) was added to an aqueous solution (50%, w/w) of MHPTA (42 mmol). The heterogeneous solution was stirred vigorously at 45 °C for 5 h under nitrogen. After evaporating the solvent, the crude product was reprecipitated from methanol-tetrahydrofuran system to give bis(perfluoropropylated) 3-methacryloxy-2-hydroxypropyltrimethylammonium chloride oligomers (Run 2 in Table 3-1; 6.48 g). This oligomer showed the following spectral data: IR ν (cm^{-1}) 3440 (OH), 1716 (C=O), 1319 (CF_3), 1245 (CF_2); ^1H NMR (D_2O) δ 0.70 ~ 1.10 (CH_3), 1.73 ~ 2.00 (CH_2), 3.07 ~ 3.22 (CH_3), 3.35 ~ 3.50 (CH_2), 3.80 ~ 4.10 (CH_2), 4.40 ~ 4.55 (CH); ^{19}F NMR (D_2O, ext. CF_3CO_2H) δ -5.57 (6F), -43.04 (4F), -52.80 (4F).

The other products obtained exhibited the following spectral characteristics:

R_F-(MHPTA)$_n$-R_F [R_F = C_3F_7; Run 1 in Table 3-1]:

IR ν (cm^{-1}) 3448 (OH), 1716 (C=O), 1319 (CF_3), 1245 (CF_2); ^1H NMR (D_2O) δ 0.70 ~ 1.10 (CH_3), 1.73 ~ 2.00 (CH_2), 3.07 ~ 3.22 (CH_3), 3.35 ~ 3.50 (CH_2), 3.80 ~ 4.10 (CH_2), 4.40 ~ 4.55 (CH); ^{19}F NMR (D_2O, ext. CF_3CO_2H) δ -5.66 (6F), -43.02 (4F), -52.84 (4F).

R_F-(MHPTA)$_n$-R_F [R_F = $CF(CF_3)OC_3F_7$; Run 3 in Table 3-1]:

IR ν (cm^{-1}) 3457 (OH), 1725 (C=O), 1320 (CF_3), 1244 (CF_2); ^1H NMR (D_2O) δ 0.68 ~ 1.10

(CH_3), 1.60 ~ 2.10 (CH_2), 3.05 ~ 3.20 (CH_2), 3.35 ~ 3.50 (CH_2), 3.80 ~ 4.10 (CH_2), 4.43 ~ 4.55 (CH); ^{19}F NMR (D_2O, ext. CF_3CO_2H) δ -5.63 ~ -6.93 (16F), -53.17 (6F).

R_F-(MHPTA)$_n$-R_F [R_F = $CF(CF_3)OC_3F_7$; Run 4 in Table 3-1]:

IR ν (cm^{-1}) 3457 (OH), 1727 (C = O), 1321 (CF_3), 1241 (CF_2); ^1H NMR (D_2O) δ 0.68 ~ 1.11 (CH_3), 1.61 ~ 2.15 (CH_2), 3.05 ~ 3.19 (CH_3), 3.31 ~ 3.54 (CH_2), 3.79 ~ 4.19 (CH_2), 4.43 ~ 4.55 (CH); ^{19}F NMR (D_2O, ext. CF_3CO_2H) δ -5.63 ~ -6.93 (16F), -53.25 (6F).

R_F-(MHPTA)$_n$-R_F [R_F = $CF(CF_3)OC_3F_7$; Run 5 in Table 3-1]:

IR ν (cm^{-1}) 3455 (OH), 1727 (C=O), 1310 (CF_3), 1242 (CF_2); ^1H NMR (D_2O) δ 0.68 ~ 1.12 (CH_3), 1.62 ~ 2.18 (CH_2), 3.08 ~ 3.22 (CH_3), 3.38 ~ 3.55 (CH_2), 3.80 ~ 4.14 (CH_2), 4.43 ~ 4.60 (CH); ^{19}F NMR (D_2O, ext. CF_3CO_2H) δ -5.61 ~ -6.72 (16F), -53.04 (6F).

R_F-(MHPTA)$_n$-R_F [R_F = $CF(CF_3)OC_3F_7$; Run 6 in Table 3-1]:

IR ν (cm^{-1}) 3464 (OH), 1724 (C=O), 1320 (CF_3), 1242 (CF_2); ^1H NMR (D_2O) δ 0.60 ~ 1.13 (CH_3), 1.66 ~ 2.12 (CH_2), 3.06 ~ 3.33 (CH_3), 3.34 ~ 3.55 (CH_2), 3.80 ~ 4.12 (CH_2), 4.40 ~ 4.57 (CH); ^{19}F NMR (D_2O, ext. CF_3CO_2H) δ -5.66 ~ -6.65 (16F), -53.61 (6F).

R_F-(MHPTA)$_n$-R_F [R_F = $CF(CF_3)OC_3F_7$; Run 7 in Table 3-1]:

IR ν (cm^{-1}) 3438 (OH), 1724 (C=O), 1319 (CF_3), 1257 (CF_2); ^1H NMR (D_2O) δ 0.50 ~ 1.20 (CH_3), 1.22 ~ 2.38 (CH_2), 3.38 ~ 3.37 (CH_3), 3.38 ~ 3.55 (CH_2), 3.80 ~ 4.22 (CH_2), 4.30 ~ 4.55 (CH); ^{19}F NMR (D_2O, ext. CF_3CO_2H) δ -5.58 ~ -7.43 (16F), -53.59 (6F).

R_F-(MHPTA)$_n$-R_F [R_F = $CF(CF_3)OCF_2CF(CF_3)OC_3F_7$; Run 8 in Table 3-1]:

IR ν (cm^{-1}) 3462 (OH), 1715 (C=O), 1317 (CF_3), 1245 (CF_2); ^{1}H NMR (D_2O) δ 0.60 ~ 1.10 (CH_3), 1.70 ~ 2.10 (CH_2), 3.05 ~ 3.24 (CH_3), 3.34 ~ 3.51 (CH_2), 3.80 ~ 4.11 (CH_2), 4.42 ~ 4.51 (CH); ^{19}F NMR (D_2O, ext. CF_3CO_2H) δ -5.76 ~ -8.20 (26F), -53.04 (6F), -70.93 (2F).

R_F-(MHPTA)$_n$-R_F [R_F = $CF(CF_3)OCF_2CF(CF_3)OC_3F_7$; Run 9 in Table 3-1]:

IR ν (cm^{-1}) 3436 (OH), 1727 (C=O), 1323 (CF_3), 1257 (CF_2); ^{1}H NMR (D_2O) δ 0.65 ~ 1.13 (CH_3), 1.70 ~ 2.20 (CH_2), 3.05 ~ 3.25 (CH_3), 3.35 ~ 3.53 (CH_2), 3.80 ~ 4.05 (CH_2), 4.32 ~ 4.55 (CH); ^{19}F NMR (D_2O, ext. CF_3CO_2H) δ -5.76 ~ -7.84 (26F), -53.01 (6F), -70.64 (2F).

R_F-(MHPTA)$_x$-(CH_2-$CHSiMe_3$)$_y$-R_F [R_F = $CF(CF_3)OC_3F_7$; Run 17 in Table 3-2]:

IR ν (cm^{-1}) 3428 (OH), 1724 (C=O), 1257 (CF_2), 863 (Si-CH_3); ^{1}H NMR (D_2O) δ -0.20 ~ 0 (Si-CH_3), 0.65 ~ 1.10 (CH_3, CH), 1.70 ~ 2.18 (CH_2), 3.07 ~ 3.21 (CH_3), 3.35 ~ 3.48 (CH_2), 3.80 ~ 4.12 (CH_2), 4.34 ~ 4.56 (CH); ^{19}F NMR (D_2O, ext. CF_3CO_2H) δ -5.48 ~ -7.53 (16F), -53.01 (6F).

R_F-(MHPTA)$_x$-(CH_2-$CHSiMe_3$)$_y$-R_F [R_F = $CF(CF_3)OCF_2CF(CF_3)OC_3F_7$; Run 18 in Table 3-2]:

IR ν (cm^{-1}) 3467 (OH), 1730 (C=O), 1323 (CF_3), 1245 (CF_2), 860 (Si-CH_3); ^{1}H NMR (D_2O) δ -0.30 ~ 0 (Si-CH_3), 0.65 ~ 1.15 (CH_3, CH), 1.70 ~ 2.20 (CH_2), 3.07 ~ 3.25 (CH_3), 3.35 ~ 3.60 (CH_2), 3.80 ~ 4.13 (CH_2), 4.40 ~ 4.60 (CH); ^{19}F NMR (D_2O, ext. CF_3CO_2H) δ -5.56 ~ -7.92

(26F), -53.04 (6F), -70.50 (2F).

Similarly, a series of fluoroalkylated end-capped HOPPA oligomers was prepared by oligomerization with fluoroalkanoyl peroxides, and exhibited the following spectral characteristics:

R_F-(HOPPA)$_n$-R_F [R_F = C_3F_7; Run 10 in Table 3-1]:

IR ν (cm^{-1}) 3471 (OH), 3164 (NH), 1736, 1648 (C=O), 1313 (CF_3), 1261 (CF_2); ^{1}H NMR (D_2O) δ 0.90 ~ 2.40 (CH_2, CH), 5.10 ~ 5.57 (CH); ^{19}F NMR (D_2O, ext. CF_3CO_2H) δ -5.63, -7.77 (6F), -43.17, -45.48 (4F), -53.74, 54.65 (4F).

R_F-(HOPPA)$_n$-R_F [R_F = $CF(CF_3)OC_3F_7$; Run 11 in Table 3-1]:

IR ν (cm^{-1}) 3465 (OH), 3187 (NH), 1745, 1658 (C=O), 1336 (CF_3), 1257 (CF_2); ^{1}H NMR (D_2O) δ 0.98 ~ 2.48 (CH_2, CH), 5.09 ~ 5.62 (CH); ^{19}F NMR (D_2O, ext. CF_3CO_2H) δ -6.96 ~ -7.76 (16F), -54.15 (6F).

R_F-(HOPPA)$_n$-R_F [R_F = $CF(CF_3)OC_3F_7$; Run 12 in Table 3-1]:

IR ν (cm^{-1}) 3457 (OH), 3195 (NH), 1747, 1662 (C=O), 1334 (CF_3), 1226 (CF_2); ^{1}H NMR (D_2O) δ 0.80 ~ 2.51 (CH_2, CH), 5.15 ~ 5.81 (CH); ^{19}F NMR (D_2O, ext. CF_3CO_2H) δ -5.76 ~ -7.76 (16F), -54.21 (6F).

R_F-(HOPPA)$_n$-R_F [R_F = $CF(CF_3)OC_3F_7$; Run 13 in Table 3-1]:

IR ν (cm^{-1}) 3457 (OH), 3181 (NH), 1743, 1653 (C=O), 1255 (CF_2); ^{1}H NMR (D_2O) δ 0.96 ~

2.49 (CH_2, CH), 5.01 ~ 5.80 (CH); ^{19}F NMR (D_2O, ext. CF_3CO_2H) δ -4.43 ~ -8.62 (16F), -55.53 (6F).

R_F-(HOPPA)$_n$-R_F [R_F = $CF(CF_3)OCF_2CF(CF_3)OC_3F_7$; Run 14 in Table 3-1]:

IR ν (cm^{-1}) 3465 (OH), 3178 (NH), 1753, 1670 (C=O), 1338 (CF_3), 1240 (CF_2); ^1H NMR (D_2O) δ 0.93 ~ 2.48 (CH_2, CH), 5.00 ~ 5.63 (CH); ^{19}F NMR (D_2O, ext. CF_3CO_2H) δ -5.76 ~ -7.06 (26F), -53.77 ~ -54.68 (6F), -74.98 (2F).

R_F-(HOPPA)$_n$-R_F [R_F = $CF(CF_3)OCF_2CF(CF_3)OC_3F_7$; Run 15 in Table 3-1]:

IR ν (cm^{-1}) 3432 (OH), 3195 (NH), 1745, 1660 (C=O), 1335 (CF_3), 1249 (CF_2); NMR spectra were not measured due to gelling (highly viscoelastic) of the sample.

R_F-(HOPPA)$_n$-R_F [R_F = $CF(CF_3)OCF_2CF(CF_3)OC_3F_7$; Run 16 in Table 3-1]:

IR ν (cm^{-1}) 3465 (OH), 3178 (NH), 1743, 1662 (C=O), 1338 (CF_3), 1240 (CF_2); NMR spectra were not measured due to gelling (highly viscoelastic) of the sample.

R_F-(HOPPA)$_x$-(CH_2-$CMeCO_2Me$)$_y$-R_F [R_F = $CF(CF_3)OC_3F_7$; Run 19 in Table 3-2]:

IR ν (cm^{-1}) 3463 (OH), 3184 (NH), 1747, 1662 (C=O), 1325 (CF_3), 1240 (CF_2); ^1H NMR (D_2O) δ 0.88 ~ 2.89 (CH_2, CH_3, CH), 3.57 ~ 3.67 (CH_3), 5.15 ~ 5.50 (CH); ^{19}F NMR (D_2O, ext. CF_3CO_2H) δ -5.82 ~ -7.66 (16F), -54.23 (6F).

R_F-(HOPPA)$_x$-(CH_2-$CMeCO_2Me$)$_y$-R_F [R_F = $CF(CF_3)OC_3F_7$; Run 20 in Table 3-2]:

IR ν (cm^{-1}) 3463 (OH), 3180 (NH), 1738, 1676 (C=O), 1327 (CF_3), 1242 (CF_2); ^1H NMR (D_2O)

δ 0.99 ~ 2.70 (CH_2, CH_3, CH), 3.47 ~ 3.63 (CH_3), 5.10 ~ 5.64 (CH); ^{19}F NMR (D_2O, ext. CF_3CO_2H) δ -5.76 ~ -6.88 (16F), -54.36 (6F).

3.2.4 Viscosity measurements

Viscosity of aqueous solution of fluoroalkylated end-capped MHPTA oligomers was measured at 30 °C using a falling-sphere viscometer (Haake Viscometer D1-G).

3.2.5 A typical procedure for gelation test

The procedure for studying the gel-formation ability was essentially that of Hanabusa *et al*.[16, 17] Briefly, weighed fluoroalkylated end-capped oligomer was mixed with water or organic fluid in a tube. The mixture was treated under ultrasonic conditions until the solid was dissolved. The resulting solution was kept at 30 °C for 1 h, and gelation was checked visually. The gel was stable and the tube could be inverted without changing the shape of the gel.

3.2.6 Metal ions binding or releasing by fluoroalkylated end-capped oligomer hydrogels

Fluoroalkylated end-capped oligomer hydrogels were swollen with water in a measuring flask. After the addition of the required amount of aqueous metal ion solution into the flask, the flask was allowed to stand for 1 day at 25 °C. The metal-ion concentration of supernatant liquid after incubation was spectrophotometrically determined.

Metal ion was released from the metal binding to the hydrogel into water for 1 day at 25 °C, and its concentration in the supernatant liquid was determined spectrophotometrically.

3.3 Results and discussion

Reactions of fluoroalkanoyl peroxides with methacrylate monomer containing trimethylammonium and hydroxy segments (MHPTA) were found to proceed under very mild conditions to afford fluoroalkylated end-capped 3-methacryloxy-2-hydroxypropyltrimethylammonium chloride oligomers as shown in Scheme 3-1.

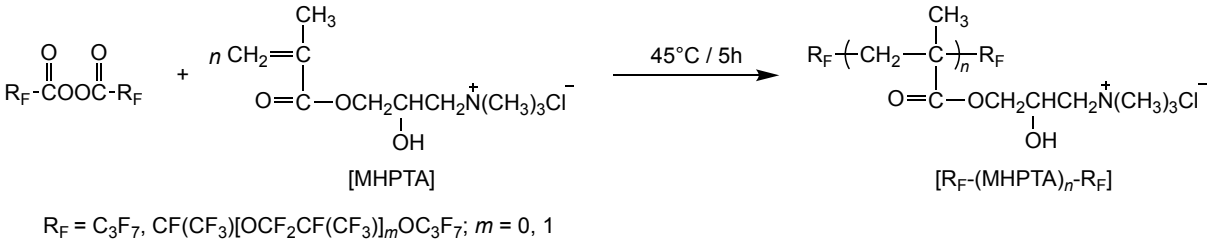

Scheme 3-1 Synthesis of R_F-(MHPTA)$_n$-R_F homo-oligomers at 45 ºC for 5 h

A series of fluoroalkylated end-capped oligomers containing hydroxy and carboxy segments were synthesized by reactions of fluoroalkanoyl peroxides with 2-hydroxy-2-[(1-oxoprop-2-enyl)amino]acetic acid [HOPPA] as shown in Scheme 3-2.

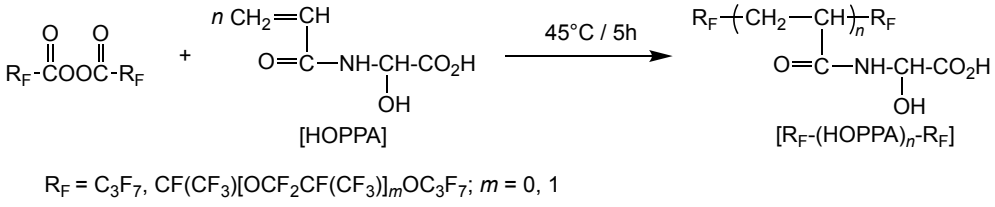

Scheme 3-2 Synthesis of R_F-(HOPPA)$_n$-R_F homo-oligomers at 45 ºC for 5 h

The results of the reactions of fluoroalkanoyl peroxides with MHPTA or HOPPA are summarized in Table 3-1.

Table 3-1 Reactions of fluoroalkanoyl peroxides with MHPTA (or HOPPA)

Run	R_F in peroxide / mmol		MHPTA or HOPPA / mmol	Product Yield / %[a)]	Product $\overline{M}_n(\overline{M}_w/\overline{M}_n)$
			MHPTA	R_F-(MHPTA)$_n$-R_F	
1	C_3F_7	4	21	21	2630 (3.02)
2	C_3F_7	4	42	30	2060 (3.86)
3	$CF(CF_3)OC_3F_7$	4	11	17	6760 (11.0)
4	$CF(CF_3)OC_3F_7$	5	25	36	—
5	$CF(CF_3)OC_3F_7$	4	42	12	—
6	$CF(CF_3)OC_3F_7$	4	65	39	—
7	$CF(CF_3)OC_3F_7$	4	85	25	—
8	$CF(CF_3)OCF_2CF(CF_3)OC_3F_7$	4	22	32	—
9	$CF(CF_3)OCF_2CF(CF_3)OC_3F_7$	4	43	88	—
			HOPPA	R_F-(HOPPA)$_n$-R_F	
10	C_3F_7	4	41	83	—
11	$CF(CF_3)OC_3F_7$	4	8	8	—
12	$CF(CF_3)OC_3F_7$	4	20	20	—
13	$CF(CF_3)OC_3F_7$	5	50	71	—
14	$CF(CF_3)OCF_2CF(CF_3)OC_3F_7$	3	5	15	—
15	$CF(CF_3)OCF_2CF(CF_3)OC_3F_7$	3	13	50	—
16	$CF(CF_3)OCF_2CF(CF_3)OC_3F_7$	3	26	85	—

a) Yields based on starting materials [MHPTA (or HOPPA)] and the decarboxylated peroxide unit (R_F-R_F).

Fluoroalkylated end-capped MHPTA or HOPPA co-oligomers were also synthesized by the use of co-monomers such as trimethylvinylsilane and methyl methacrylate as shown in

Scheme 3-3 and Table 3-2.

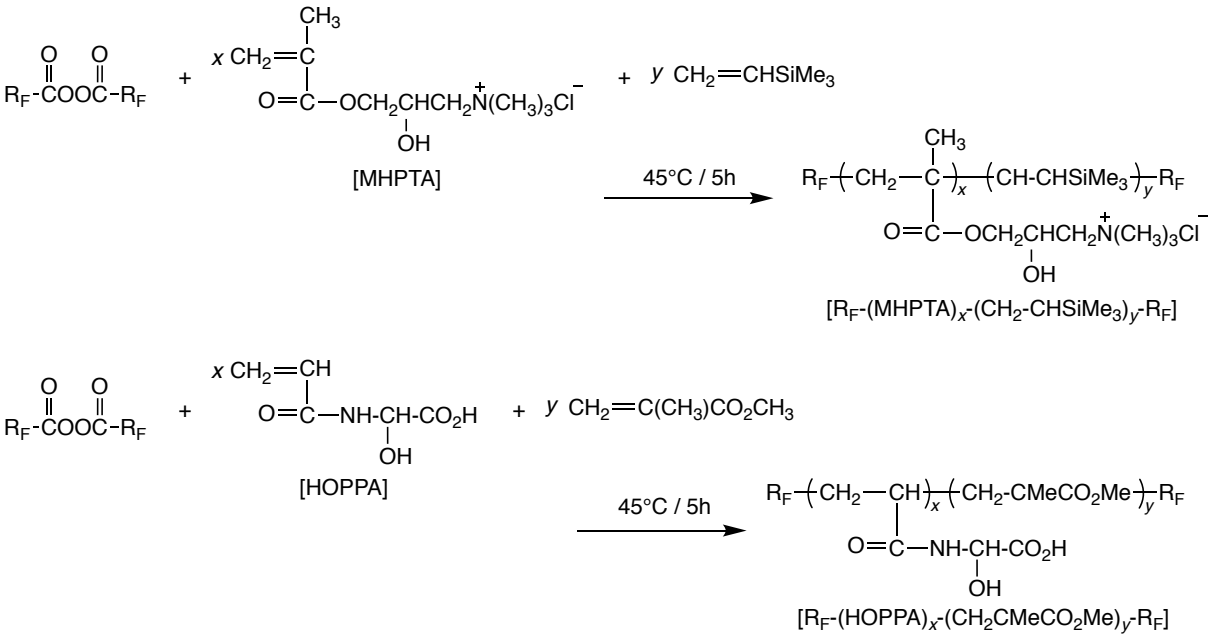

R_F = C_3F_7, $CF(CF_3)[OCF_2CF(CF_3)]_mOC_3F_7$; m = 0, 1

Scheme 3-3 Synthesis of R_F-(MHPTA)$_x$-(CH$_2$-CHSiMe$_3$)$_y$-R_F co-oligomers and R_F-(HOPPA)$_x$-(CH$_2$-CMeCO$_2$Me)$_y$-R_F co-oligomers

Table 3-2 Reactions of fluoroalkanoyl peroxides with MHPTA (or HOPPA) and trimethylvinylsilane (or methyl methacrylate)

Run	R_F in peroxide		MHPTA or HOPPA	Co-monomer	Product	
	/ mmol		/ mmol	/ mmol	Yield / %[a]	x : y[b]
			MHPTA	CH_2=CHSiMe$_3$	R_F-(MHPTA)$_x$-(CH$_2$-CHSiMe$_3$)$_y$-R_F	
17	$CF(CF_3)OC_3F_7$	4	17	8	31	96 : 4
18	$CF(CF_3)OCF_2CF(CF_3)OC_3F_7$	4	16	8	27	95 : 5
			HOPPA	CH_2=CMeCO$_2$Me	R_F-(HOPPA)$_x$-(CH$_2$CMeCO$_2$Me)$_y$-R_F	
19	$CF(CF_3)OC_3F_7$	4	8	8	45	70 : 30
20	$CF(CF_3)OC_3F_7$	4	13	84	9	30 : 70

a) Yields based on starting materials [MHPTA (or HOPPA), trimethylvinylsilane (or methyl methacrylate)] and the decarboxylated peroxide unit (R_F-R_F).
b) Co-oligomerization ratio determined by ^{1}H NMR.

As Tables 3-1 and 3-2 show, perfluoropropylated and some perfluoro-oxaalkylated MHPTA or HOPPA homo- and co-oligomers were obtained in excellent to moderate isolated yields under very mild conditions. The yields of perfluoro-1-methyl-2-oxapentylated MHPTA oligomers (Runs 3 ~ 7 in Table 3-1) and perfluoro-1-methyl-2-oxa-pentylated HOPPA-methyl methacrylate co-oligomers (Runs 19, 20 in Table 3-2) are not dependent upon the molar ratios of monomers and peroxides, but possibly on homo- and co-oligomerization of MHPTA (or HOPPA) with peroxides that are heterogeneous systems including water.

In these fluoroalkylated end-capped oligomers, perfluoropropylated and perfluoro-1-methyl-2-oxapentylated MHPTA oligomers (Runs 1, 2, 3 in Table 3-1) were soluble in water, and molecular weights were measured by GPC (gel permeation chromatography) analysis calibrated with standard poly(ethylene glycol) using 30% acetonitrile solution containing 0.5 M acetic acid and 0.5 M sodium acetate as the eluent [$\overline{Mn}$($\overline{Mw}$/$\overline{Mn}$) = 2630 (3.02) (Run 1); 2060 (3.86) (Run 2); 6760 (11.0) (Run 3)]. In perfluoro-1-methyl-2-oxapentylated MHPTA oligomers, the oligomers with greater molar ratios of MHPTA in MHPTA/peroxide (Runs 4 ~ 9) became "gel-like" or formed gels with water and polar organic solvents such as methanol, ethanol, dimethylformamide and dimethyl sulfoxide, and their molecular weights were unable to measure owing to the highly viscoelastic fluids or the gel formation. Both perfluoropropylated and perfluoro-oxaalkylated HOPPA oligomers were found to cause

gelation with water, dimethylformamide and dimethyl sulfoxide under the non-crosslinked conditions, and the molecular weight of all oligomers were not determined by GPC measurements. It is important to note that corresponding non-fluorinated MHPTA or HOPPA oligomer [-(MHPTA)$_n$- or -(HOPPA)$_n$-] forms no gels with these solvents, and these non-fluorinated oligomers are completely soluble in these solvents.

Perfluoro-1-methyl-2-oxapentylated end-capped MHPTA-trimethylvinylsilane co-oligomer (Run 17) in Table 3-2 formed highly viscoelastic fluid (gel-like) in water and polar organic solvents such as MeOH, EtOH, *N,N*-dimethylformamide (DMF), and dimethyl sulfoxide (DMSO), and longer perfluoro-oxaalkylated co-oligomer (Run 18) in Table 3-2 was shown to cause gelation in these solvents. Fluoroalkylated HOPPA-methylmethacrylate co-oligomer (Run 19) in Table 3-2 caused gelation in water, DMF, and DMSO. In contrast, fluoroalkylated HOPPA co-oligomer (Run 20) was insoluble in water, and cause gelation only in organic polar solvents such as DMF and DMSO. This would depend upon higher oleophilic property than the corresponding co-oligomer (Run 19).

To study the unique gelation of these fluorinated oligomers under non-crosslinked conditions, the viscosity of aqueous solutions of gel-like perfluoro-1-methyl-2-oxapentylated MHPTA oligomer (Run 5) and soluble perfluoropropylated MHPTA oligomer (Run 2) was measured at 30 ºC. The results are shown in Figure 3-1.

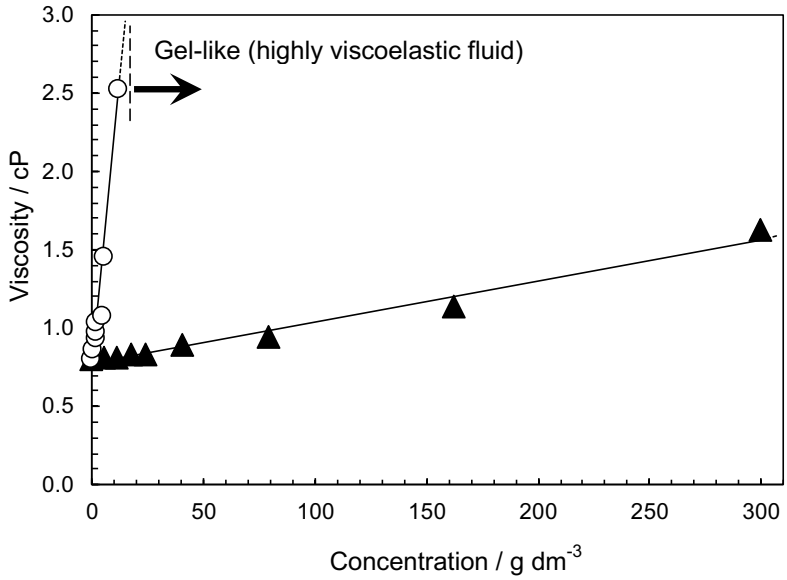

Figure 3-1 Effects of concentration on viscosity of R_F-(MHPTA)$_n$-R_F at 30 °C

As shown in Figure 3-1, the viscosity of perfluoropropylated MHPTA oligomer (Run 2) did not increase remarkably with concentrations, and gels or highly viscoelastic fluids did not form even under a higher concentration (300 g dm^{-3}). In contrast, the viscosity of perfluoro-1-methyl-2-oxapentylated MHPTA oligomer (Run 5) increased remarkably with concentration, and the viscosity was not measured owing to the formation of highly viscoelastic fluids (gel-like) above *ca.* 10 g dm^{-1}. These results suggest that interactions of the aggregation of longer fluoroalkyl segments become stronger to establish highly viscous gel-like fluid or a physical gel network. For low-molecular compounds, Hanabusa *et al.* reported a similar remarkable rise of viscosity of organic solvents containing trialkyl-1,3,5-benzenetricarboxyamides to that of aqueous solutions of the present fluorinated oligomer in Figure 3-1 and intermolecular hydrogen bonding as the main driving force for the gelation.[18)]

The gelation ability of fluoroalkylated end-capped MHPTA or HOPPA homo- and co-oligomers was also studied by measuring minimum concentrations (C_{min}) of these oligomers necessary for gelation in water, MeOH and DMSO at 30°C according to the method reported of Hanabusa *et al.*,[16, 17] and the results are summarized in Table 3-3.

Table 3-3 Minimum gel concentration (c_{min}) of fluoroalkylated MHPTA (or HOPPA) homo- and co-oligomers (in g per dm^3 solvent) for gelation at 30 °C

Run [a]	R_F in oligomer	C_{min} [b] / g dm^{-3} (gelator/midium)		
		H_2O	MeOH	DMSO
	R_F-(MHPTA)$_n$-R_F			
1	C_3F_7	Soln	Soln	Soln
2	C_3F_7	Soln	Soln	Soln
3	$CF(CF_3)OC_3F_7$	Soln	Soln	Soln
4	$CF(CF_3)OC_3F_7$	Gel-like	Gel-like	Gel-like
5	$CF(CF_3)OC_3F_7$	Gel-like	Gel-like	Gel-like
6	$CF(CF_3)OC_3F_7$	102	121	191
7	$CF(CF_3)OC_3F_7$	7	15	30
8	$CF(CF_3)OCF_2CF(CF_3)OC_3F_7$	330	Gel-like	Gel-like
9	$CF(CF_3)OCF_2CF(CF_3)OC_3F_7$	51	84	102
	R_F-(HOPPA)$_n$-R_F			
10	C_3F_7	88	—	145
11	$CF(CF_3)OC_3F_7$	100	—	147
12	$CF(CF_3)OC_3F_7$	93	—	87
13	$CF(CF_3)OC_3F_7$	91	—	—
14	$CF(CF_3)OCF_2CF(CF_3)OC_3F_7$	94	—	151
15	$CF(CF_3)OCF_2CF(CF_3)OC_3F_7$	87	—	—
16	$CF(CF_3)OCF_2CF(CF_3)OC_3F_7$	53	—	119
	R_F-(MHPTA)$_x$-(CH_2-CHSiMe_3)$_y$-R_F			
17	$CF(CF_3)OC_3F_7$	Gel-like	Gel-like	Gel-like
18	$CF(CF_3)OCF_2CF(CF_3)OC_3F_7$	255	330	Gel-like
	R_F-(HOPPA)$_x$-(CH_2CMeCO_2Me)$_y$-R_F			
19	$CF(CF_3)OC_3F_7$	89	—	262
20	$CF(CF_3)OC_3F_7$	—	—	125

a) Each different from those in Table 3-1 and 3-2.
b) Gel-like = highly viscoelastic fluid.

As shown in Table 3-3, C_{min}s of a series of fluoroalkylated homo- and co-oligomers necessary to gel one liter of water, MeOH, and DMSO was 7 ~ 330 g dm^{-3}, and oligomers with greater molar ratios of MHPTA (Runs 1, 2; Runs 3 ~ 7; Runs 8, 9) or HOPPA (Runs 11 ~ 13; Runs 14 ~ 16) in MHPTA (or HOPPA)/peroxide or longer perfluoro-oxaalkylated oligomers exhibited higher gelling ability. These results strongly suggest that the main driving force for gelation is the synergistic interactions with the aggregation of fluoroalkyl units in oligomers and intermolecular hydrogen bonding between hydroxy segments or carboxy segments including the interactions of hydroxy (-OH) and trimethylammonium ($-N^+Me_3$) segments. Oligomers with longer fluoroalkyl segments and greater molar ratios of monomer in monomer/peroxide are likely to have stronger association through aggregation of fluoroalkyl moieties and intermolecular hydrogen bondings between hydroxy or carboxy segments to cause physical gelation. In particular, fluorinated HOPPA oligomers possessing perfluoropropyl and perfluoro-1-methyl-2-oxapentyl segments (Runs 10, 11 in Table 3-3) caused gelation in water and DMSO. The corresponding MHPTA oligomers (Runs 2, 3 in Table 3-3) were soluble in these solvents. Hydrogen bonding interactions between hydroxy or carboxy segments in HOPPA oligomers may thus become stronger than those between hydroxy segments in MHPTA oligomers when fluorinated oligomers form gels in these solvents.

The fluoroalkylated end-capped MHPTA or HOPPA oligomers form gels not only in

water but also in organic polar solvents such as MeOH, EtOH, DMF, and DMSO under non-crosslinked conditions, since fluoroalkyl segments are solvophobic in aqueous and organic media, and enhance the aggregation due to the strong interaction between fluoroalkyl end-capped segments in oligomers. Fluoroalkyl segments in the double-chain amphiphiles possessing long perfluoroalkyl chains in the hydrophobic portion such as $\{[CF_3(CF_2)_7\text{-}CH_2CH_2C(=O)OCH_2CH_2]_2N\text{-}C(=O)CH_2N^+Me_3Cl^-\}$ should provide the solvophobic property to form stable bilayer membrances in water and organic solvents.[19 ~ 23] Thus, such unique aggregate of fluoroalkyl segments in these media would be remarkably enhanced due to the stability by the self-organization of oligomers to cause gelation. It was clarified that non-fluorinated MHPTA or HOPPA oligomers do not form gels either in water or polar organic solvents. This suggests that only hydrogen bonding interactions cannot be involved in physical gelation, and the aggregation of fluoroalkylated end-capped segments is essential for gelation.

It is of particular interest to clarify the surface properties of these gelling or gel-like oligomers. Thus, the reduction of surface tension of aqueous solutions of gel-like perfluoro-1-methyl-2-oxapentylated MHPTA oligomers (Run 5 in Table 3-1) was measured with the Wilhelmy plate method at 30°C. The surface tension of aqueous solutions of non-fluorinated MHPTA oligomers was also measured for comparison. The results are shown

in Figure 3-2.

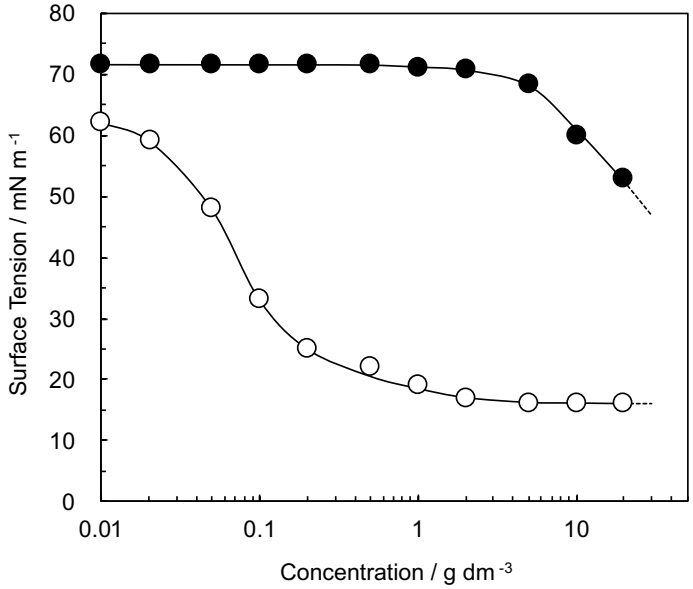

Figure 3-2 Surface tension of aqueous solutions of R_F-(MHPTA)$_n$-R_F (○: Run 5) and -(MHPTA)$_n$- (●) at 30 ºC.

As shown in Figure 3-2, significant decrease in the surface tension of water, around 15 mN m^{-1}, was found for this gel-like fluorinated oligomer in contrast to the corresponding non-fluorinated oligomer. This fluorinated oligomer exhibited a clear break point resembling a CMC (critical micell concentration). This indicates the formation of molecular aggregate, that is, the formation of macromolecular aggregates (gel-like). Thus, these fluoroalkylated end-capped oligomers should interact with aggregations of fluoroalkyl segments as well as have surface active property imparted by fluorine.

Hitherto, much attention has been focused on the uptake or release of metal ions by chemically crosslinked polymer gels. Osada *et al.* reported the adsorptive properties against

metal ions on the swelling equilibrium of polymer gels.[24] Therefore, it is much interesting to study the adsorptive properties against metal ions on the swelling equilibrium of the new fluoroalkylated end-capped MHPTA or HOPPA oligomer hydrogels. Thus, the uptake and release of Cr^{3+} and Co^{2+} by these oligomer hydrogels were studied for a wide range of metal-ion concentrations (15 ~ 60 mmol dm^{-3}). The metal-ion concentration of supernatant liquid after the incubation (at 25°C for 24 h) was spectrophotometrically determined from a calibration curve showing the relationship between metal ion concentration and absorbance at 580 nm (Cr^{3+}) or 510 nm (Co^{2+}). The results are shown in Figures 3-3 and 3-4, respectively.

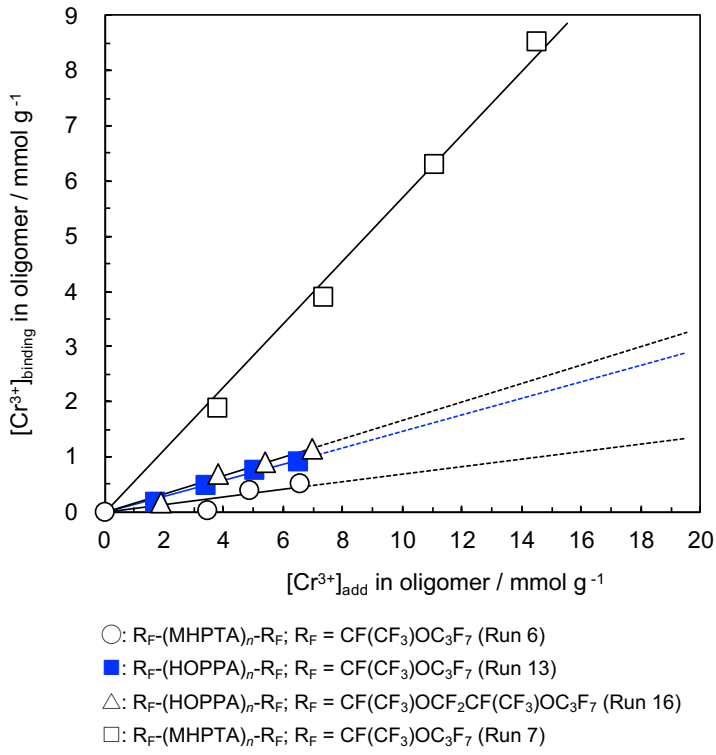

Figure 3-3 Relationship between relative amounts of Cr^{3+} binding to fluoroalkylated oligomers and initial Cr^{3+}.

.

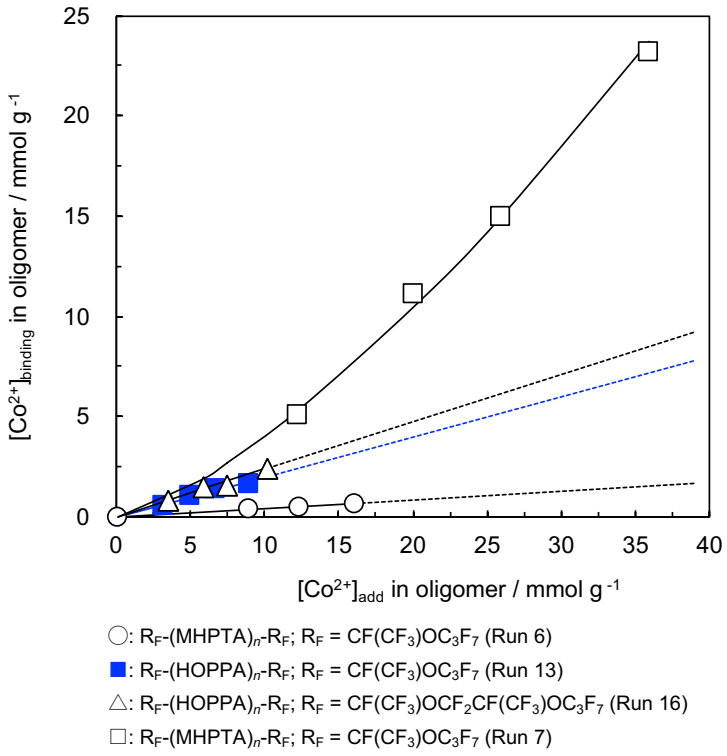

Figure 3-4 Relationship between relative amounts of Co^{2+} binding to fluoroalkylated oligomers and initial Co^{2+}.

As shown in Figures 3-3 and 3-4, the uptake of Cr^{3+} or Co^{2+} increased linearly with initial concentration of Cr^{3+} or Co^{2+}. Fluorinated hydrogels possessing lower C_{min} values (*i.e.*, Run 7: C_{min} = 7 g dm^{-3}) had stronger binding power with *ca.* 60% binding ratio [ratio based on relative amount of Cr^{3+} (or Co^{2+}) binding to gel ($[Cr^{3+}]_{binding}$/oligomer) and relative amount of initial Cr^{3+} ($[Cr^{3+}]_{add}$/oligomer)]. R_F-$(MHPTA)_n$-R_F (Run 6 in Table 3-1) hydrogel possessing higher C_{min} than Run 7 in Table 3-1 had weaker Cr^{3+} and Co^{2+} binding power (*ca.* 10% and *ca.* 5% binding ratios, respectively) under the similar conditions. R_F-$(HOPPA)_n$-R_F (Run 16 and 13 in Table 3-1) hydrogels had Cr^{3+} binding power (*ca.* 17% and *ca.* 15% binding ratios, respectively)

as shown in Figure 3-3, and the hydrogel (Run 16) possessing lower C_{min} had a slightly higher metal binding power. Similar results for the uptake of Co^{2+} by R_F-$(HOPPA)_n$-R_F were obtained as in Figure 3-4, and there was no uptake selectivity of the fluorinated hydrogels for these metal ions. From these results, it can be said that the fluoroalkylated end-capped oligomer networks in the hydrogels possessing lower C_{min} are likely to bind strongly to the metal ion, since the stronger aggregation of fluoroalkyl segments is necessary for establishment of a physical gel network to exhibit lower C_{min}.

The release of Cr^{3+} or Co^{2+} increases linearly with initial concentration of Cr^{3+} (or Co^{2+}) binding to the hydrogels (data not shown) to afford *ca.* 60% releasing ratio [ratio based on the relative amount of Cr^{3+} (or Co^{2+}) released into water and relative amount of Cr^{3+} (or Co^{2+}) binding to gel], respectively, after incubation at 25°C for 24 h. On the other hand, Cr^{3+} (or Co^{2+}) was not released from Cr^{3+} (or Co^{2+}) bound R_F-$(HOPPA)_n$-R_F hydrogels at all under similar releasing conditions. This is because interactions of Cr^{3+} (or Co^{2+}) and R_F-$(HOPPA)_n$-R_F hydrogels are ionic, whereas the main driving force for Cr^{3+} (or Co^{2+}) binding to R_F-$(MHPTA)_n$-R_F is coordinate bonds between Cr^{3+} (or Co^{2+}) and OH segments. The electrostatic repulsion between the cation (N^+) segments in these MHPTA hydrogels and the metal ions may promote the release of metal ions into water.

Gelling fluoroalkylated end-capped oligomers containing betaine segments have been

reported to act as potent and selective inhibitors against anti-human immunodeficiency virus (HIV)-1.[11] Therefore, the present gelling (or gel-like) fluoroalkylated oligomers would be expected to behave as novel polymeric inhibitors of HIV-1 and for this reason such fluoroalkylated MHPTA oligomers have been evaluated for activity against HIV-1 replication in MT-4 cells. However, each oligomer was found inactive against HIV-1 replication, and the oligomers were toxic to the host cells. It was previously reported that the activity against HIV-1 is sensitive to the oleophilic property of fluoroalkylated end-capped oligomers, and the fluoroalkylated oligomers become more hydrophilic, activity is, in general, not observed.[25] Hence, the present oligomers possessing no anti-HIV-1 activity would be due to these oligomers having strong hydrophilic trimethylammonium and hydroxy segments.

The present fluoroalkylated end-capped MHPTA oligomers were toxic to host cells, and thus should show antibacterial activity. They have been evaluated for antibacterial activity against *Staphylococcus aures* by viable cell counting method as already reported.[26, 27] 1.5×10^8 cells ml^{-1} of *Staphylococcus aures* were exposed to 1 mg ml^{-1} oligomers in saline, and the colony-forming units (cfu) *versus* exposure for these oligomers against *Staphylococcus aures* were as follows:

R_F-(MHPTA)$_n$-R_F;

R_F = $CF(CF_3)OCF_2CF(CF_3)OC_3F_7$ (Run 8) 3.3×10^5 cfu

R_F = $CF(CF_3)OCF_2CF(CF_3)OC_3F_7$ (Run 9) 2.1×10^7 cfu

R_F-(MHPTA)$_x$-(CH_2-$CHSiMe_3$)$_y$-R_F;

R_F = $CF(CF_3)OCF_2CF(CF_3)OC_3F_7$ (Run 18) 1.1×10^5 cfu

Fluoroalkylated end-capped MHPTA homo- and co-oligomers showed bacterial activity to some extent (~ 10^5 colony forming units levels). In these oligomers, fluoroalkylated MHPTA-trimethylvinylsilane co-oligomer was the most active, with 1.1×10^5 cfu.

3.4 Conclusions

It was demonstrated that fluoroalkylated end-capped oligomers containing hydroxy segment can cause gelation under the non-crosslinked conditions, especially the aggregation of fluoroalkyl units in water and/or in organic media becomes a new driving factor for gelation as well as interactions such as hydrogen bonding and ionic interaction. Fluoroalkylated MHPTA oligomers had high metal-binding or releasing power. The gelling or gel-like fluoroalkylated MHPTA oligomers exhibited not only the properties imparted by fluorine such as surface activity, but also some antibacterial activity. Therefore, the present fluorintaed oligomer gels should be used in various fields as novel fluorinated functional materials.

References

1) R. E. Banks, B. E. Smart, and J. C. Tatlow, Ed., "Organofluorine Chem.," Plenum, New York, N. Y., 1994.

2) Z.-Y. Yang, A. E. Feiring, and B. E. Smart, *J. Am. Chem. Soc.,* **116**, 4135 (1994).

3) H. Sawada, *Chem. Rev.,* **96**, 1779 (1996).

4) J. F. Elman, B. D. Johs, T. E. Long, and J. T. Koberstein, *Macromolecules*, **27**, 5341 (1994).

5) S. Affrossman, M. Hartshorne, T. Kiff, R. A. Pethrick, and R. W. Richards, *Macromolecules*, **27**, 1588 (1994).

6) M. O. Hunt, Jr., A. M. Belu, R. W. Linton, and J. M. DeSimone, *Macromolecules*, **26**, 4854 (1993).

7) S. Affrossman, P. Bertrand, M. Hartshorne, T. Kiff, D. Leonard, R. A. Pethrick, and R. W. Richards, *Macromolecules*, **29**, 5432 (1996).

8) B. Xu, L. Li, A. Yekta, Z. Masoumi, S. Kanagalingam, M. A. Winnik, K. Zhang, P. M. Macdonald, and S. Menchen, *Langmuir*, **13**, 2447 (1997).

9) J. Wang, G. Mao, C. K. Ober, and E. J. Kramer, *Polym. Prepr., Am. Chem. Soc., Div. Polym. Chem.,* **38**, 953 (1997).

10) Z. Su, D. Wu, S. L. Hsu, and T. J. McCarthy, *Polym. Prepr., Am. Chem. Soc., Div. Polym. Chem.,* **38**, 951 (1997).

11) H. Sawada, S. Katayama, Y. Nakamura, T. Kawase, Y. Hayakawa, and M. Baba, *Polymer*, **39**, 743 (1998).

12) H. Sawada, Y. Nakamura, S. Katayama, and T. Kawase, *Bull. Chem. Soc. Jpn.,* **70**, 2839 (1997).

13) R. J. Twieg, T. P. Russell, R. Siemens, and J. F. Rabolt, *Macromolecules*, **18**, 1361 (1985).

14) H. Sawada and M. Nakayama, *J. Fluorine Chem.,* **51**, 117 (1990).

15) H. Sawada, M. Yoshida, H. Hagii, K. Aoshima, and M. Kobayashi, *Bull. Chem. Soc. Jpn.,* **59**, 215 (1986).

16) K. Hanabusa, R. Tanaka, M. Suzuki, M. Kimura, and H. Shirai, *Adv. Mater.,* **9**, 1095 (1997).

17) K. Hanabusa, K. Okui, K. Karaki, M. Kimura, and H. Shirai, *J. Colloid Interface Sci.,* **195**, 86 (1997).

18) K. Hanabusa, C. Koto, M. Kimura, H. Shirai, and A. Kakehi, *Chem. Lett.,* 429 (1997).

19) T. Kunitake, Y. Okahata, and S. Yasunami, *J. Am. Chem. Soc.,* **104**, 5547 (1987).

20) T. Kunitake and N. Higashi, *J. Am. Chem. Soc.,* **107**, 692 (1985).

21) T. Kunitake and N. Higashi, *Macromol. Chem. Phys. Suppl.,* 81 (1985).

22) Y. Ishikawa, H. Kuwahara, and T. Kunitake, *Chem. Lett.,* 1737 (1989).

23) Y. Ishikawa, H. Kuwahara, and T. Kunitake, *J. Am. Chem. Soc.,* **111**, 8530 (1989).

24) Y. Osada and M. Takase, *Nippon Kagaku Kaishi,* 439, (1983).

25) H. Sawada, K. Tanba, N. Itoh, C. Hosoi, M. Oue, M. Baba, T. Kawase, M. Mitani, and H.

Nakajima, *J. Fluorine Chem.,* **77**, 51 (1996).

26) H. Sawada, S. Katayama, M. Oue, T. Kawase, Y. Hayakawa, M. Baba, T. Tomita, and M. Mitani, *J. Jpn. Oil Chem. Soc.,* **45**, 161 (1996).

27) H. Sawada, K. Tanba, T. Tomita, T. Kawase, M. Baba, and T. Ide, *J. Fluorine Chem.,* **84**, 141 (1997).

CHAPTER 4

Preparation of Fluoroalkyl End-Capped Vinyltrimethoxysilane Oligomeric Silica Nanocomposites Containing Gluconamide Units Possessing Highly Oleophobic/Superhydrophobic, Highly Oleophobic/Superhydrophilic, and Superoleophilic/Superhydrophobic Characteristics on the Modified Surfaces

4.1 Introduction

It is well known that fluoroalkanoyl peroxide [R_F-C(=O)OO(O=)C-R_F: R_F = fluoroalkyl group] is a useful tool for the synthesis of two-fluoroalkyl end-capped oligomers [R_F-(M)$_n$-R_F: M = radical polymerizable monomers].[1 ~ 3] These fluoroalkyl end-capped oligomers are attractive polymeric materials because they can exhibit a variety of unique properties such as high solubility, surface active properties, and nanometer size-controlled self-assembled molecular aggregates through the aggregation of end-capped fluoroalkyl segments in oligomers, which cannot be achieved by the corresponding non-fluorinated and randomly fluoroalkylated polymers.[4, 5] In these fluoroalkyl end-capped oligomers, especially, fluoroalkyl end-capped oligomers containing various hydroxy segments such as monool, triol, and tetraol can cause gelation in water and polar organic media such as methanol and ethanol, whose behavior is governed by the synergistic interactions of the aggregation of fluoroalkyl segments within oligomers and the intermolecular hydrogen bonding related to the hydroxy segments.[6 ~ 9] In this way, the exploration of novel fluoroalkyl end-capped oligomers containing numerous hydroxy segments is of particular interest, from the developmental viewpoints of new fluorinated functional materials. In a variety of hydroxylated polymers, much attention has been focused on the synthetic sugar-containing polymers (glycopolymers), which possess the pendent gluconic residues (pentaol units), owing to their role as biomimetic analogues and their

applications in biomedical and technological fields such as paints and cosmetics.[10 ~ 19)] In fact, poly(allylamine) can react with gluconolactone in water to provide the gluconamide-substituted polymers, successively affording the hydrogel through the interaction of the corresponding polymers with borax.[20)] Similarly, the D-gluconamide unit-containing methacrylate monomer can be copolymerized with AIBN (2,2′-azobisisobutyronitrile) in the presence of methyl acrylate as comonomer to afford the corresponding glycopolymers.[21)] These glycopolymers also have high potential use as polymeric surfactants.[22)] Therefore, the studies on the preparation of novel gluconamide unit-containing polymers bearing longer fluoroalkyl groups are of particular interest, because these polymers would exhibit not only the unique characteristics related to the gluconamide units but also the surface active characteristics imparted by longer fluoroalky groups. However, such studies have been very limited so far. In the fluoroalkyl end-capped oligomers, especially, two fluoroalkyl end-capped vinyltrimethoxysilane oligomer [R_F-(CH_2-$CHSi(OMe)_3$)$_n$-R_F] can undergo the sol-gel reaction under alkaline conditions to afford the corresponding fluorinated oligomeric silica nanoparticles [R_F-(CH_2-$CHSiO_2$)$_n$-R_F].[22)] These fluorinated oligomeric silica nanoparticles have been also applied to the surface modification of glass to supply the superhydrophobic characteristic (water contact angle value: 180 degrees) with the oleophobic property.[22)] From these findings, it is highly suggested that the composite reactions of the present fluorinated

vinyltrimethoxysilane oligomer with the gluconamide derivatives should lead the obtained composites to the creation of the unique surface characteristics imparted by not only longer fluoroalkyl groups, but also the gluconamide units. This chapter shows that two fluoroalkyl end-capped vinyltrimethoxysilane oligomers [R_F-(CH_2–$CHSi(OMe)_3$)$_n$-R_F] can undergo the sol-gel reaction in the presence of *N*-(3-triethoxysilylpropyl)gluconamide [Glu-$Si(OEt)_3$] under alkaline conditions to afford the corresponding fluorinated oligomeric silica nanocomposites containing gluconamide units [R_F-(VM-SiO_2)$_n$-R_F/Glu-SiO_2]. The modified surfaces treated with these obtained nanocomposites can provide the unique wettability states such as the highly oleophobic/superhydrophobic, highly oleophobic/superhydrophilic, and superoleophilic/superhydrophobic characteristics. These results will be described in this chapter.

4.2 Experimental

4.2.1 Materials

1,4-Bis[4-methylphenyl]amino]-9,10-anthracenedione (Quinizarin Green SS) and PET (polyethylene terephthalate) fabric (Polyester Tropical 13001) were received from Chugaikasei Co., Ltd. (Fukushima, Japan) and Unitika Ltd. (Osaka, Japan), respectively. *N*-(3-triethoxysilylpropyl)gluconamide [Glu-Si(OEt)$_3$] was purchased from AZmax. Co. (Chiba, Tokyo). Dodecane and 1*H*-tridecafluorohexane were received from Tokyo Chemical Industrial Co., Ltd. (Tokyo, Japan). 25 wt % ammonia was provided by Wako Pure Chemical Industries (Osaka, Japan). Fluoroalkyl end-capped vinyltrimethoxysilane oligomer was prepared according to the previously reported method.[23] Glass plate (borosilicate glass) [micro cover glass: 18 mm × 18 mm] was purchased from Matunami glass Ind. Ltd. (Osaka, Japan) and was used after washing well with dichloromethane.

4.2.2 Measurements

Dynamic light scattering (DLS) measurements were measured by using Otsuka Electronics DLS-7000 HL (Tokyo, Japan). Contact angles were recorded using a Kyowa Interface Science Drop Master 300 (Saitama, Japan). Field emission scanning electron micrographs (FE-SEM) and energy dispersive X-ray (EDX) spectra were obtained by using

JEOL JSM-7000F (Tokyo, Japan). Dynamic force microscope (DFM) was recorded by using SII Nano Technology Inc. E-sweep (Chiba, Japan).

4.2.3 Preparation of fluoroalkyl end-capped vinyltrimethoxysilane oligomeric silica nanocomposites containing gluconamide units [R_F-(VM-SiO_2)$_n$-R_F/Glu-SiO_2]

A typical procedure for the preparation of nanocomposites is as follows: To methanol solution (5.0 mL) containing fluoroalkylated vinyltrimethoxysilane oligomer [200 mg; R_F-($CH_2CHSi(OMe)_3$)$_n$-R_F; R_F = $CF(CF_3)OC_3F_7$; M_n = 730 (R_F-(VM)$_n$-R_F)] was added 50 wt % Glu-$Si(OEt)_3$ ethanol solution (1400 mg). The mixture was stirred with a magnetic stirring bar at room temperature for 30 min. 25% aqueous ammonia solution (1.0 mL) was added to this mixture, and then stirred for 5 h at room temperature. Methanol was added to the obtained crude products after the solvent was evaporated off. The methanol suspension was stirred with magnetic stirring bar at room temperature for 1 day. The fluorinated oligomeric silica/Glu-SiO_2 nanocomposites were isolated after centrifugal separation for 30 min. The nanocomposite product was washed well with methanol several times, and then was dried under vacuum at 50 °C for 1 day to afford the expected nanocomposites as white powders (774 mg) (see Scheme 4-1 and Table 4-1).

4.2.4 Preparation of the modified glass treated with the R_F-(VM-SiO_2)$_n$-R_F/Glu-SiO_2 nanocomposites by dipping method

To methanol solution (5.0 mL) containing R_F-(VM)$_n$-R_F oligomer (200 mg) was added 50 wt % Glu-Si(OEt)$_3$ ethanol solution (700 mg) and 25% aqueous ammonia solution (1.0 mL). The mixture was stirred with a magnetic stirring bar at room temperature for 5 h. The glass plates (18 × 18 mm^2 pieces) were dipped into this methanol solution at room temperature and left for 1 min. The glass plate was lifted from the solutions at a constant rate of 0.5 mm/min and were left to dry at room temperature for 1 day; finally, these were dried under vacuum for 1 day at room temperature to afford the modified glass. The modified PET fabric swatch (25 × 25 mm^2 pieces) was prepared under similar conditions. The contact angle values for dodecane and water were measured by depositing a drop of dodecane (2 μL) or water (2 μL) on the modified plate surfaces.

4.3 Results and discussion

Sol-gel reaction of fluoroalkyl end-capped vinyltrimethoxysilane oligomer [R_F-($CH_2CHSi(OMe)_3$)$_n$-R_F; R_F = $CF(CF_3)OC_3F_7$ (R_F-(VM)$_n$-R_F)] proceeded smoothly in the presence of *N*-(3-triethoxysilylpropyl)gluconamide [Glu-$Si(OEt)_3$] under alkaline conditions to afford the corresponding fluorinated oligomeric silica/Glu-SiO_2 nanocomposites [R_F-(VM-SiO_2)$_n$-R_F/Glu-SiO_2]. These results are shown in Scheme 4-1 and Table 4-1.

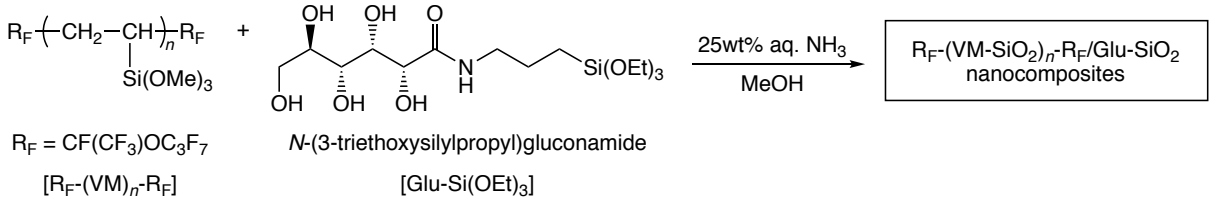

Scheme 4-1 Preparation of R_F-(VM-SiO_2)$_n$-R_F/Glu-SiO_2 nanocomposites

Table 4-1 Preparation of the R_F-(VM-SiO_2)$_n$-R_F/Glu-SiO_2 nanocomposites

Run	R_F-(VM)$_n$-R_F (mg) [mmol]	Glu-Si(OEt)$_3$ (mg)[c] [mmol]	MeOH (ml)	25 wt% aq. NH_3 (ml)	Yield[a] (%)	Size of composites[b] (nm ± STD)
1	200 [0.27]	10 [0.01]	5.0	1.0	54	32.7 ± 3.1
2	200 [0.27]	25 [0.03]	5.0	1.0	39	38.1 ± 7.1
3	200 [0.27]	50 [0.06]	5.0	1.0	43	53.8 ± 17.3
4	200 [0.27]	90 [0.11]	5.0	1.0	39	37.4 ± 9.0
5	200 [0.27]	170 [0.21]	5.0	1.0	31	71.8 ± 14.0
6	200 [0.27]	350 [0.44]	5.0	1.0	43	35.5 ± 2.3
7	200 [0.27]	700 [0.88]	5.0	1.0	69	51.1 ± 6.5
8	200 [0.27]	1400 [1.75]	5.0	1.0	86	42.8 ± 8.7

a) Yield was based on oligomer and Glu-Si(OEt)$_3$
b) Determined by dynamic light scattering (DLS) measurements in methanol
c) 50 % EtOH solution

The expected fluorinated composites were obtained in 31% ~ 86% isolated yields, and the obtained composites revealed a good dispersibility and stability in traditional organic media such as methanol, tetrahydrofuran, and 1,2-dichloroethane. Especially the fluorinated composites (Runs: 1 ~ 5), which were prepared under the feed amounts of Glu-Si(OEt)$_3$ from 10 to 170 mg, afforded no dispersibility toward water; however, the fluorinated composites (Runs: 6 ~ 8), which were prepared under a higher feed amount of Glu-Si(OEt)$_3$ greater than 170 mg, were found to give a good dispersibility and stability toward water.

The size of the fluorinated composites in Table 4-1 was measured in methanol by dynamic light-scattering (DLS) measurements at 25 °C, because these composites can reveal the good dispersibility in methanol. Table 4-1 also shows that each size of the composites is

nanometer size-controlled fine particles from 33 to 72 nm (number-average diameter).

FE-SEM photograph of the R_F-(VM-SiO_2)$_n$-R_F/Glu-SiO_2 nanocomposites (Runs 4 and 7 in Table 4-1) methanol solutions was recorded, and the results are shown in Figure 4-1.

Electron micrograph also shows the formation of fluorinated nanocomposite fine cubic-type particles with a mean diameter of 56 and 45 nm, respectively, and the similar size values to those (37.4 ± 9.0 and 51.1 ± 6.5 nm) of DLS measurements were observed in FE-SEM measurements (see Runs 4 and 7 in Table 4-1).

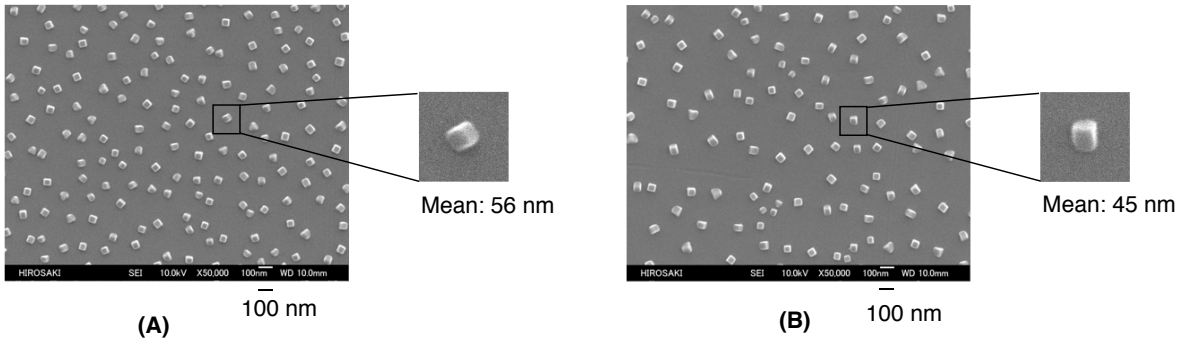

Figure 4-1 FE-SEM (Field Emission Scanning Electron Microscopy) images of well-dispersed methanol solutions of the R_F-(VM-SiO_2)$_n$-R_F/Glu-SiO_2 nanocomposite particles: (A): Run 4; (B): Run 7 in Table 4-1.

To verify the surface active characteristics of the nanocomposites in Table 4-1, these fluorinated nanocomposites have been applied to the surface modification of glass, and the dodecane and water contact angle values have been measured on these modified surfaces. The results are shown in Table 4-2.

Table 4-2 Contact angles of dodecane and water on the modified glasses treated with the R_F-(VM-SiO_2)$_n$-R_F/Glu-SiO_2 nanocomposites

Run*	Feed amount (mmol/mmol) [R_F-(VM)$_n$-R_F/Glu-Si(OEt)$_3$]	Contact angle (degree)							
		Dodecane	Water						
			Time (min.)						
			0	5	10	15	20	25	30
1	[0.27/0.01]	74	180	—**	—	—	—	—	—
2	[0.27/0.03]	112	180	—**	—	—	—	—	—
3	[0.27/0.06]	107	142	130	132	131	128	127	104
4	[0.27/0.11]	97	137	134	134	129	127	127	122
5	[0.27/0.21]	94	135	133	132	132	128	113	101
6	[0.27/0.44]	97	137	143	122	91	62	0	—**
7	[0.27/0.88]	58	133	132	104	0	—**	—	—
8	[0.27/1.75]	56	108	106	102	99	93	86	80
Parent R_F-(VM-SiO_2)$_n$-R_F		46	180	—**	—	—	—	—	—
Non-treated glass		0	50						

* Each Run No corresponds to that of Table 4-1.
** no change

As shown in Table 4-2, water contact angle values are, in general, dependent upon the feed ratios of the R_F-(VM)$_n$-R_F oligomer and the Glu-Si(OEt)$_3$ employed, increasing with lower feeds amounts of Glu-Si(OEt)$_3$ in R_F-(VM)$_n$-R_F – Glu-(Si(OEt)$_3$ from 108 to 180 degrees (superhydrophobic surface). A similar result was observed in the dodecane contact angle values, increasing from 56 to 112 degrees except for Run 1, although the original fluoroalkyl end-capped vinyltrimethoxysilane oligomeric silica nanoparticles [R_F-(VM-SiO_2)$_n$-R_F] can give a usual oleophobic (dodecane contact angle value: 46 degrees) with a superhydrophobic property (water contact angle value: 180 degrees).

The water contact angle values on the modified glass surfaces treated with the fluorinated nanocomposites, which were prepared under the greater feed amounts of Glu-Si(OEt)$_3$ from 0.44 to 1.75 mmol, were found to decrease from 133–137 to 0 degrees (superhydrophilic surface) over 15 or 25 min except for Run 8, indicating that the hydrophobic fluoroalkyl segments are replaced by the hydrophilic gluconamide segments in the nanocomposites when the environment is changed from air to water. The relatively higher feed amounts (0.44–0.88 mmol) of Glu-Si(OEt)$_3$ in the nanocomposite preparation illustrated in Scheme 4-1 would enable the smooth surface arrangement of the hydrophilic gluconamide segments to provide the completely superhydrophilic surface through the flip-flop motion between the fluoroalkyl groups and gluconamide segments in the nanocomposites. A similar flip-flop motion between longer fluoroalkyl groups and hydrophilic segments has been already reported to exhibit the hydrophilic characteristic with an oleophobic property on the modified surfaces.[24 ~ 28] Therefore, the nanocomposites which were prepared under relatively lower feed amounts (0.03 mmol) of Glu-Si(OEt)$_3$, can supply a highly oleophobic/superhydrophobic characteristic (dodecane and water contact angle values: 112 and 180 degrees) on the modified surface, due to the lower content of hydrophilic gluconamide segments in the nanocomposites.

The fabrication of a superoleophobic surface is, in general, difficult due to the lower surface tension of oils than that of water. Thus, a highly oleophobic (superoleophobic) surface

can be realized by lowering the surface energy and enhancing the surface roughness.[29 ~ 33] Similarly, it is well known that a superhydrophobic surface can be created by the architecture of the roughness surface through the sol-gel reactions of the longer alkyl chain-containing silane coupling agents such as octadecyltrichlorosilane and hexadecyltriethoxysilane in the presence of silica nanoparticles and tetraethoxysilane under alkaline conditions.[34, 35] Therefore, in order to clarify such unique surface wettability illustrated in Table 4-2, the surface roughness has been studied toward the modified glasses treated with the R_F-(VM-SiO_2)$_n$-R_F/Glu-SiO_2 nanocomposites possessing the highly oleophobic/superhydrophobic characteristic (Run 2 in Table 4-2: dodecane contact angle value: 112 degrees and water contact angle value: 180 degrees) by using FE-SEM (field emission scanning electron microscopy) measurements and DFM (dynamic force microscopy) measurements, respectively. The surface roughness has been also studied toward the modified surfaces possessing a similar wettability (highly oleophobic/superhydrophobic characteristic) (Run 1 in Table 4-2) and usual oleophobic and hydrophobic characteristics (Run 8 in Table 4-2) including the original fluoroalkyl end-capped vinyltrimethoxysilane oligomeric silica nanoparticles [R_F-(VM-SiO_2)$_n$-R_F], for comparison. The results are shown in Figures 4-2 ~ 4-5.

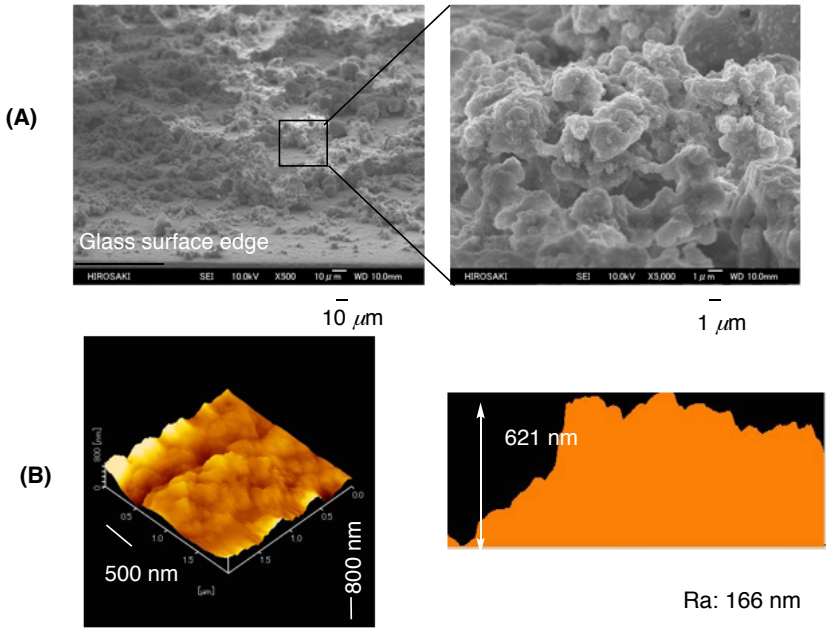

Figure 4-2 FE-SEM (Field Emission Scanning Electron Microscopy) images (**A**) and DFM (Dynamic Force Microscopy) topography (**B**) of the modified glass surface treated with the R_F-(VM-SiO_2)$_n$-R_F/Glu-SiO_2 nanocomposites (Run 2 in Table 4-1).

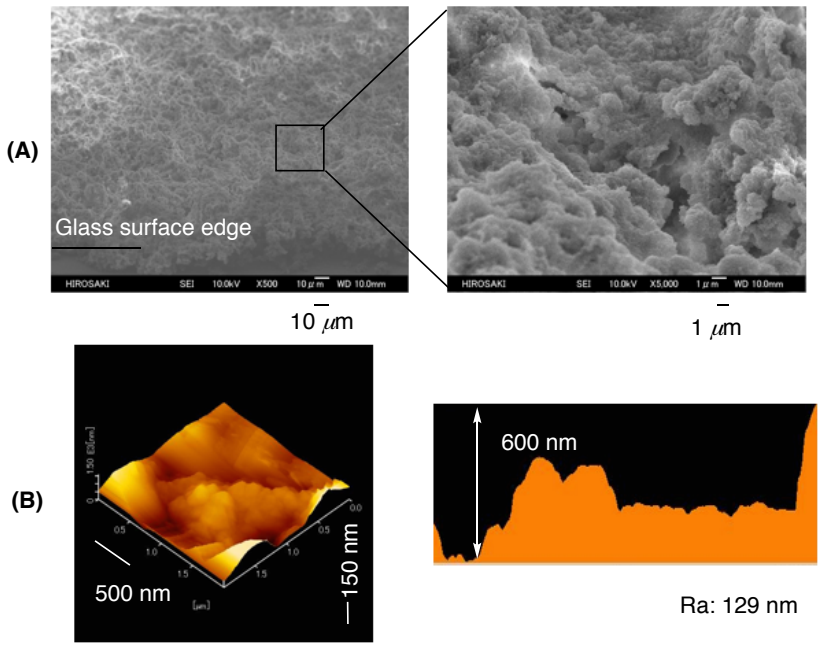

Figure 4-3 FE-SEM (Field Emission Scanning Electron Microscopy) images (**A**) and DFM (Dynamic Force Microscopy) topography (**B**) of the modified glass surface treated with the R_F-(VM-SiO_2)$_n$-R_F/Glu-SiO_2 nanocomposites (Run 1 in Table 4-1).

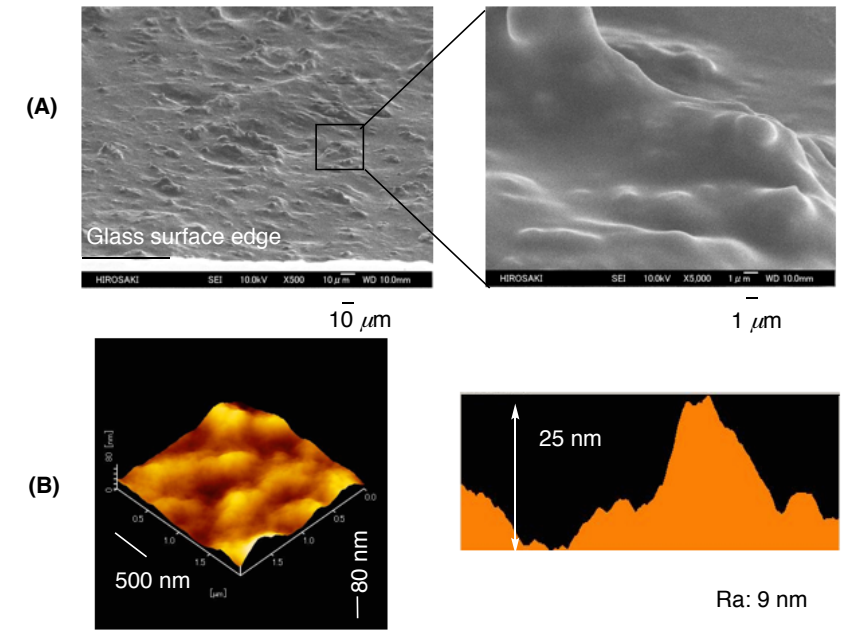

Figure 4-4 FE-SEM (Field Emission Scanning Electron Microscopy) images (**A**) and DFM (Dynamic Force Microscopy) topography (**B**) of the modified glass surface treated with the R_F-(VM-SiO_2)$_n$-R_F/Glu-SiO_2 nanocomposites (Run 8 in Table 4-1).

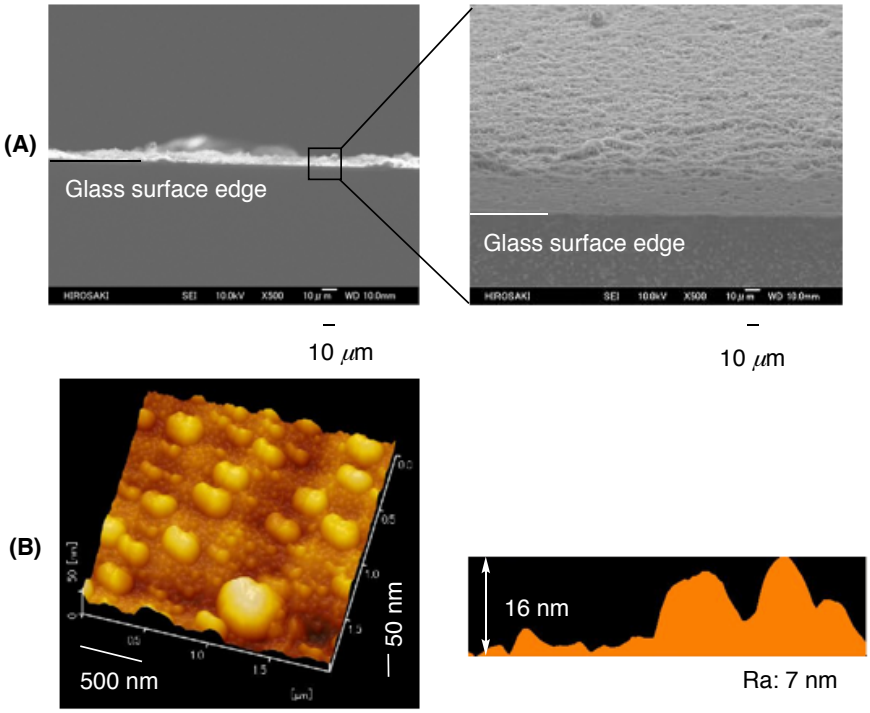

Figure 4-5 FE-SEM (Field Emission Scanning Electron Microscopy) images (**A**) and DFM (Dynamic Force Microscopy) topography (**B**) of the modified glass surface treated with the pristine R_F-(VM-SiO_2)$_n$-R_F/Glu-SiO_2 nanocomposites (see Table 4-1).

As shown in Figure 4-2**(A)**, the architecture of the effective roughness was observed on the modified surface treated with the R_F-(VM-SiO_2)$_n$-R_F/Glu-SiO_2 nanocomposites possessing a highly oleophobic/superhydrophobic property. Such roughness of surface was also observed in the nanocomposites possessing a similar wettability depicted in Figure 4-3**(A)**. The topographical image of the modified glass surface treated with the nanocomposites possessing a highly oleophobic/superhydrophobic property [Figure 4-2**(B)**] can afford a higher roughness characteristic (the roughness average value: Ra value = 166 nm), compared with that (Ra value = 129 nm) of the modified surface possessing a lower dodecane contact angle value: 74 degrees [see Figure 4-3**(B)**]. Such a higher Ra value should enable the modified surface to supply a highly oleophobic/superhydrophobic characteristic. Especially, the introduction of an air cushion into rough deposits of the present nanocomposite particles could create such a unique superoleophobic/superhydrophobic characteristic on the modified surface. In fact, it was reported that the introduction of a proper rough surface microstructure could make a flat hydrophobic surface more hydrophobic due to the introduction of an air cushion beneath the water droplet.[36] On the other hand, the FE-SEM and DFM measurements (see Figures 4-4 and 4-5) show that the modified surfaces treated with the R_F-(VM-SiO_2)$_n$-R_F/Glu-SiO_2 nanocomposites possessing a usual oleophobic/hydrophobic property and the pristine R_F-(VM-SiO_2)$_n$-R_F oligomeric nanoparticles can provide relatively smooth roughness, because

these Ra values are 9 and 7 nm, respectively, indicating that such relatively smooth surfaces should supply the usual oleophobic/hydrophobic or oleophobic/superhydrophobic characteristic to the modified surfaces.

The surface modification has been tried toward not only the glass but also the polyethylene terephthalate (PET) fabric swatch by using the R_F-(VM-SiO_2)$_n$-R_F/Glu-SiO_2 nanocomposites (Run 2 in Table 4-1) under similar conditions, and the dodecane and water contact angle values on the modified PET fabric swatch were measured. The modified PET fabric swatch can exhibit the similar dodecane and water contact angle values: 111 and 180 degrees to those of the modified glass surfaces depicted for Run 2 in Table 4-2. Especially, FE-SEM pictures of the modified PET fabric swatch show that the fluorinated nanocomposite particles are not only filled up between the PET fibers, but are also uniformly coated on the PET fibers [Figure 4-6**(B)**], compared with that of the pristine PET fabric [Figure 4-6**(A)**]. Here, this modified PET fabric swatch has been applied to the separation membrane for the separation of the mixture of the fluorocarbon oil (1*H*-tridecafluorohexane) and the hydrocarbon oil (dodecane: blue-colored with Quinizarin Green SS), because the modified PET fabric swatch can provide a highly oleophobic/superhydrophobic characteristic on the modified surface, and the results are illustrated in Figure 4-7.

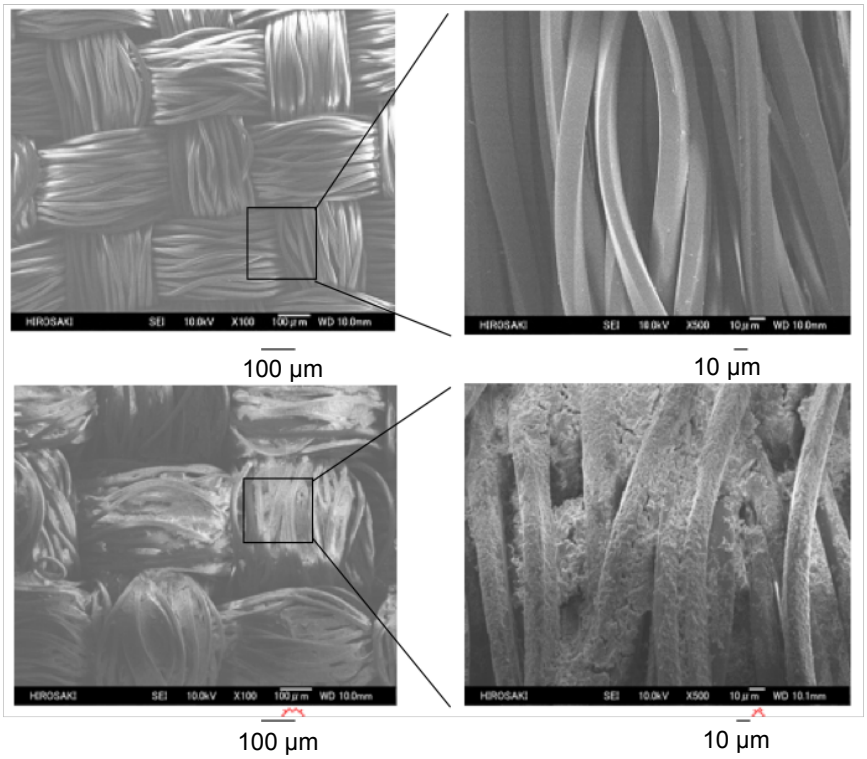

Figure 4-6 FE-SEM (Field Emission Scanning Electron Microscopy) images of the pristine PET-fabric swatch (**A**) and the modified PET fabric swatch (**B**) treated with the R_F-(VM-SiO_2)$_n$-R_F/Glu-SiO_2 nanocomposites (Run 2 in Table 4-1).

As shown in Figure 4-7**(C)**, the surface appearance of the modified PET fabric swatch was quite similar to that of the pristine PET fabric swatch [Figure 4-7**(B)**]. In addition, it was demonstrated that the modified PET fabric swatch is effective for the separation of blue-colored hydrocarbon oil and fluorocarbon oil to isolate the transparent colorless fluorocarbon oil as shown in Figure 4-7**(C)**; although the pristine PET fabric swatch was not able to separate the mixture under similar conditions [see Figure 4-7**(B)**]. This finding is due to the highly oleophobic/superhydrophobic characteristic of the modified PET fabric swatch.

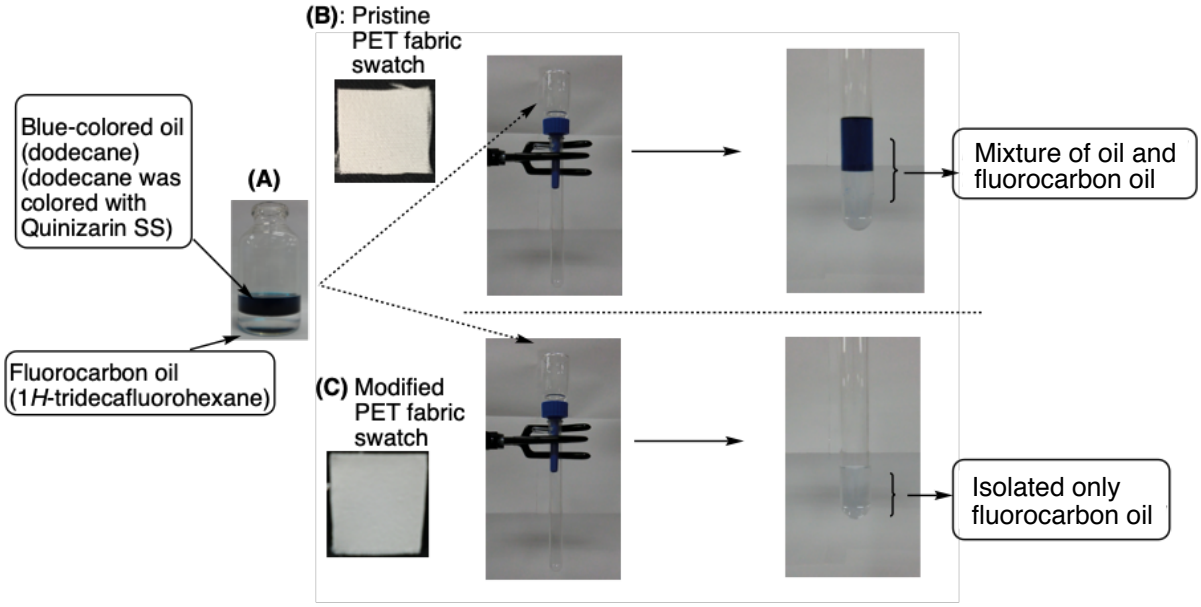

Figure 4-7 Separation of the mixture (**A**) of the blue-colored hydrocarbon oil (dodecane) and fluorocarbon oil (1*H*-tridecafluorohexane) by using the pristine PET fabric swatch (**B**) and the modified PET fabric swatch treated with the R_F-(VM-SiO_2)$_n$-R_F/Glu-SiO_2 nanocomposites (Run 2 in Table 4-1) (**C**) as the separation membrane, respectively.

As illustrated in Scheme 4-1 and Table 4-1, the expected fluorinated oligomeric silica nanocomposites containing gluconamide units are prepared through the sol-gel reactions under alkaline conditions. Especially, as mentioned before, the higher feed amounts of Glu-Si(OEt)$_3$ greater than 0.21 mmol can lead the obtained nanocomposites to a good dispersibility toward water. This finding suggests that the fluorinated nanocomposites can cause gelation toward water through the synergistic interaction between the aggregation of the end-capped fluoroalkyl groups and the intermolecular hydrogen bonding related to the hydroxy segments in the gluconamide units in the nanocomposites by controlling the sol-gel conditions (for example; by changing the alkaline concentrations). In fact, the R_F-(VM-SiO_2)$_n$-R_F/Glu-SiO_2

nanocomposites, which can cause gelation toward water, were prepared by changing the feed amounts of both 25 % aqueous ammonia and methanol from 1.0 to 0.6 and 5.0 to 15 mL, respectively, as shown in Table 4-3.

Table 4-3 Preparation of the R_F-(VM-SiO_2)$_n$-R_F/Glu-SiO_2 nanocomposite hydrogels

Run No.	Feed amounts (mg/mg) of R_F-(VM)$_n$-R_F/Glu-Si(OEt)$_3$	25% *aq*. NH_3 (mL)	Methanol (mL)
9	200/90	0.6	15
10	200/170	0.6	15

The gelling fluorinated nanocomposites (see Figure 4-8) were applied to the surface modification of the PET fabric swatch under similar conditions to those of Table 4-2, and the dodecane and water contact angle values on the modified PET fabric swatch were measured. The results are shown in Table 4-4.

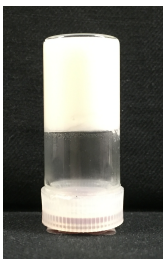

Figure 4-8 Gelation of water by using the R_F-(VM-SiO_2)$_n$-R_F/Glu-SiO_2 nanocomposites (Run 9 in Table 4-3).

Table 4-4 Contact angles of dodecane and water on the modified PET fabrics swatch treated with the R_F-(VM-SiO_2)$_n$-R_F/Glu-SiO_2 nanocomposite gels before and after immersing into water at room temperature for 1 day

Run	Feed amount (mmol/mmol) [R_F-(VM)$_n$-R_F/Glu-Si(OEt)$_3$]	Contact angle (degree)							
		Dodecane	Water						
			Time (min.)						
			0	5	10	15	20	25	30
Before immersing into water									
9	[0.27/0.11]	102	180	— [a]	—	—	—	—	—
10	[0.27/0.21]	89	180	— [a]	—	—	—	—	—
After immersing into water									
9	[0.27/0.11]	0	180	— [a]	—	—	—	—	—
10	[0.27/0.21]	0	180	— [a]	—	—	—	—	—

a) No change

As shown in Table 4-4, the modified PET fabric swatches were found to give a highly oleophobic/superhydrophobic characteristic, because the dodecane and water contact angle values are 89 ~ 102 and 180 degrees, respectively, quite different from the corresponding modified glass surfaces possessing a highly oleophobic/hydrophobic characteristic (see Runs 4 and 5 in Table 4-2). The surface appearance of the modified PET fabric swatch is almost the same as that of the pristine PET fabric swatch (see Figure 4-9), and the adhesion ability of the PET fabric swatch is strong enough that even after rubbing the modified surface with a finger. Especially, any released nanocomposites powder cannot be detected toward the modified PET fabric swatch [see Figure 4-10**(B)**]. In contrast, the adhesion ability of the modified PET fabric swatch treated with the pristine R_F-(VM-SiO_2)$_n$-R_F oligomeric nanoparticles is not enough, and

the corresponding fluorinated oligomeric nanoparticles were easily released from the modified surface after rubbing the surface with a finger [see Figure 4-10**(A)**]. Such strong adhesion ability would be due to the uniform modification on the PET fiber surface by the R_F-(VM-SiO_2)$_n$-R_F/Glu-SiO_2 nanocomposite gels. In fact, FE-SEM images of the modified PET fabric and the pristine PET fabric swatches show that the nanocomposite gels can be uniformly coated on the PET fibers [see Figure 4-11**(A)**, **(B)**], quite different from the FE-SEM picture of the modified PET fabric treated with the R_F-(VM-SiO_2)$_n$-R_F/Glu-SiO_2 nanocomposites possessing no gelling ability as in Figure 4-6**(B)**.

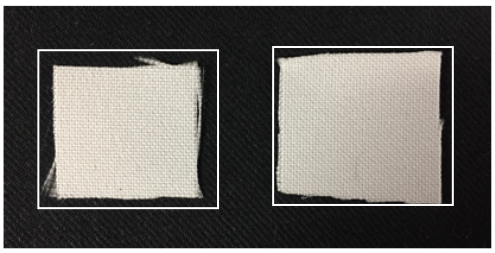

(A) Pristine PET fabric swatch

(B) Modified PET fabric swatch

Figure 4-9 Photograph of the pristine PET fabric swatch (**A**) and the modified PET fabric swatch treated with the R_F-(VM-SiO_2)$_n$-R_F/Glu-SiO_2 nanocomposites gels (Run 9 in Table 4-4).

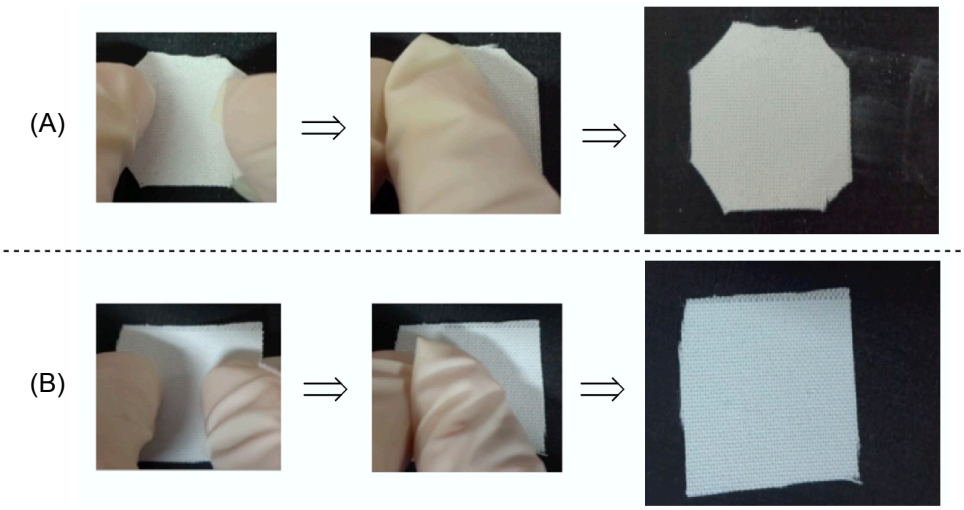

Figure 4-10 Photograph of the adhesion trial for the modified PET fabric swatch treated with the pristine R_F-(VM-SiO_2)$_n$-R_F oligomeric nanoparticle (**A**) and the modified PET fabric swatch treated with the R_F-(VM-SiO_2)$_n$-R_F/Glu-SiO_2 nanocomposite gels (Run 9 in Table 4-4) (**B**).

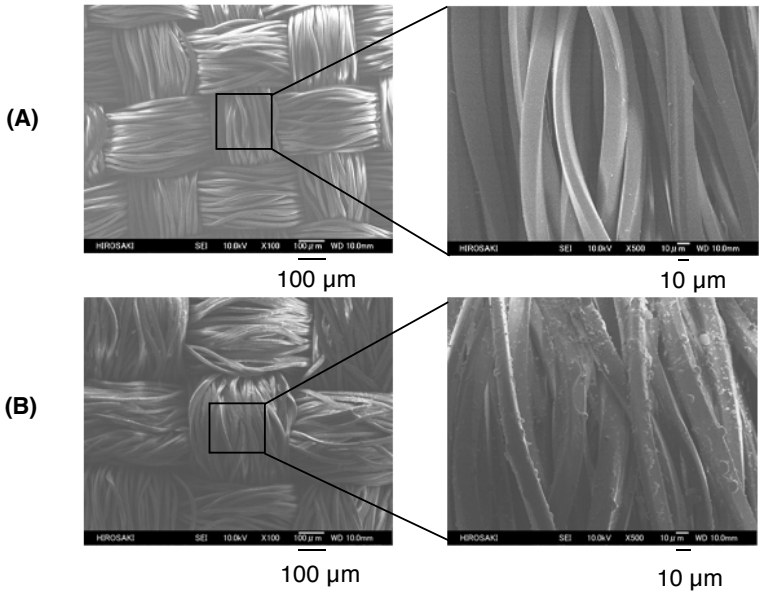

Figure 4-11 FE-SEM (Field Emission Scanning Electron Microscopy) images of the pristine PET fabric swatch (**A**) and the modified PET fabric swatch treated with the R_F-(VM-SiO_2)$_n$-R_F/Glu-SiO_2 nanocomposite gels (Run 9 in Table 4-4) (**B**).

Furthermore, the dodecane and water contact angle values on the modified PET fabric swatches treated with the nanocomposite gels (Runs 9 and 10 in Table 4-4) have been measured after immersing the corresponding swatches in water at room temperature for 1 day, and the results are also shown in Table 4-4.

Quite interestingly, the wettability change from the highly oleophobic to the superoleophilic characteristic can be observed, while keeping the superhydrophobic characteristic on the modified fabric swatches only after immersing into water, because the dodecane contact angle values extremely decreased from 89 ~ 102 to 0 degrees after immersing into water. The FE-SEM measurments of the modified PET fabric swatch were studied after immersing this swatch into water, and the results are illustrated in Figure 4-12**(B)**. The FE-SEM images show that the nanocomposite gels are uniformly coated on each PET fiber to enhance the roughness on the PET fibers, different from that before immersing into water [see Figure 4-12**(A)**]. Such enhanced roughness would afford the different wettability through the immersing process into water.

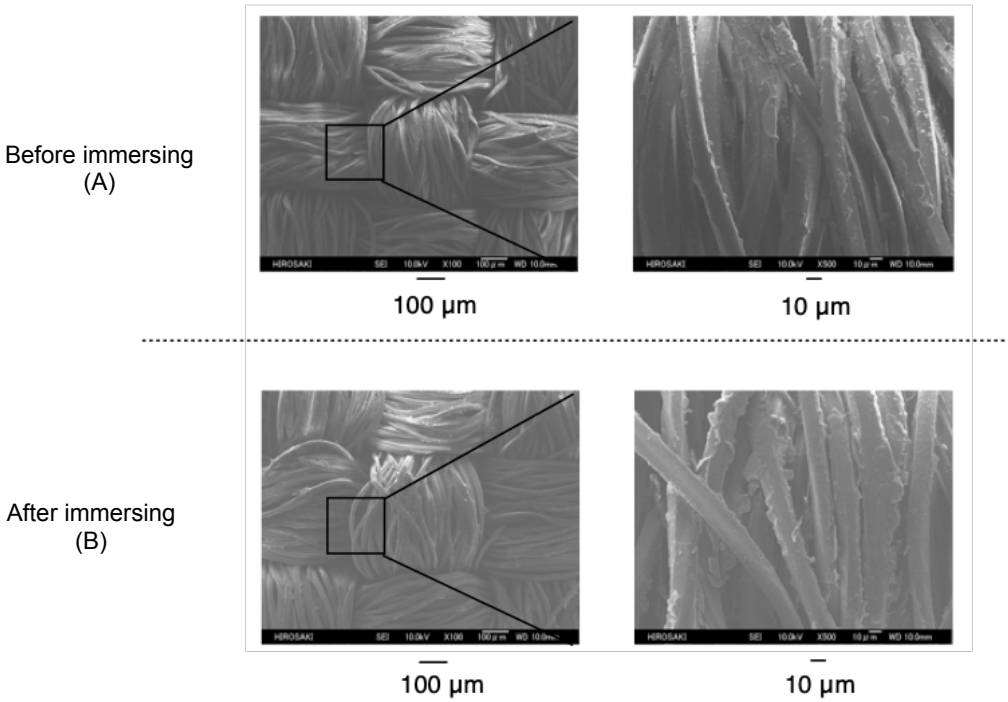

Figure 4-12 FE-SEM (Field Emission Scanning Electron Microscopy) images of the modified PET fabric swatch treated with the R_F-(VM-SiO_2)$_n$-R_F/Glu-SiO_2 nanocomposites gels (Run 9 in Table 4-4) before (**A**) and after (**B**) immersing into water at room temperature for 1 day.

In order to clarify the presence of fluorinated nanocomposites in the modified PET fabric swatch even after immersing into water, the EDX (Energy Dispersive X-ray) spectra of the modified PET fabric swatch treated with the R_F-(VM-SiO_2)$_n$-R_F/Glu-SiO_2 nanocomposites (Runs 9 and 10 in Table 4-4) have been measured before and after immersing into water, the results are shown in Figures 4-13 and 4-14.

EDX measurements show that the atomic contents of carbon, oxygen, nitrogen, fluorine, and silicon of the modified PET fabric swatch before and after immersing into water are as follows (see Table 4-5).

Table 4-5 Atomic contents of the modified PET-fabric surface treated with the R_F-(VM-SiO_2)$_n$-R_F/Glu-SiO_2 composite gels (Run 9 in Table 4-4) before and after after immersing into water at room tempreture for 1 day

	Atomic contents (atomic %)				
	C	O	N	F	Si
Before immersing	39.9	33.1	20.1	6.3	0.6
After immersing	40.0	31.6	19.7	7.9	0.7

Similar atomic values were observed even after immersing into water. In addition, it was verified that fluorine and silicon atoms related to the fluorinated nanocomposites are uniformly dispersed on the modified PET fabric swatch before and after immersing into water by EDX mapping images illustrated in Figures 4-13 and 4-14.

In this way, it was demonstrated that the present R_F-(VM-SiO_2)$_n$-R_F/Glu-SiO_2 nanocomposite gels can be strongly coated into the PET fabric fiber networks due to the gelling ability of the nanocomposites.

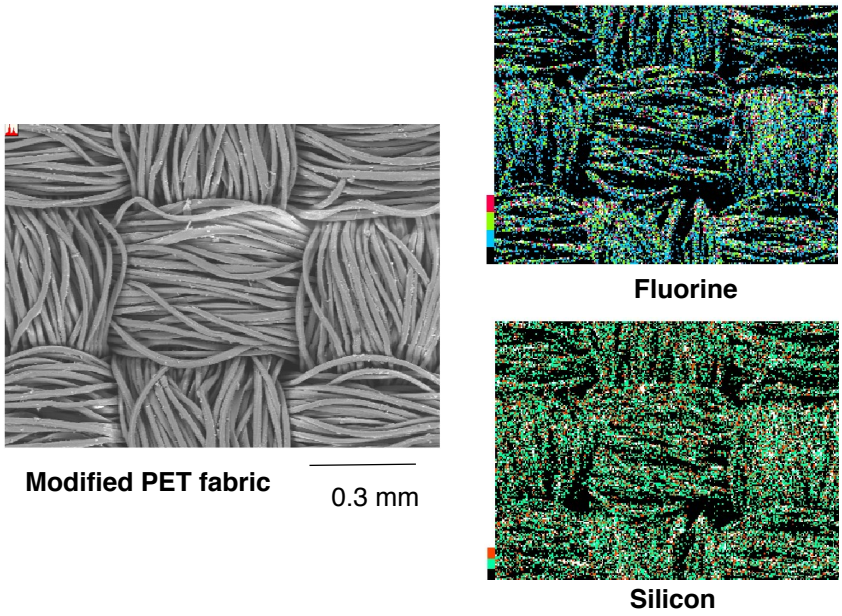

Figure 4-13 EDX (Energy Dispersive X-ray) mapping micrographs of the fluorine and silicon atoms on the modified PET fabric swatch surface treated with the R_F-(VM-SiO_2)$_n$-R_F/ Glu-SiO_2 nanocomposite gels (Run 9 in Table 4-4) before immersing into water.

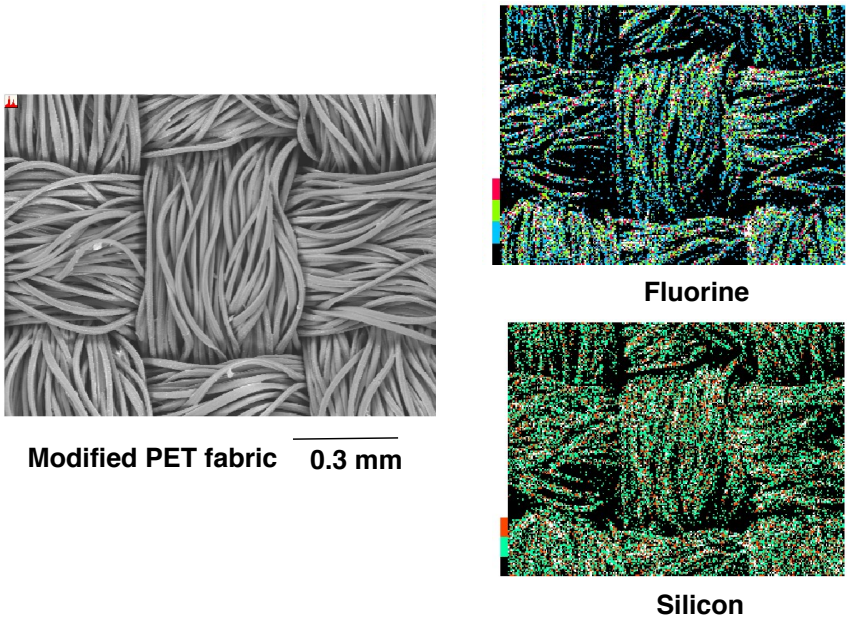

Figure 4-14 EDX (Energy Dispersive X-ray) mapping micrographs of the fluorine and silicon atoms on the modified PET fabric swatch surface treated with the R_F-(VM-SiO_2)$_n$-R_F/ Glu-SiO_2 nanocomposite gels (Run 9 in Table 4-4) after immersing into water at room temperature for 1 day.

4.4 Conclusions

Fluoroalkyl end-capped viniyltrimethoxysilane oligomeric silica nanocomposites containing gluconamide units [R_F-(VM-SiO_2)$_n$-R_F/Glu-SiO_2] were prepared by the sol-gel reactions of the corresponding oligomers in the presence of gluconamide unit-containing silane coupling agent [Glu-Si(OEt)$_3$] under alkaline conditions. Wettability control between the highly oleophobic/superhydrophobic and highly oleophobic/superhydrophilic states was observed on the modified glass surfaces treated with the R_F-(VM-SiO_2)$_n$-R_F/Glu-SiO_2 nanocomposites. Such wettability can be easily controlled by changing the feed amount ratios of Glu-Si(OEt)$_3$ and R_F-(VM)$_n$-R_F oligomer for the preparation of the nanocomposites. Lower feed amounts of Glu-Si(OEt)$_3$ can provide a highly oleophobic/superhydrophobic surface; in contrast, a higher feed amount of Glu-Si(OEt)$_3$ enables the modified surface to reveal a highly oleophobic/superhydrophilic characteristic. Such a highly oleophobic/superhydrophobic characteristic was also observed on the modified PET fabric swatch, and this modified PET fabric was applied to the separation membrane to separate the mixture of fluorocarbon oil and hydrocarbon oil.

R_F-(VM-SiO_2)$_n$-R_F/Glu-SiO_2 nanocomposites were also shown to cause gelation toward water. Especially, the gelling nanocomposites were applied to the surface modification of the PET fabric swatch to exhibit a highly oleophobic/superhydrophobic characteristic on the

modified surface. However, interestingly, the wettability change can be observed on the modified PET fabric surface from a highly oleophobic state to a superoleophilic state, while keeping the superhydrophobic characteristic by immersing this modified fabric into water.

References

1) H. Sawada, *Chem. Rev*., **96**, 1779 (1996).

2) H. Sawada, *J. Fluorine Chem*., **105**, 219 (2000).

3) H. Sawada, *J. Fluorine Chem*., **121**, 111 (2003).

4) H. Sawada, H. *Prog. Polym. Sci*., **32**, 509 (2007).

5) H. Sawada, *Polym. Chem.,* **3**, 46 (2012).

6) H. Sawada, T. Tanimura, S. Katayama, and T. Kawase, *J. Chem. Soc. Chem. Commun*., 1391 (1997).

7) H. Sawada, T. Tanimura, S. Katayama, T. Kawase, T. Tomita, and M. Baba, *Polym. J*., **30**, 797 (1998).

8) H. Sawada, Y. Nakamura, S. Katayama, and T. Kawase, *Bull. Chem. Soc. Jpn*., **70**, 2839 (1997).

9) H. Sawada, Y. Murai, M. Kurachi, T. Kawase, T. Minami, J. Kyokane, and T. Tomita, *J. Mater. Chem*., **12**, 188 (2002).

10) R. Narain and D. Jhurry, *Polym. Int*., ***51***, 85 (2001).

11) A. Carter, D. W. Morton, and D. E. Kiely, *J. Polym. Sci*. *Part A Polym. Chem*., **38**, 3892 (2000).

12) K. Ohno, T. Fukuda, and H. Kitano, *Macromol. Chem. Phys*., **199**, 2193 (1998).

13) A. Munoz-Bonilla, O. Leon, M. L. Cerrada, J. Rodriguez-Hernandez, M. Sanchez-Chaves, and M. Fernandez-Garcia, *Eur. Polym. J.*, **62**, 167 (2015).

14) M. Goto, K. Kobayashi, A. Hachikawa, K. Saito, C. Cho, and T. Akaike, *Macromol. Chem. Phys.*, **202**, 1161 (2001).

15) R. Wagner, L. Richter, R. Wersig, G. Schmaucks, B. Weiland, J. Weissmuller, and J. Reiners, *Appl. Organomet. Chem.*, **10**, 421 (1996).

16) K. Babiuch, D. Pretzel, T. Tolstik, A. Vollrath, S. Stanca, F. Foertsch, C. R. Becer, M. Gottschaldt, C. Biskup, and U. S. Schubert, *Macromol. Biosci.*, **12**, 1190 (2012).

17) R. Wagner, L. Richter, B. Weiland, J. Reiners, and J. Weissmuller, *Appl. Organomet. Chem.*, **10**, 437 (1996).

18) K. Hashimoto, H. Saito, and R. Ohsawa, *J. Polym. Sci. A*, **44**, 4895 (2006).

19) C. R. Becer, *Macromol. Rapid Commun.*, **33**, 742 (2012).

20) E. K. Oikonomou, E. Audebeau, S. Norvez, and I. Iliopoulos, *Macrmol. Symp.*, **331**, 152 (2013).

21) V. Bordege, A. Munoz-Bonillia, O. Leon, R. Cuervo-Rodriguez, M. Sanchez-Chaves, and M. Fernandez-Garcia, *J. Polym. Sci. A* **2011**, **49**, 526 (2011).

22) H. Sawada, T. Suzuki, H. Takashima, and K. Takishita, *Colloid Polym. Sci.*, **286**, 1569 (2008).

23) H. Sawada and M. Nakayama, *J. Chem. Soc. Chem. Commun.*, **10**, 677 (1991).

24) H. Sawada, Y. Ikematsu, T. Kawase, and Y. Hayakawa, *Langmuir*, **12**, 3529 (1996).

25) Y. Oikawa, T. Saito, M. Yamada, M. Sugita, and H. Sawada, *ACS Appl. Mater. Interfaces*, **7**, 13782 (2015).

26) E. Sumino, T. Saito, T. Noguchi, and H. Sawada, *Polym. Adv. Technol*., **26**, 345 (2015).

27) T. Saito, Y. Tsushima, and H. Sawada, *Colloid Polym. Sci*., **293**, 65 (2015).

28) T. Saito, Y. Tsushima, T. Honda, T. Kamiya, M. Fujita, and H. Sawada, *J. Compos. Mater*., **50**, 3831 (2016).

29) X. Deng, L. Mammen, H.-J. Butt, and D. Vollmer, *Science*, **335**, 67 (2012).

30) X. Yao, Y. Song, and L. Jiang, *Adv. Mater*., **23**, 719 (2011).

31) J. Feng, B. Huang, and M. Zhong, *J. Colloid Interface Sci*., **336**, 268 (2009).

32) R. Taurino, E. Fabbri, M. Messori, F. Pilati, D. Pospiech, and A. Synytska, *J. Colloid Interface Sci*., **325**, 149 (2008).

33) A. K. Kota, Y. Li, J. M. Mabry, and A. Tuteja, *Adv. Mater*., **24**, 5838 (2012).

34) F. Liu, M. Ma, D. Zhang, Z. Gao, and C. Wang, *Carbohydr. Polym*., **103**, 480 (2014).

35) L. Wu, J. Zhang, B. Li, and A. Wang, *J. Colloid Interface Sci*., **413**, 112 (2014).

36) X. Feng and L. Jiang, *Adv. Mater*., **18**, 3063 (2006).

CHAPTER 5

Preparation and Properties of Fluoroalkyl End-Capped 2-Acrylamido-2-methylpropanesulfonic Acid Oligomer/Poly(vinyl alcohol) Composite Film

5.1 Introduction

ABA-triblock type two fluoroalkyl end-capped oligomers [R_F-$(M)_n$-R_F; M = radical polymerizable monomers; R_F = fluoroalkyl group] are attractive fluorinated polysoaps, due to their exhibiting a wide variety of unique properties such as high surface active property, self-assembled molecular aggregate ability which cannot be achieved by the corresponding randomly fluoroalkylated and AB-block type fluoroalkylated polysoaps.[1 ~ 3] In these two fluoroalkyl end-capped oligomers, fluoroalkyl end-capped oligomers possessing sulfobetaine-type units can cause a gelation not only in water but also in organic polar solvents such as methanol, ethanol and dimethyl sulfoxide through the synergistic interaction between the aggregation of fluoroalkyl segments at the oligomer end-sites and the ionic interaction of the sulfobetaine-type segments under non-crosslinked conditions.[4, 5] Two fluoroalkyl end-capped oligomers possessing hydroxy segments can also form gels in water and polar organic media through the synergistic interaction between the aggregation of fluoroalkyl groups at the oligomer end-sites and the intermolecular hydrogen bonding interactions of the hydroxy units at the oligomer side chains under similar conditions.[6 ~ 8] Moreover, fluoroalkyl end-capped 2-acrylamido-2-methylpropanesulfonic acid oligomer can cause a gelation in ionic liquids such as 1-methylpyrazolium tetrafluoroborate under non-crosslinked conditions.[9] This fluorinated oligomer gel formed in the ionic liquid afforded a high ionic (proton) conductivity

of 10^{-2} S/cm level at room temperature.[9] Fluoroalkyl end-capped 2-acrylamido-2-methylpropanesulfonic acid cooligomers containing poly(oxyethylene) units can also form gels in dimethyl sulfoxide under non-crosslinked conditions, and these fluorinated oligomeric gelling electrolytes containing lithium salts exhibit a considerably high ionic conductivity of 10^{-3} S/cm level at room temperature.[10] Therefore, from the developmental viewpoint of new fluorinated functional materials, it is of particular interest to develop the new fluorinated oligomeric composite gels through the interaction with the traditional polymers. In these traditional polymers, poly(vinyl alcohol) [PVA] is commercially among the most promising polymers; however, application of PVA into a wide variety of fields is extremely restricted due to its poor resistance toward water.[11] To improve such water-sensitive characteristic, there have been heretofore numerous reports on the crosslinking reactions of PVA with maleic acid, glutaraldehyde and formaldehyde to increase the strength of the PVA films.[12 ~ 16] The hybridizations of PVA with alkoxysilanes such as tetraethoxysilane, vinyltriethoxysilane and 2,2-bis(triethoxysilyl)ethane are also useful for the improvement of the strength and the permeation properties of the PVA films.[17 ~ 19] Aomi *et al.* have very recently reported that two fluoroalkyl end-capped vinyltrimethoxysilane oligomer/boric acid/poly(vinyl alcohol) composite films [R_F-$(VM)_n$-R_F/$B(OH)_3$/PVA] can provide not only the high amphiphobic characteristic but also the water resistant ability.[20] Therefore, it is suggested

that two fluoroalkyl end-capped oligomer gels will have high potential for affording the unique characteristic toward PVA. In fact, PVA hydrogels serves as a candidate for artificial cartilage[21 ~ 23]; however, such hydrogels in general suffer from lack of mechanical strength.[24] From this point of view, Gong *et al.* have already reported on the mechanically strong hydrogels obtained by inducing a double-network structure for numerous combinations of hydrophilic polymers such as poly(2-acrylamido-2-methylpropanesulfonic acid) and polyacrylamide.[24, 25] This chapter shows that fluoroalkyl end-capped 2-acrylamido-2-methylpropanesulfonic acid oligomer [R_F-(AMPS)$_n$-R_F] can react with poly(vinyl alcohol) [PVA] to supply the corresponding R_F-(AMPS)$_n$-R_F/PVA composite gels. The transparent colorless R_F-(AMPS)$_n$-R_F/PVA composite films were prepared by casting the homogeneous aqueous methanol solutions of the corresponding fluorinated composites. Interestingly, it was clarified that mechanical properties and the water-adsorption ability of these films are superior to those of the original PVA film, which was prepared under acidic conditions. These results will be described in this chapter.

5.2 Experimental

5.2.1 Measurements

Stress-strain curve testing was performed using a A&D STB-1225S (Tokyo, Japan). Molecular weights of fluoroalkyl end-capped 2-acrylamido-2-methylpropanesulfonic acid oligomer [R_F-$(AMPS)_n$-R_F; molecular weight (Mn): 20,500 g/mol] were determined by using a Shodex DS-4 (pump) and Shodex RI-71 (detector) gel permeation1 chromatography (Tokyo, Japan) calibrated with poly(ethylene glycol) (molecular weight: 1000 ~ 40000) standards by using 0.5 mol dm^{-3} Na_2HPO_4 aqueous solution as the eluent. Thermal analyses were recorded by raising the temperature around 800 °C (the heating rate: 10 °C/min) under atmospheric conditions by the use of Bruker axs TG-DTA2000SA differential thermobalance (Kanagawa, Japan).

5.2.2 Materials

2-Acrylamido-2-methylpropanesulfonic acid was purchased from FUJIFILM Wako Pure Chemical Industries (Osaka, Japan). Fluoroalkyl end-capped 2-acrylamido-2-methylpropanesulfonic acid oligomer [R_F-$(CH_2$-$CHC(=O)NH_2^+CMe_2CH_2SO_3^-)_n$-$R_F$; R_F = $CF(CF_3)OC_3F_7$] was synthesized by reaction of fluoroalkanoyl peroxide with the corresponding monomer according to the previously reported method.[4, 5)] The R_F-$(AMPS)_n$-R_F oligomer was

obtained as a white powder by reprecipitation with water-tetrahydrofuran, and was dried under vacuum at 50 °C for 2 days. Poly(vinyl alcohol) (KL-118^{TR}; molecular weight (Mw): 200,000 g/mol; degree of hydrolysis: 95.0 ~ 99.0 %) was kindly supplied from Kuraray Co., Ltd. (Tokyo, Japan).

5.2.3 Preparation of fluoroalkyl end-capped 2-acrylamido-2-methylpropanesulfonic acid oligomer [R_F-(AMPS)$_n$-R_F]/poly(vinyl alcohol) [PVA] composites

To a methanol solution (10 ml) of R_F-(AMPS)$_n$-R_F oligomer; R_F = $CF(CF_3)OC_3F_7$ (80 mg), was added an aqueous homogeneous solution (10 ml) containing PVA (420 mg). The mixture was stirred with a magnetic stirring bar at room temperature for 1 day. After the removal of solvent, the obtained product was dried under vacuum at 50 ºC for 1 day to afford the expected product [375 mg; isolated yield based on the used oligomer (80 mg) and PVA (420 mg): 89 %]. The material loss (125 mg) would be due to the recovery process of the expected composites. Other composites were also prepared under similar conditions. Each isolated composite was successively mixed with water in a tube. The mixture was treated under ultrasonic conditions until the solid was dissolved. The resulting solution was kept at 25 ºC for 1 h, and then the gelation was checked out visually. When it was formed, the gel was stable and the tube was able to be inverted without changing the shape of the gel.

5.2.4 Preparation of fluoroalkyl end-capped 2-acrylamido-2-methylpropanesulfonic acid oligomer/poly(vinyl alcohol) composite films

To a methanol solution (10 ml) containing fluoroalkyl end-capped 2-acrylamido-2-methylpropanesulfonic acid oligomer [R_F = $CF(CF_3)OC_3F_7$: R_F-$(AMPS)_n$-R_F] (80 mg) was added an aqueous solution (10 ml) of poly(vinyl alcohol) (420 mg). The mixture was stirred at room temperature for 6 hours to provide the low viscosity and transparent colorless solution. The R_F-$(AMPS)_n$-R_F/PVA composite film was easily prepared by casting this homogeneous solution on glass plate. The solvent was evaporated at room temperature, and the film formed peeled off and dried at room temperature for 1 day under vacuum to afford the expected composite film. The other composite films were also prepared under similar conditions.

5.2.5 Mechanical property of the R_F-$(AMPS)_n$-R_F/PVA composite films

The film samples were cut into the dumbbell-type specimen (35 mm long at two ends, thickness of 61 ~ 75 μm, and 2 mm wide at the neck) were loaded into the sample grips of materials testing machine (A&D STB-1225S, Tokyo, Japan) with a grip distance of 12 mm; a crosshead speed was 200 mm/min. The three films of each sample were used to determine the average values of Young's modulus, tensile strength, and elongation at break.

5.2.6 Swelling ratio of the R_F-(AMPS)$_n$-R_F/PVA composite films

The R_F-(AMPS)$_n$-R_F/PVA composite film was cut into a square of 10 mm × 10 mm × 61 μm (thickness), and was dried at room temperature for 1 day under vacuum. Swelling ratio of the film was measured after the preweight dried film was swollen in water at 25 ºC. The swollen film was weighed after being slightly removed from the surface water. The swelling ratio was calculated by the following equation: swelling ratio (g/g) = (W_s - W_d)/W_d, where W_d is the weight of dried film, and *Ws* is the weight of swollen film.

5.3 Results and discussion

Fluoroalkyl end-capped 2-acrylamido-2-methylpropanesulfonic acid oligomer [R_F-(AMPS)$_n$-R_F] was found to react with poly(vinyl alcohol) (PVA) in aqueous methanol solutions at room temperature for 1 day to afford the expected R_F-(AMPS)$_n$-R_F/PVA composite gel as shown in Scheme 5-1.

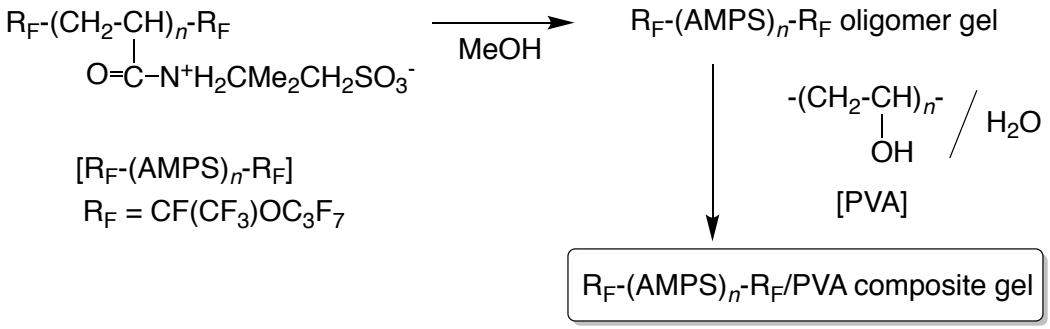

Scheme 5-1 Preparation of R_F-(AMPS)$_n$-R_F/PVA composite gel

It was demonstrated that the fluorinated composites thus obtained can cause a gelation in water as shown in Runs 2 ~ 4 in Figure 5-1.

R_F-$(AMPS)_n$-R_F/PVA composites (Run 1)*

R_F-$(AMPS)_n$-R_F/PVA composites (Run 2)*

R_F-$(AMPS)_n$-R_F/PVA composites (Run 3)*

R_F-$(AMPS)_n$-R_F/PVA composites (Run 4)*

*Each Run No corresponds to that of Table 5-1

Original R_F-$(AMPS)_n$-R_F oligomer

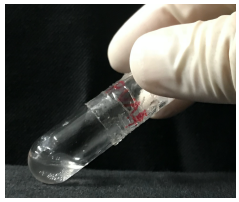

original PVA

Figure 5-1 Photograph of the R_F-$(AMPS)_n$-R_F /PVA composite hydrogels

To clarify this gelling behavior, the minimum concentrations (C_{min}) of these oligomers for gelation at 25 ºC have been measured according to the method reported by Hanabusa *et al*.[26, 27], and the results are summarized in Table 5-1.

Table 5-1 Minimum concentration C_{min} values (%) for gelation of the R_F-$(AMPS)_n$-R_F/PVA composites in water

Run*	Feed ratio of oligomer/PVA mg/mg (mol/mol)	C_{min}
1	20/480 (0.41/1.00)	no gelation
2	40/460 (1.00/1.00)	12
3	80/420 (1.86/1.00)	7
4	160/340 (4.59/1.00)	9
Original R_F-$(AMPS)_n$-R_F		9
Original PVA		no gelation

As shown in Table 5-1, original PVA and the R_F-(AMPS)$_n$-R_F/PVA composites (Run 1), which were prepared under a lower feed amount (20 mg) of oligomer based on PVA (480 mg), are unable to reveal the gelling ability. However, the C_{min} values were found to decrease from 12 to 7 or 9 %, with the increase of the feed amounts of oligomer from 40 to 160 mg, indicating that this gelation behavior is governed by the synergistic interaction between the aggregation of the end-capped fluoroalkyl groups in oligomer and the ionic interaction of the sulfobetine-type segments. Thus, the higher feed amounts of oligomer such as Run 4 should enable the R_F-(AMPS)$_n$-R_F/PVA composites to provide the similar gelling ability to that of the original R_F-(AMPS)$_n$-R_F oligomer.

The R_F-(AMPS)$_n$-R_F/PVA composite films were prepared by using the corresponding composites (Runs 1 ~ 4 in Table 5-1). The photograph of the obtained composite films is depicted in Figure 5-2. Original PVA film and the PVA film (PVA/HCl film), which was prepared under acidic conditions, were also illustrated in Figure 5-2, for comparison.

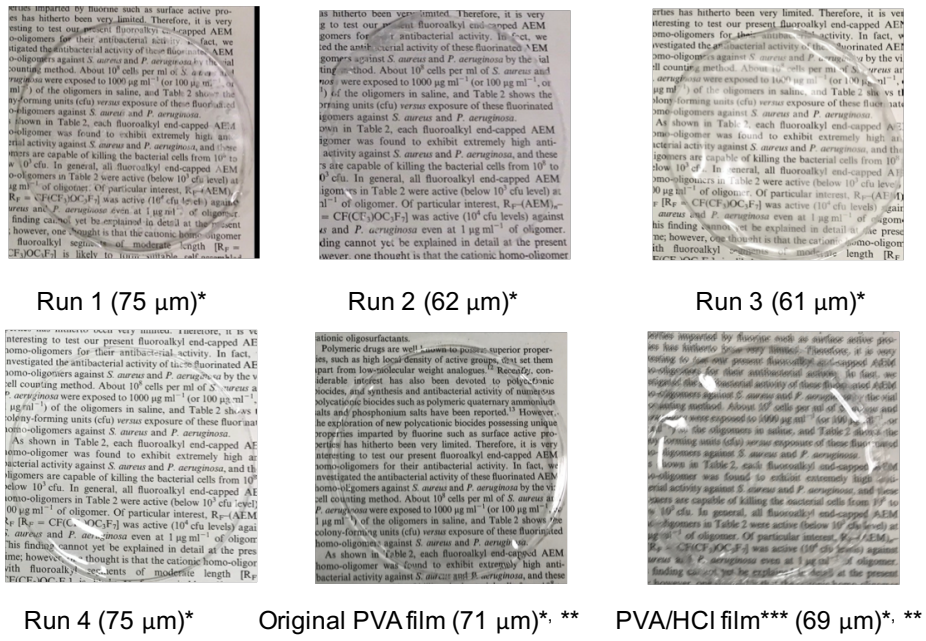

Run 1 (75 μm)* Run 2 (62 μm)* Run 3 (61 μm)*

Run 4 (75 μm)* Original PVA film (71 μm)*, ** PVA/HCl film*** (69 μm)*, **

Figure 5-2 Photograph of the R_F-$(AMPS)_n$-R_F/PVA composite films, which were prepared by using the corresponding composites (Runs 1 ~ 4) in Table 5-1, original PVA film, and the PVA/HCl film, which was prepared under acidic conditions (1 N HCl: 1 ml); *)Film thickness; **)Used PVA: 500 mg

As shown in Figure 5-2, the transparent colorless composite films (Runs 1 ~ 4) were prepared, quite similar to that of the original PVA film and the PVA/HCl film. Original PVA film is very sensitive toward water, and this film was completely soluble after immersion into water within 1 min. However, the PVA/HCl film was unable to give a solubility toward water, and a swelling behavior of this film was observed after immersion into water. This finding would be due to the crosslinking reaction between the hydroxy groups on the PVA main chain to produce the crosslinked acetal units under acidic conditions.[28] In addition, the TGA (thermogravimetric analyses) measurements of these composite films were studied in order to

clarify the presence of the residual solvent in the composite films. The results are shown in Figure 5-3.

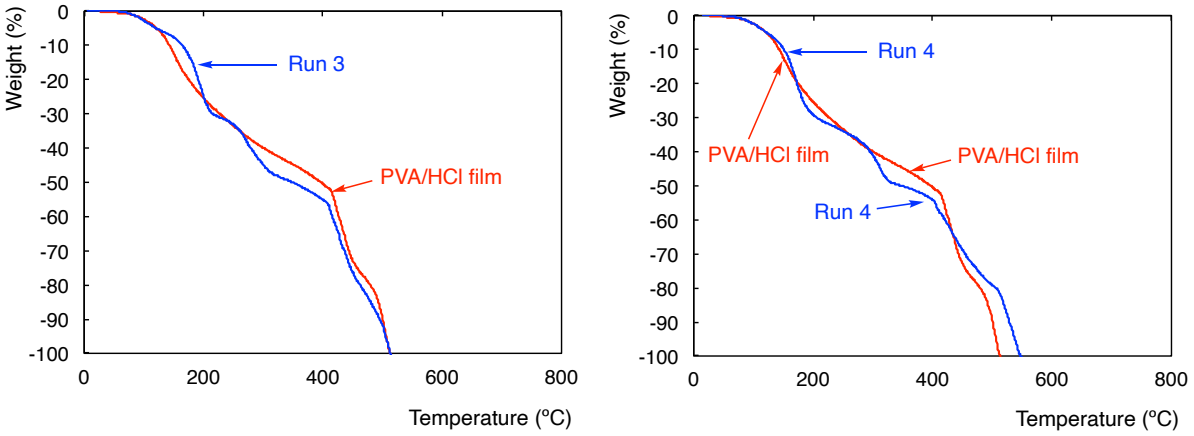

Figure 5-3 TGA (Thermogravimetric analyses) of R_F-(AMPS)$_n$-R_F/PVA composite films Runs 3* and 4* and the PVA/HCl film*

* Run numbers and PVA/HCl film correspond to those of Figure 5-2

As shown in Figure 5-3, the composite films cannot afford any residual solvent at around 100 ºC quite similar to that of the PVA/HCl film. Thus, the mechanical property has been studied toward the R_F-(AMPS)$_n$-R_F/PVA composite films (Runs 1 ~ 4 in Figure 5-2) and the PVA/HCl film. The mechanical property of the original PVA film was not performed due to its higher solubility toward water. The composite films were subjected to tensile testing to evaluate the stress-strain relationship. The typical stress-strain behavior for the R_F-(AMPS)$_n$-R_F/PVA composite film (Run 3 in Figure 5-2) and the PVA/HCl film at the crosshead speed of 200 mm/min at room temperature is shown in Figure 5-4.

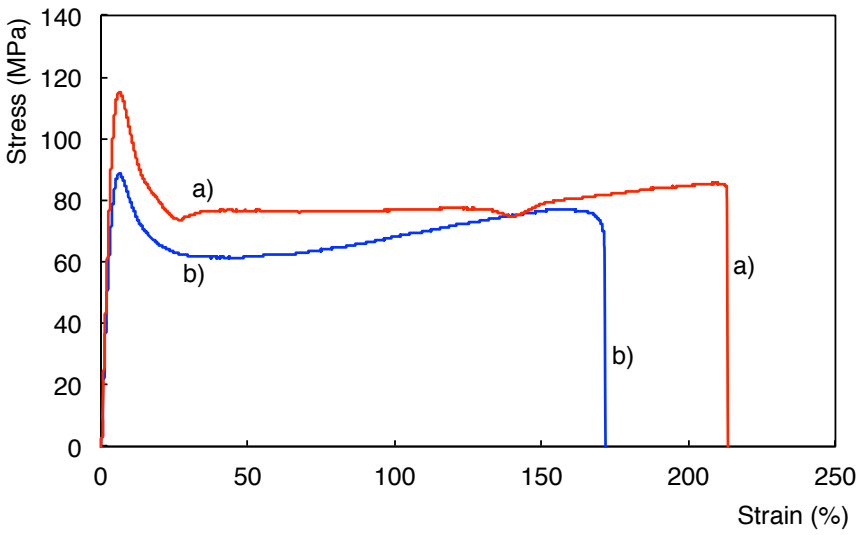

Figure 5-4 Stress-Strain curves of the R_F-$(AMPS)_n$-R_F/PVA composite film (a); Run 3) and the PVA/HCl film (b))

Interestingly, the R_F-$(AMPS)_n$-R_F/PVA composite film (Run 3) had an elongation at break of 215 % level, higher than that (170 %) of the PVA/HCl film, as illustrated in Figure 5-4. The higher tensile strength and the Young's modulus were also observed for this R_F-$(AMPS)_n$-R_F/PVA composite film. The polymer film having a higher Young's modules is in general tough and brittle to provide the lower elongation at break. However, this composite film can provide a significant increase in both the tensile strength and elongation at break, compared to those of the PVA/HCl film. This would be due to the architecture of a double-network structure for the combination of R_F-$(AMPS)_n$-R_F oligomeric gel network and PVA gel network. The crosslinking reactions of PVA by the use of traditional cross-linkers such as maleic acid, glutaraldehyde and formaldehyde are well-known to provide the PVA

hydrogel.[12 ~ 16] Aqueous hydrochloric acid is also effective for the formation of PVA hydrogels through the crosslinking between hydroxy groups on the PVA main chain to produce the acetal units.[28] Kijima *et al.* reported that aqueous R_F-(AMPS)$_n$-R_F oligomer solution can exhibit the acidic characteristic (pH 2.86), due to the presence of the sulfobetaine-type segments on the oligomer side-chain.[29] Therefore, PVA should form the corresponding hydrogel in the presence of R_F-(AMPS)$_n$-R_F oligomer to create the new R_F-(AMPS)$_n$-R_F/PVA double-network gel. Such double-network gel can derive into the superior mechanical property to that of the PVA/HCl film.

The Young's modulus, the tensile strength, and the elongation at break for the composite films (Runs 1 ~ 4) and the PVA/HCl film are summarized in Figure 5-5, which are the average values of each three films.

As shown in Figure 5-5, the R_F-(AMPS)$_n$-R_F/PVA composite films (Runs 1 ~ 4) were found to have a higher Young's modulus and tensile strength than those of the PVA/HCl film. Especially, the composite films (Runs 3 and 4) possessing a higher gelling ability, of whose the minimum concentrations (C_{min}) are 7 ~ 9 (see Table 5-1), can give a higher Young's modulus and tensile strength than that of the PVA/HCl film. Of particular interest, only the composite film: Run 3 can supply a higher elongation at break than that of the PVA/HCl film. This finding is due to the higher gelling ability, compared to that of the other composite films. Thus, the

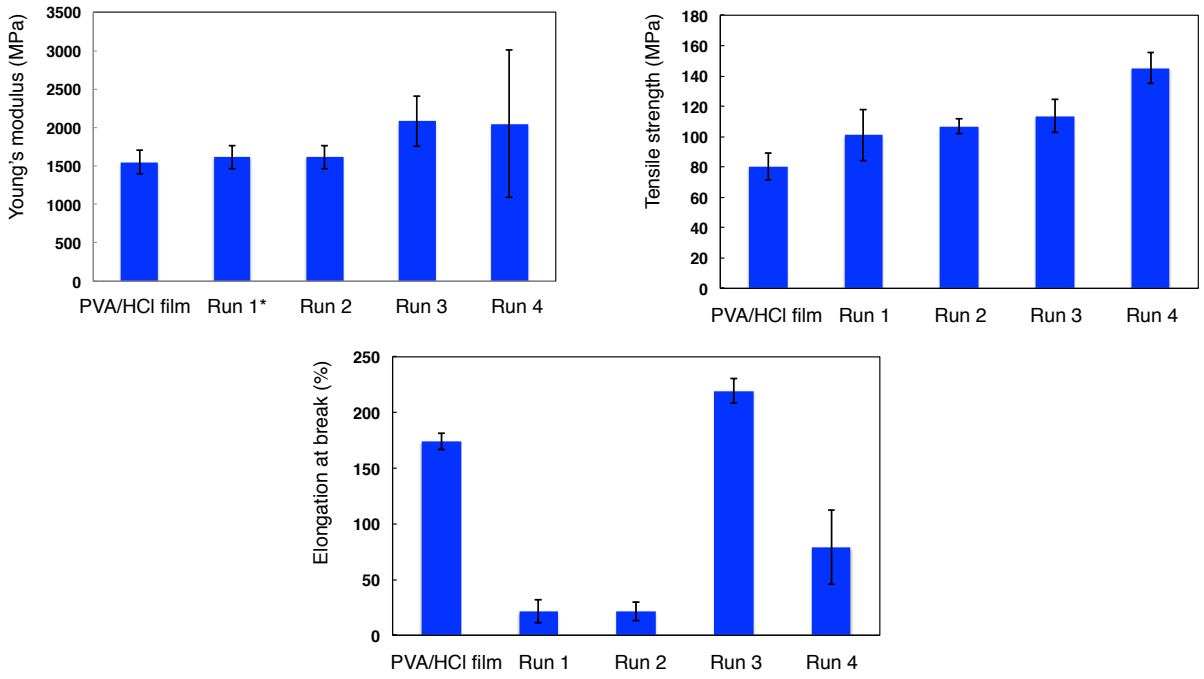

Figure 5-5 Mechanical properties (Young's modulus, tensile strength, and elongation at break) of the R_F-$(AMPS)_n$-R_F/PVA composite films (*each Run No corresponds to that of Figure 5-2)

R_F-$(AMPS)_n$-R_F/PVA composites (Run 3) possessing a higher gelling ability should establish the mechanically strong double-network gel to provide a higher elongation at break for the composite films. Usually, it is well known that the double-network gels are synthesized through the two-step crosslinking reactions; that is, first step consists of the synthesis of crosslinked hydrophilic polymers such as poly(2-acrylamido-2-methylpropanesulfonic acid) [PAMPS], of whose polymer is obtained by the photopolymerization of AMPS monomer in the presence of crosslinking agent (*N, N'*-methylenebisacrylamide (MBAAm) initiated by 2-oxoglutaric acid. In the second step, the subsequently photopolymerization of acrylamide (AAm) containing MBAAm and 2-oxoglutaric acid in the presence of the crosslinked PAMPS hydrogel can

proceed to provide the double-network hydrogel as illustrated in Scheme 5-2.[24, 25, 30)]

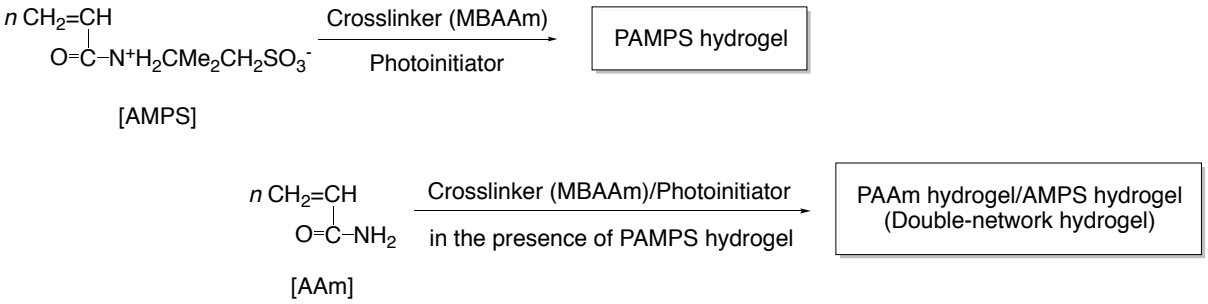

Scheme 5-2 Formation of the traditional double-network hydrogel

On the other hand, R_F-$(AMPS)_n$-R_F oligomer can form the gel in water through the synergistic interaction between the aggregation of the end-capped fluoroalkyl groups and the ionic interaction of sulfobetaine-type segments under non-crosslinked conditions (see Scheme 5-3). Especially, PVA should afford the crosslinked PVA hydrogel related to the acetal units formed from hydroxy groups between the PVA main chain in the presence of the acidic R_F-$(AMPS)_n$-R_F oligomer solution (pH 2.86).[29)] Thus, the double-network hydrogel can be easily prepared by the reaction of the R_F-$(AMPS)_n$-R_F oligomer with PVA in aqueous solutions in only one step, quite different from the traditional synthesis of the double-network hydrogels, as shown in the following Schematic illustration.

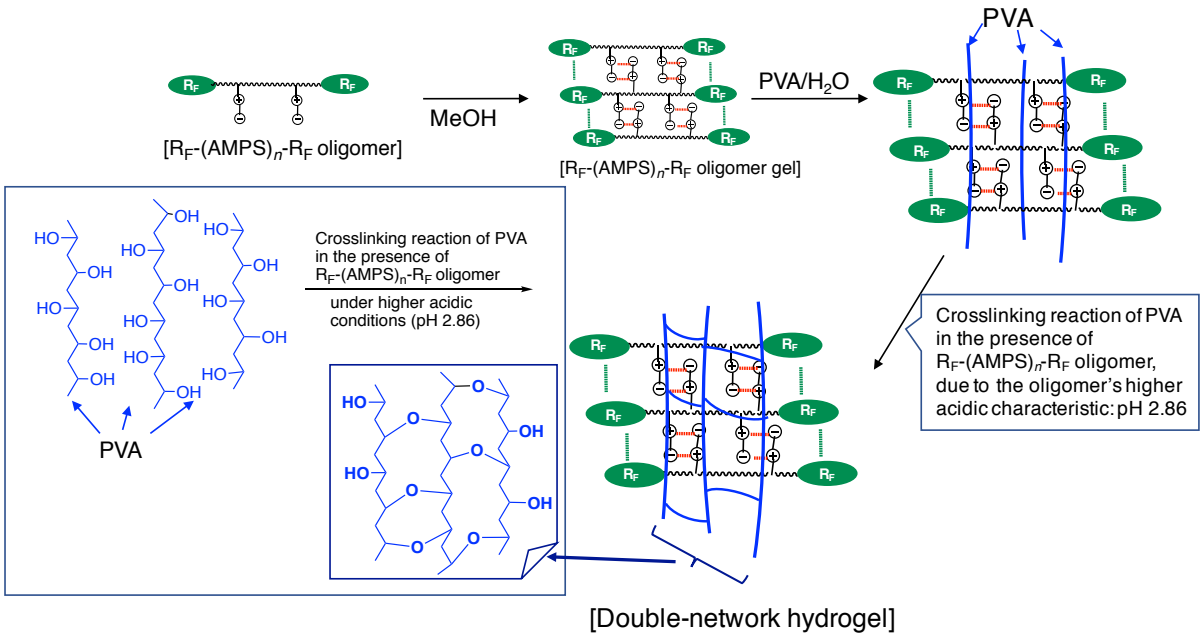

Scheme 5-3 Schematic illustration of the formation of double-network hydrogel through the interaction of R_F-(AMPS)$_n$-R_F oligomer and PVA

In this way, such double-network formation would enable the R_F-(AMPS)$_n$-R_F/PVA composite possessing a higher gelling ability to create the mechanically strong composite film.

It is of particular interest to clarify the water-adsorption ability of the present the R_F-(AMPS)$_n$-R_F/PVA composite films in order to apply these films into a variety of fields. Because the application of the original PVA film is very limited due to its higher solubility toward water.[11] Thus, the water-adsorption behaviors have been studied toward the R_F-(AMPS)$_n$-R_F/PVA composite films [square of 10 mm × 10 mm × 61 ~ 76 μm (film thickness)]. The PVA/HCl film [a square of 10 mm × 10 mm × 69 μm (film thickness)] was also studied under similar conditions, for comparison. The results are shown in Figure 5-6.

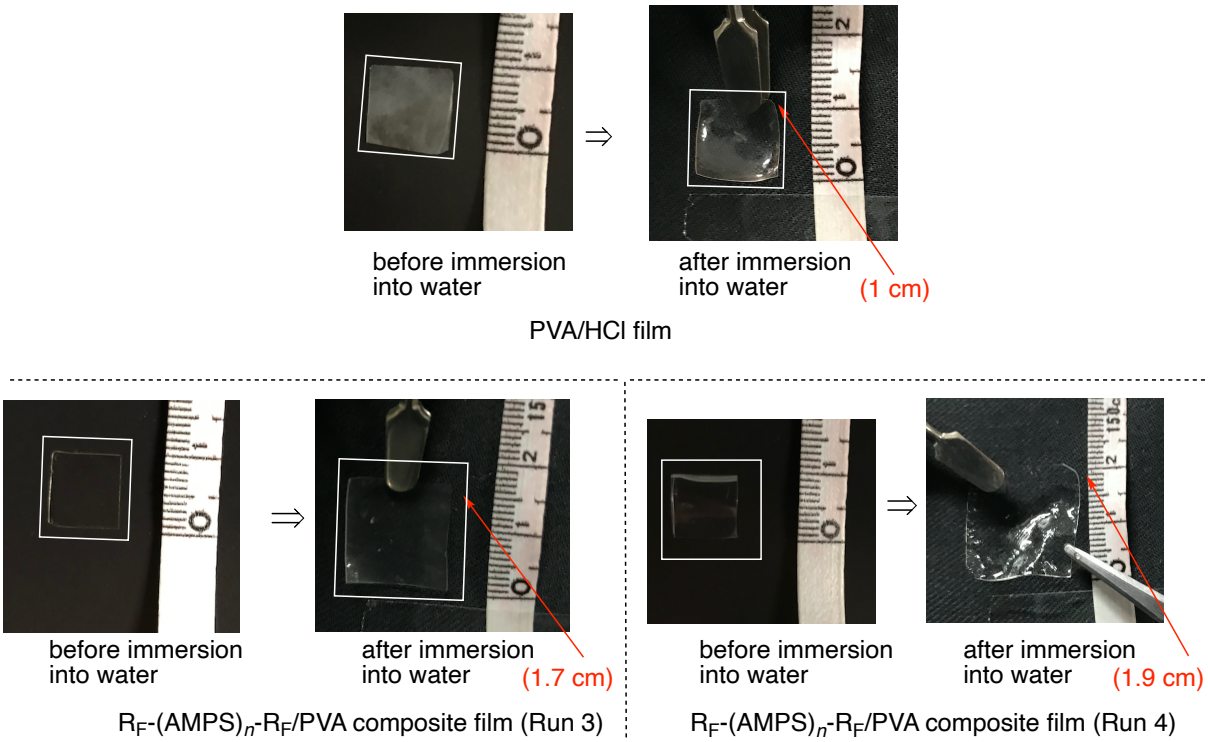

Figure 5-6 Photograph of the PVA/HCl film and the R_F-(AMPS)$_n$-R_F/PVA composites films before and after immersion into water

In the case of the PVA/HCl film, a swelling behavior was observed with keeping the shape of this film after immersion into water for 60 min. On the other hand, interestingly, the shape of the R_F-(AMPS)$_n$-R_F/PVA composite films (Runs 3 and 4) were found to swell to about two times under similar immersion conditions as shown in Figure 5-6. Thus, the relationship between the swelling ratio (g/g) of the composite films and the immersion time into water was studied, and the results are summarized in Figure 5-7.

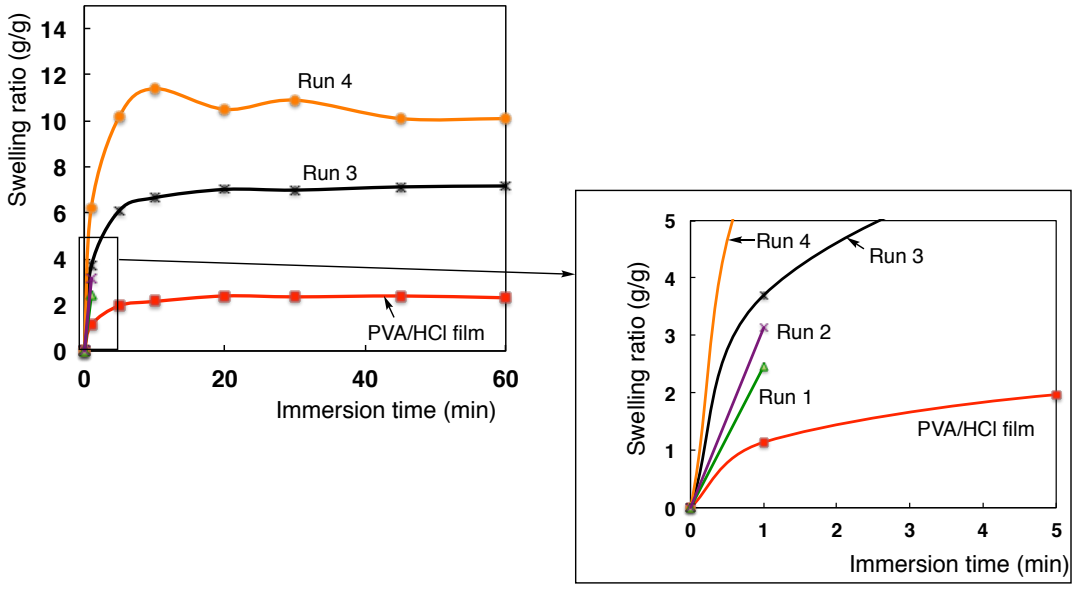

Figure 5-7 Relationship between the immersion time and swelling ratio of the R_F-$(AMPS)_n$-R_F/PVA composite films

Figure 5-7 shows that the PVA/HCl film can adsorb water to form the gelling film (swelling ratio of the film: ca. 2 g/g) after immersion into water for 5 min, and this film keeps the constant swelling ratio (2 g/g) even after immersion into water for 60 min. On the other hand, the R_F-$(AMPS)_n$-R_F/PVA composite films (Runs 1 and 2), of whose composites exhibit no gelation and a poor gelling ability (C_{min} = 12 %), respectively, afforded a soluble characteristic after immersion into water for 1 min, indicating that these composites cannot construct the double-network structure to lead the mechanically strong hydrogel films. However, of particular interest, the R_F-$(AMPS)_n$-R_F/PVA composite films (Runs 3 and 4), of whose composites supply a higher gelling ability (C_{min} = 7 and 9 %), can give a higher

water-adsorption behavior (6 ~10 times), compared to that (2 times) of the PAV/HCl film after immersion into water for 5 min.

The water cycling stability has been studied toward the R_F-(AMPS)$_n$-R_F/PVA composite films (Runs 3 and 4) for the water-adsorption and -desorption behavior by using the corresponding fresh composite films. Especially, the dried composite films after completely releasing water was used in the case of 2 cycle, and the swelling ratio was successively measured under similar conditions. The results are shown in Figure 5-8.

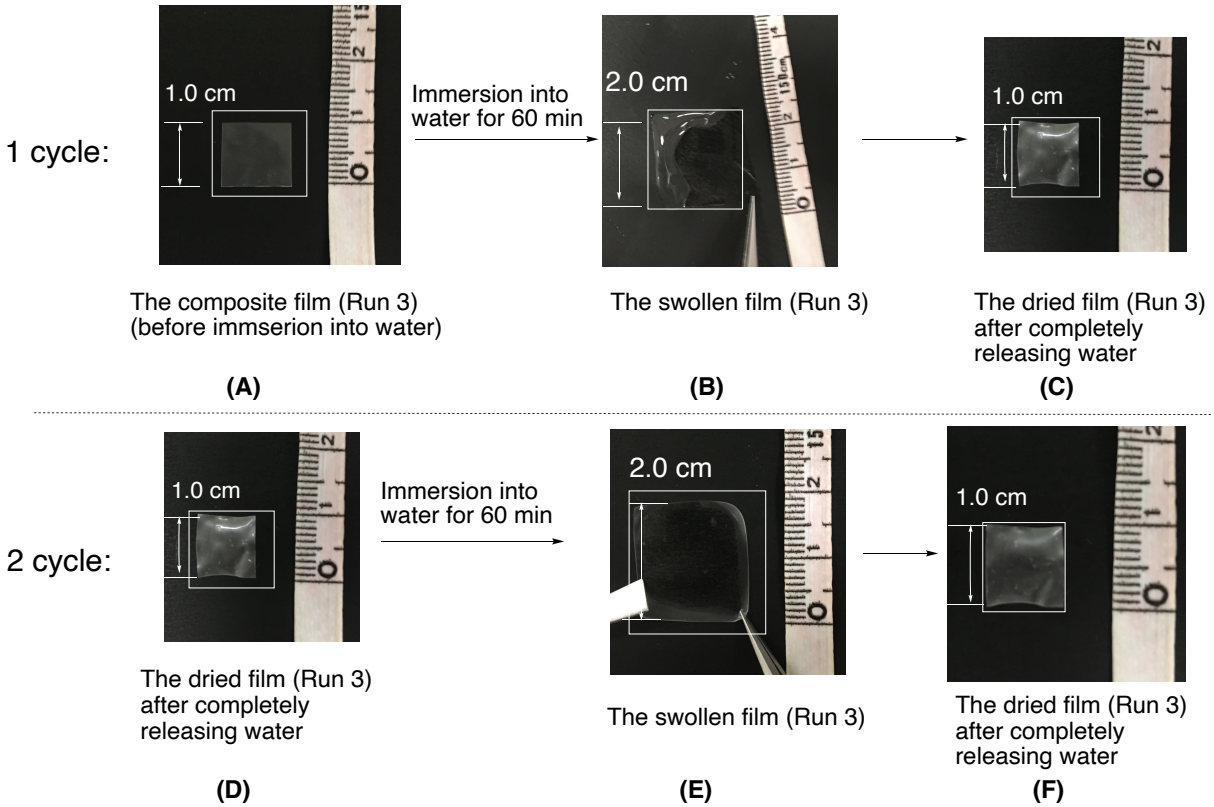

Figure 5-8 Photograph of the R_F-(AMPS)*n*-R_F/PVA composite film (Run 3) before immersion into water **(A)**, the swollen film (Run 3) after immersion into water for 60 min **(B)**, and the dried film (Run 3) after completely releasing water **(C)** in the case of 1cycle. The same dried film (Run 3) **(D)** was used in the case of 2 cycle [**(D)** ~ **(F)**]

As shown in Figure 5-8, the good water cycling stability was observed for the swelling behavior of the composite film (Run 3). The shape of the composite film [square of 10 mm × 10 mm × 61 μm (film thickness)] was found to swell to approximately two times after immersion into water for 60 min, quite similar to that of Figure 5-6. However, interestingly, the shape of this swollen film was recovered to the original one through the drying process [see Figure 5-8-**(C)**]. The similar swelling behavior was observed toward the dried composite film (Run 3) in 2 cycle as shown in Figure 5-8- **(D)** ~ **(F).** In addition, a similar swelling characteristic was observed in the composite film (Run 4) (data not shown). Furthermore, the water cycling stability was studied toward the swelling ratio of the composite films (Runs 3 and 4), and the results are shown in Table 5-2.

Table 5-2 Swelling ratio of the R_F-$(AMPS)_n$-R_F/PVA composite films immersing into water at room temperature for 1 hour

The composite film	Immersion time (min)						
	1	5	10	20	30	45	60
Run 3	Swelling ratio [g/g (swollen film/dried film before immersion]						
1 cycle	4.6	5.5	5.7	5.8	5.8	6.0	6.0
2 cycle	4.8	5.6	5.6	5.8	5.7	5.8	5.8
Run 4	Swelling ratio [g/g (swollen film/dried film before immersion]						
1 cycle	6.7	9.2	10.2	10.4	10.7	10.9	11.1
2 cycle	7.1	9.8	10.5	10.7	10.7	10.8	10.6

As indicated above, each swelling ratio for the film: Run 3 or Run 4 in 1 cycle was found to be quite similar to that of Run 3 or Run 4 in Figure 5-7, respectively, and a good water cycling stability of the composite films: Runs 3 and 4 was observed for the water-adsorption process in 2 cycle. This finding would be due to the construction of mechanically strong double-network hydrogel. In fact, as shown in Figure 5-4, the composite films (Runs 3 and 4) can exhibit the higher Young's modulus, tensile strength, and elongation at break than those of the other composite films (Runs 1 and 2).

In this way, it was clarified that the R_F-(AMPS)$_n$-R_F/PVA composite films, of whose composites possess a higher gelling ability, can exhibit a higher water-adsorption ability with keeping the shape of the swollen composite films.

5.4 Conclusions

The R_F-$(AMPS)_n$-R_F/PVA composites have been newly prepared by the reactions of the R_F-$(AMPS)_n$-R_F oligomer with PVA at room temperature for 1 day. The transparent colorless films were subsequently prepared by casting their aqueous methanol solutions. It was demonstrated that the mechanical properties such as Young's modulus and tensile strength of the obtained composite films were superior to that of the PVA/HCl film. The R_F-$(AMPS)_n$-R_F/PVA composite films possessing a higher gelling ability can provide the significant increase in the Young's modulus, tensile strength and elongation at break, compared to the other composite films possessing a poor gelling ability. The polymer film possessing the higher Young's modulus is in general tough and brittle to give the lower elongation at break; however, such excellent mechanical property would be due to the formation of the double-network structure in the corresponding composite film. Mechanically strong composite films were also clarified to afford a higher water-adsorption ability with keeping the shape of the swollen films, quite different from that of the PVA/HCl film. In this way, it is suggested that the present R_F-$(AMPS)_n$-R_F/PVA composite films have high potential for a wide variety of fields, especially the biomedical area, because the R_F-$(AMPS)_n$-R_F oligomer hydrogels are known to be potent and selective inhibitors of HIV-1 and other enveloped viruses.[31)]

References

1) H. Sawada, *Chem. Rev*., **96**, 1779 (1996).

2) H. Sawada, *Prog. Polym. Sci*., **32**, 509 (2007).

3) H. Sawada, *Polym. Chem*., **3**, 46 (2012).

4) H. Sawada, S. Katayama, Y. Nakamura, T. Kawase, Y. Hayakawa, and M. Baba, *Polymer*, **39**, 743 (1998).

5) H. Sawada, S. Katayama, Y. Ariyoshi, T. Kawase, Y. Hayakawa, T. Tomita, and M. Baba, *J. Mater. Chem*., **8**, 1517 (1998).

6) H. Sawada, Y. Nakamura, S. Katayama, and T. Kawase, *Bull. Chem. Soc. Jpn*., **70**, 2839 (1997).

7) H. Sawada, T. Tanimura, S. Katayama, and T. Kawase, *Chem. Commun*., 1391 (1997).

8) H. Sawada, T. Tanimura, S. Katayama, T. Kawase, T. Tomita, and M. Baba, *Polymer J*., **30**, 797 (1998).

9) H. Sawada, K. Shima, J. Kyokane, K. Oharu, H. Nakagawa, and T. Kitazume, *Eur. Polym. J*., **40**, 1595 ~ 1597 (2004).

10) H. Sawada, Y. Ariyoshi, K. Lee, J. Kyokane, and T. Kawase, *Eur. Polym. J*., **36**, 2523 (2000).

11) J. Wang, X. Wang, C. Xu, M. Zhang, and X. Shang, *Polym. Int*., **60**, 816 (2011).

12) R. Y. M. Huang and J. W. Rhim, *Polym. Int*., **30**, 129 (1993).

13) C. K. Yeom and R. Y. M. Huang, *Angew. Makromol. Chem*., **184**, 27 (1991).

14) C. K. Yeom and K. H. Lee, *J. Membr. Sci*., **109**, 257 (1996).

15) J.-W. Rhin, S.-W. Yoon, S.-W. Kim, and K.-H Lee, *J. Appl. Polym. Sci*., **63**, 521 (1997).

16) A. Bandyopadhyay, M. DE Sarkar, and A. K. Bhowmick, *J. Mater. Sci*., **40**, 5233 (2005).

17) T. Uragami, K. Okazaki, H. Matsugi, and T. Miyata, *Macromolecules*, **35**, 9156 (2002).

18) W. W. Hu, H. H. Zhang, Q. G. Zhang, Q. L. Liu, and A. M. Zhu, *J. Appl. Polym. Sci*., **126**, 778 (2012).

19) Q. G. Zheng, Q. L. Liu, A. M. Zhu, Y. Xiong, and X. H. Zhang, *J. Phys. Chem*. B, **112**, 16559 (2008).

20) Y. Aomi and H. Sawada, *J. Coat. Technol. Res*., **16**, 651 (2019).

21) J. A. Stammen, S. Williams, D. N. Ku, and R. E. Guldberg, *Biomaterials*, **22**, 799 (2001).

22) K. S. Anseth, C. N. Bowman, and L. Brannon-Peppas, *Biomaterials,* **17**, 1647 (1996).

23) Z.-Q. Gu, J.-M. Xiao, and X.-H. Zhang, *Biomed. Mater. Eng*., **8**, 75 (1998).

24) J. P. Gong, Y. Katsuyama, T. Kurokawa, and Y. Osada, *Adv. Mater*., **15**, 1155 (2003).

25) J. P. Gong, T. Kurokawa, T. Narita, G. Kagata, Y. Osada, G. Nishimura, and M. Kinjo, *J. Am. Chem. Soc*., **123**, 5582 (2001).

26) K. Hanabusa, R. Tanaka, M. Suzuki, M. Kimura, and H. Shirai, *Adv. Mater*., **9**, 1095

(1997).

27) K. Hanabusa, K. Okui, K. Karaki, M. Kimura, and H. Shirai, *J. Colloid Interface Sci*., **195**, 86 (1997).

28) I. Sakurada and S. Matsuzawa, *Kobunshi Kagaku*, **20**, 353 (1963).

29) T. Kijima, M. Nishida, H. Fukaya, M. Yoshida, and H. Sawada, *J. Polym. Sci*. Part A: *Polym. Chem*., **51**, 2555 (2013).

30) T. Suekama, J. Hu, T. Kurokawa, J. P. Gong, and S. H. Gehrke, *Macromol. Symp*., **329**, 9 (2013).

31) M. Fujiwara, N. Ashida, M. Okamoto, T. Mizuta, T. Ide, Y. Hanasaki, K. Katsuura, H. Sawada, S. Shigeta, K. Konno, T. Yokota, and M. Baba, *Antiviral Res*., **38**, 141 (1998).

Conclusions

The results obtained from this study are summarized as follows.

1. Fluoroalkylated end-capped 2-acrylamido-2-methylpropanesulfonic acid homo-oligomers [R_F-(AMPS)$_n$-R_F] containing sulfobataine-type segment were synthesized by reaction of fluoroalkanoyl peroxides with 2-acrylamido-2-methylpropanesulfonic acid (AMPS). Similarly, fluoroalkylated end-capped co-oligomers [R_F-(AMPS)$_x$-(CH_2-CR^1R^2)$_y$-R_F] were synthesized by reaction of fluoroalkanoyl peroxides with AMPS and the comonomers such as trimethylvinylsilane and methyl methacrylate. These fluoroalkylated end-capped AMPS oligomers were found to form gels not only in water but also in organic polar solvents such as methanol, ethanol, *N,N*-dimethylformamide and dimethyl sulfoxide under non-crosslinked conditions. On the other hand, AMPS polymer containing fluoroalkylene units {[-R_F-(AMPS)$_q$]$_p$-} could cause no gelation under similar conditions. Thus, fluoroalkylated end-capped AMPS oligomers can cause gelation where strong aggregation of the end-capped fluoroalkyl segments is involved sterically in establishing the physical gel network in these media. These fluoroalkylated end-capped AMPS oligomer hydrogels had a strong metal-ion binding power for Cr^{3+} and Co^{2+}. Moreover, these fluoroalkylated gelling oligomers are potent

and selective inhibitors of HIV-1 replication in cell culture. In addition, one of these gelling oligomers was found to possess antibacterial activity against *Staphylococcus aureus*.

2. Fluoroalkylated end-capped *N*-tris(hydroxymethyl)methylacrylamide oligomers [R_F-(NAT)$_n$-R_F] containing triol segments were synthesized under very mild conditions by reaction of fluoroalkanoyl peroxides with *N*-tris(hydroxymethyl)methylacrylamide (NAT). These fluoroalkylated NAT oligomers were found to cause a physical gelation not only in water, but also in organic solvents, such as DMSO and DMF, whose behavior is governed by the synergistic interaction of strong aggregations of fluoroalkyl segments in oligomers and intermolecular hydrogen bonding between triol segments under non-crosslinked conditions. It was demonstrated that the aggregation of fluoroalkyl segments in polymeric compounds in water and/or in organic media become a new driving factor for gelation as well as the well-known interactions, such as hydrogen bond and ionic interaction. Hitherto, it is well known that longer fluoroalkylated compounds exhibit a strong repellent property against water or hydrocarbons owing to the strong electronegativity of fluorine. However, since fluoroalkyl groups are introduced into only oligomer end-sites, these fluoroalkyl segments could aggregate easily each other rather than have repellent interactions in aqueous or organic media. Additionally, these fluoroalkylated oligomer hydrogels have not only a metal-ion binding, for

Cr^{3+}, but also a metal-ion releasing power. Especially, these oligomer hydrogels possessing lower minimum concentrations for gelation (C_{min}) values had a higher metal binding power, whereas, the hydrogels possessing higher C_{min} values had a higher releasing power.

3. Fluoroalkyated end-capped 3-methacryloxy-2-hydroxypropyltrimethylammonium chloride oligomers [R_F-(MHPTA)$_n$-R_F] containing hydroxy segment were synthesized under very mild conditions by oligomerization reaction of fluoroalkanoyl peroxides with 3-methacryloxy-2-hydroxypropyltrimethylammonium chloride (MHPTA). Similarly, fluoroalkyated end-capped 2-hydroxy-2-[(1-oxoprop-2-enyl)amino]acetic acid oligomers containing hydroxy and carboxy segment [R_F-(HOPPA)$_n$-R_F] were synthesized by using fluoroalkanoyl peroxides. A series of these fluoroalkylated end-capped oligomer containing hydroxy segment or hydroxy and carboxy segments can cause gelation under non-crosslinked conditions not only in water but also polar organic media such as methanol, *N,N*-dimethylformamide, and dimethyl sulfoxide. Especially, longer perfluoro-oxaalkylated oligomers exhibited higher gelling ability. Thus, these results suggest that the main driving force for gelation is the synergistic interactions with the aggregation of fluoroalkyl units in oligomers and intermolecular hydrogen bonding between hydroxy segments or carboxy segments including the interactions of hydroxy (-OH) and trimethylammonium (-N^+Me_3)

segments. Oligomers with longer fluoroalkyl segments and greater molar ratios of monomer in monomer/peroxide are to have stronger association through aggregation of fluoroalkyl moieties and intermolecular hydrogen bondings between hydroxy or carboxy segments to cause physical gelation. In addition, fluoroalkylated MHPTA oligomer: R_F-(MHPTA)$_n$-R_F had high metal-ion binding or releasing power for Cr^{3+} and Co^{2+}. The gelling or gel-like fluoroalkylated MHPTA oligomers exhibited not only the properties imparted by fluorine such as surface activity, but also some antibacterial activity for *Staphylococcus aures*.

4. Sol-gel reaction of fluoroalkyl end-capped vinyltrimethoxysilane oligomer [R_F-($CH_2CHSi(OMe)_3$)$_n$-R_F: R_F-(VM)$_n$-R_F] proceeded smoothly in the presence of *N*-(3-triethoxysilylpropyl)gluconamide [Glu-Si(OEt)$_3$] under alkaline conditions to afford the corresponding fluorinated oligomeric silica/Glu-SiO_2 nanocomposites [R_F-(VM-SiO_2)$_n$-R_F/ Glu-SiO_2]. Wettability control between the highly oleophobic/superhydrophobic and highly oleophobic/superhydrophilic states was observed on the modified glass surfaces treated with the R_F-(VM-SiO_2)$_n$-R_F/Glu-SiO_2 nanocomposites. Such wettability can be easily controlled by changing the feed amount ratios of Glu-Si(OEt)$_3$ and R_F-(VM)$_n$-R_F oligomer for the preparation of the nanocomposites. Lower feed amounts of Glu-Si(OEt)$_3$ can provide a highly oleophobic/superhydrophobic surface; in contrast, a higher feed amount of Glu-Si(OEt)$_3$

enables the modified surface to reveal a highly oleophobic/superhydrophilic characteristic. Such a highly oleophobic/superhydrophobic characteristic was also observed on the modified PET fabric swatch, and this modified PET fabric was applied to the separation membrane to separate the mixture of fluorocarbon oil and hydrocarbon oil. R_F-(VM-SiO_2)$_n$-R_F/Glu-SiO_2 nanocomposites were also shown to cause gelation toward water. Especially, the gelling nanocomposites were applied to the surface modification of the PET fabric swatch to exhibit a highly oleophobic/superhydrophobic characteristic on the modified surface. However, interestingly, it can be observed that the wettability change on the modified PET fabric surface from a highly oleophobic state to a superoleophilic state, while keeping the superhydrophobic characteristic by immersing this modified PET fabric into water.

5. Fluoroalkylated end-capped 2-acrylamido-2-methylpropanesulfonic acid oligomer/poly(vinyl alcohol) composites [R_F-(AMPS)$_n$-R_F/PVA] were prepared by reaction of the corresponding fluorionated end-capped AMPS oligomer with poly(vinyl alcohol (PVA). The transparent colorless films were subsequently prepared by casting their aqueous methanol solutions. The mechanical properties such as Young's modulus and tensile strength of the obtained composite films were superior to that of the PVA/HCl film, which was prepared by casting the aqueous methanol solution of PVA in the presence of 1 N hydrochloric acid. The

R_F-(AMPS)$_n$-R_F/PVA composite films possessing a higher gelling ability can provide the significant increase in the Young's modulus, tensile strength and elongation at break, compared to the other composites films possessing a poor gelling ability. The polymer film possessing the higher Young's modulus is in general tough and brittle to give the lower elongation at break; however, such excellent mechanical property would be due to the formation of the double-network structure in the corresponding composite film. Mechanically strong composite films were also clarified to afford a higher water-adsorption ability with keeping the shape of the swollen films, quite different from that of the PVA/HCl film.

Publications

1) H. Sawada, S. Katayama, Y. Nakamura, T. Kawase, Y. Hayakawa, and M. Baba, "Gelation of fluoroalkylated 2-acrylamido-2-methylpropanesulfonic acid oligomers as potential for prevention of HIV-1 transmission", *Polymer*, **39**, 743 ~ 745 (1998).

2) H. Sawada, S. Katayama, Y. Ariyoshi, T. Kawase, Y. Hayakawa, T. Tomita, and M. Baba, "Fluorinated functional materials possessing biological activities: gel formation of novel fluoroalkylated end-capped 2-acrylamido-2-methylpropanesulfonic acid polymers under non-crosslinked conditions", *J. Mater. Chem.,* **8**, 1517 ~ 1524 (1998).

3) H. Sawada, Y. Nakamura, S. Katayama, and T. Kawase, "Gelation of Fluoroalkylated End-Capped Oligomers Containing Triol Segments under Non-Crosslinked Conditions, and Binding or Releasing of Metal Ions by These Oligomers", *Bull. Chem. Soc. Jpn.,* **70**, 2839 ~ 2845 (1997).

4) H. Sawada, T. Tanimura, S. Katayama, and T. Kawase, “Aggregation of fluoroalkyl units: synthesis of gelling fluoroalkylated end-capped oligomers containing hydroxy segments possessing metal ion binding and releasing abilities”, *Chem. Commun.,* 1391 ~ 1392 (1997).

5) H. Sawada, T. Tanimura, S. Katayama, T. Kawase, T. Tomita, and M. Baba, “Synthesis and Properties of Gelling Fluoroalkylated End-Capped Oligomers Containing Hydroxy Segments”, *Polym. J.,* **30**, 797 ~ 804 (1998).

6) S. Katayama, S. Fujii, T. Saito, S. Yamazaki, and H. Sawada, “Preparation of Fluoroalkyl End-Capped Vinyltrimethoxysilane Oligomeric Silica Nanocomposites Containing Gluconamide Units Possessing Highly Oleophobic/Superhydrophobic, Highly Oleophobic/Superhydrophilic, and Superoleophilic/Superhydrophobic Characteristics on the Modified Surfaces”, *Polymers*, **9**, 292 ~ 308 (2017).

7) S. Katayama, M. Yasuta, and H. Sawada, “Preparation and properties of fluoroalkyl end-capped 2-acrylamido-2-methylpropanesulfonic acid oligomer/poly(vinyl alcohol) composite film”, *J. Coat. Technol. Res.,* **17**, 219 ~ 230 (2020).

(not described in this thesis)

8) H. Sawada, S. Katayama, M. Oue, T. Kawase, Y. Hayakawa, M. Baba, T. Tomita, and M. Mitani, “Synthesis and Properties of Fluoroalkylated 2-Acryloxyethyltrimethylammonium Chlodide Oligomers”, *J. Jpn. Oil Chem. Soc.,* **45**, 161 ~ 169 (1996).

Acknowledgements

The author is particularly indebted to Professor Hideo Sawada, Department of Frontier Materials Chemistry, Graduate School of Science and Technology, Hirosaki University, for his warm, enthusiastic, and continuous direction throughout the course of the present study.

The author wishes to express his deep appreciation to Professor Masaaki Okazaki, Associate Professor Ryo Miyamoto, Associate Professor Jun Kawakami, and Associate Professor Fumihiko Kitagawa for their kind advice and discussions.

The author also deeply thanks to Professor Masanori Baba on Kagoshima University, Professor Toshio Tomita on Tohoku University, Mr. Yusei Tsushima on Hirosaki University, Mr. Shogo Fujii, Mr. Masato Yasuta, and all students of a laboratory for their help, kind advice and discussion, respectively.

The author is grateful to Chairman Dr. Shiro Yamashita, President Mr. Junichi Hasegawa, Director and Managing Executive Officer Dr. Fuyuhiko Ishii, Director and Managing Executive Officer Mr. Yukio Takaike, Director and Executive Officer Mr. Yasunari Yamaguchi, Director and Executive Officer Mr. Takeaki Yajima, and Senior Executive Officer Mr. Masatomo Hayashi on Kanto Denka Kogyo Co., Ltd. for kindly providing an opportunity for

his studying at Hirosaki University.

Furthermore, the author would like to express gratitude to President Representative Director Mr. Katsuhiro Saito on Morishita Bengara Kogyo Co., Ltd. for providing appropriate advice for studying at Hirosaki University.

Finally, the author would like to extend his indebtedness to his families for their boundless love, understanding, support, encouragement, and sacrifice throughout his study.

Shinsuke Katayama